Cyclopalladated Metallomesogens

by

Donocadh Lydon.

A thesis submitted for the part requirement for the degree of

Doctor of Philosophy

Department of Chemistry

University of Warwick

April 1999.

Table of Contents.

D. P. Lydon and J. P. Rourke, Di-cyclopalladated Schiff's base liquid crystals: Novel metallomesogens. *J. Chem. Soc. Chem. Commun.* (1997) 1741-1742.

D. P. Lydon, G. W. V. Cave and J. P. Rourke, Cyclopalladated acac and cp liquid crystals: A comparative study. *J. Mater. Chem.*, 7(1997) 403.

G W V Cave, **D P Lydon** and J P Rourke, Cyclopalladated Schiff's base liquid crystals: the effect of the acac group on thermal behaviour. *J. Organomet. Chem.*, 1998, **555**, 81.

List of Figures.

Chapter 3.

Chapter 4.

Chapter 5.

List of Tables.

Acknowledgements.

I would like to acknowledge the assistance of the following, over the past three years :

Dr. Jonathan Rourke for his advice, help and the use of his research facilities; Mr. Gareth Cave for preparation of the β-diketone ligands his help in the laboratory; Warwick Analytical Services for elemental analysis and The University of Warwick for funding.

Declaration.

The work described in this thesis is my own work with the exception of the preparation of the β-diketonate ligands undecane-5,7-dione, pentanedecane-7,9-dione and nonadecane-9,10-dione, which were prepared by Mr. Gareth Cave.

Some of the material has been accepted for publication with the following references:

D. P. Lydon and J. P. Rourke, Di-cyclopalladated Schiff's base liquid crystals: Novel metallomesogens. *J. Chem. Soc. Chem. Commun.* (1997) 1741-1742.

D. P. Lydon, G. W. V. Cave and J. P. Rourke, Cyclopalladated acac and cp liquid crystals: A comparative study. J. Mater. Chem., 7(1997) 403.

G W V Cave, **D P Lydon** and J P Rourke, Cyclopalladated Schiff's base liquid crystals: the effect of the acac group on thermal behaviour. *J. Organomet. Chem.*, 1998, **555**, 81.

D. P. Lydon and J. P. Rourke, Homo- and hetero-bimetallic liquid crystals. Abstract papers of the American Chemical Society, 1998, Vol. 215, No.Pt1, pp.470-INOR.

D. P. Lydon (BSc., MSc.).

Summary.

This thesis describes the synthesis and characterisation of novel cyclopalladated metallomesogens from four principal N-functionalised mesogenic ligands:(i) 4-alkyloxy-N-(4'-alkyloxybiphenyl)benzylidene, (ii) terephthalylidene-bis-4-N-4'-alkyloxybenzylidene, (iii) bis(4-alkoxybenzylidene-1,4-phenylenediamine and (iv) 3, 6 bis-(alkyloxyphenyl)pyridazine).

The ligands have been studied to determine their liquid crystalline behaviour and the phase behaviour is reported for the terephthalylidene-bis-4-N-4'-alkyloxybenzylidene series and for the 3, 6 bis-(alkyloxyphenyl)pyridazine series since no comprehensive study of either system has been reported in the literature.

The co-ordination chemistry of these ligands is reported. The regiospecificity of the cyclopalladation reaction for the terephthalylidene-bis-4-N-4'-alkyloxybenzylidene and 3, 6 bis(alkyloxyphenyl)pyridazine series has been established and the influence of the primary cyclopalladation step on secondary cyclopalladation has been examined.

The co-ligands acetylacetonate, undecane-5,7-dione, pentandecane-7,9-dione, nonadecane-9,10-dione, 2,2,6,6 tetra-methyl-heptane-3,5-dione and cyclopentadienylide have been employed to enable elaboration of the geometry of the organopalladium complexes giving diversity to the structure and physical properties of these materials.

Abbreviations.

Å	angstrom (10^{-10} m)
br	broad
CD	circular dichroism
d	doublet
DSC	differential scanning calorimetry
Et	ethyl
m	multiplet
Me	methyl
NMR	nuclear magnetic resonance
p.p.m.	parts per million
q	quartet
s	singlet
t	triplet
δ	chemical shift

Chapter 1

Section 1.1.1: Introduction to palladium and platinum (II).

Platinum and palladium (II) species are favoured for a variety of reasons for the synthesis of metallomesogenic materials. In the first part of this chapter the chemistry of these metal species is discussed as a background to the physical and chemical properties of which arise in palladium and platinum metallomesogens. In particular, the formation and structural properties of palladium metallocycles are discussed in detail. The topics discussed are listed below:

1 Co-ordination chemistry of divalent platinum group metals.

2 Trends in bonding of platinum and palladium (II) to donor ligands.

3 *Cis* and *trans* influences and effects.

4 Cyclopalladation.

5 Trends in cyclopalladation for benzylidene systems.

6 Mechanism of cyclopalladation for benzylidene systems.

7 Regiospecificity of cyclopalladation reaction.

8 Structure of palladocycles benzylidene systems versus benzylamine type systems.

9 Summary.

Section 1.1.2: Co-ordination chemistry of divalent platinum group metals.

The divalent (d^8) oxidation state is common to the three platinum group metals and has produced a vast number of complexes. Nickel (II) principally forms octahedral and square planar complexes, though examples of trigonal bipyramidal and square pyramidal complexes are also known. Trends for the formation of square planar, octahedral and tetrahedral geometries are known to change going down the group.

Four co-ordinate complexes are the most popular species formed by the divalent Pd and Pt ions. The vast majority of these complexes have square planar geometries or distortions of this geometry. The complexation of palladium (II) and platinum (II) has a more dramatic effect in splitting its d orbitals than for nickel (II), as complexes of these second and third row metals in this oxidation state generally have a square planar geometry and they are less likely

to dissociate than other divalent metal ions.[1] Competition between square planar, octahedral and tetrahedral geometries occurs for nickel (II) with the prevailing structure for a given complex depending on the steric requirements and field strength of the donor ligands. The major factor which determines which of the three geometries is observed is whether it is more energetically favourable for the d orbitals to have all their electrons paired thus leading the square planar geometry, or to have two electrons occupying two d orbitals singly (in two degenerate orbitals), forming the octahedral or tetrahedral geometries.[2] The eighteen electron rule is normally used to gauge the stability of organometallic compounds. However square planar complexes of the platinum group have an electron count of sixteen and are quite stable. Examples of eighteen electron palladium (II) systems do exist and they have a trigonal bipyramidal geometry.

Section 1.1.3: Bonding of ligand donors to M(II) metal centres.

Section 1.1.3.1: Oxygen donors.

The lone pairs on oxygen donor ligands do not form strong bonds with platinum (II) or palladium (II) and complexes formed from unidentate ligands of this type easily undergo substitution reactions. Stabilisation of oxygen donor ligands can be brought about by using bidentate ligands containing two oxygen donor ligands. This strategy is particularly effective in the formation of five and six membered rings. The affinity of these ligands for the class b platinum (II) and palladium (II) metal centres is augmented by a favourable entropy change when the complex forms. The presence of another donor heteroatom such as sulfur or nitrogen increases the affinity of the bidentate ligand further due to stronger binding. If the bidendate ligand contains two different donor atoms, geometrical isomerism is theoretically possible but one of these complexes may be excluded by the preferential formation of the other as a result of the *trans* effect.

Section 1.1.3.2: Nitrogen donors.

Nitrogen donor ligands form strong σ-bonds with palladium (II) and also form complexes by π-back bonding, as in the case of the CN^- ligand.

Section 1.1.3.3: Sulfur donors.

Sulfur ligands such as RSH and R_2S form strong co-ordinate bonds with platinum (II) and palladium (II).[3] This is a consequence of two factors: the ability of the sulfur atom to

generate a large induced dipole moment, in conjunction with its permanent dipole moment will increase its co-ordinating ability; these platinum (II) and palladium (II) bonds to sulfur are also strengthened by the π-back-bonding from the metal to the vacant low lying d orbitals on the sulfur atom. While halogen bridged complexes of platinum (II) and palladium (II) are readily cleaved by monodenate ligands such as pyridine and triphenylphosphine, the corresponding thio-bridged complexes are stable to attack from these nucleophiles. Note also that the thio-bridged product is *cis* for palladium (II) and *trans* for the platinum (II) species due to isomerisation of the palladium species.[4-6]

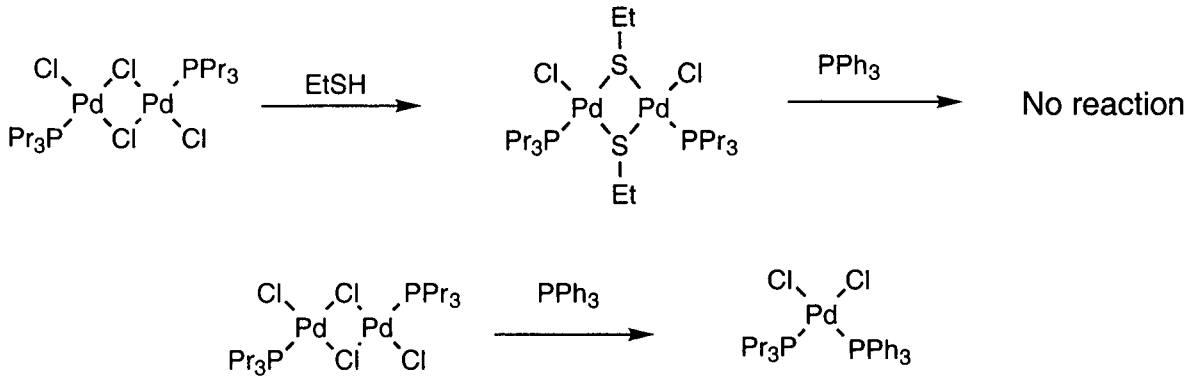

Fig. 1.1: Stability of thio-bridged complexes to nucleophilic attack.

Section 1.1.3.4: Phosphorus donors.

Platinum (II) and palladium (II) bonds to phosphorus are formed by σ-donation of a lone pair of electrons to a vacant orbital on the metal and π-back-bonding from the metal to the phosphorus atom. Lower members of this group also form co-ordination complexes with palladium (II) and platinum (II), although there is some doubt over whether π-back-bonding effects become more or less important on descending the group. This is because the size of the d orbitals increase on going down the group, increasing overlap with the d orbitals of the metal atom, while electronegativity also decreases, reducing the tendency for π-back-bonding to occur. It is likely that these two effects cancel each other out leading to similar bond order throughout the series.[7,8]

Section 1.1.3.5: Halide donors.

As mentioned above platinum (II) and palladium (II) are soft acids or class b metal centres, since they have relatively full d orbitals and are less electropositive metal species, preferring to form complexes with elements of high atomic number in a given group such as phosphorus in group VB and bromine in group VIIB. The stability of halide complexes increases in the

following order enabling heavy members of the group to displace lighter ones.[9]

$$I^- > Br^- > Cl^- >> F^-$$

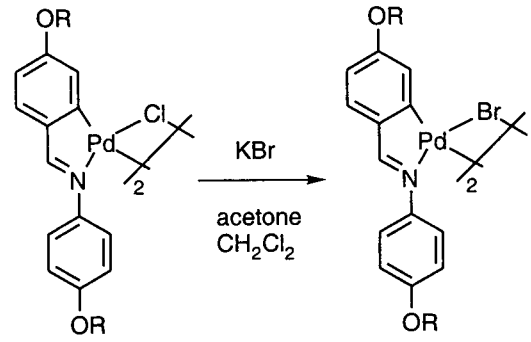

Fig. 1.2: Exchange of bridging ligand due to class b properties of palladium.

These metal centres form their most stable complexes with ligands which have vacant π-orbitals which can engage in π-back-bonding with the metal.

Section 1.1.3.6.1: Carbon donors.

Palladium forms both π-bonds and σ-bonds with carbon. π-Cyclopentadienyl complexes can be formed from sodium or thallium cyclopentadienides.[10] These are eighteen electron systems where the cyclopentadienyl group has a hapticity of five. Complexes of this kind containing halogen ligands are the most stable, which is as a result of the electron withdrawing effect of this electronegative group on the electron rich eighteen electron complex. Their proton NMR spectra exhibit a single proton resonance in the range of δ 3.71-5.40 down field from TMS. The thermal stability of the complexes increases in the order of Ni < Pd <Pt.

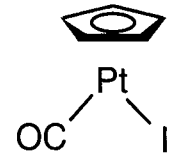

Fig. 1.3: 18 electron Pt (II) π-cyclopentadienyl complex.

Palladium (II) and platinum (II) are known to form σ-bonds with both aryl and alkyl carbon atoms. Indeed these metals form a large group of organometallic complexes more stable than any other of the transition metals.[11] The orbitals involved in the metal-alkyl σ–bonds arise from the interaction of the filled sp^3 orbital on the alkyl carbon atom with the $sp_xp_yd_{x2-y2}$ orbitals on the metal; some back donation from the metal to alkyl carbon atom also takes place. The metal-carbon σ–bond for aryl complexes is formed by the sp^2 orbital on the

carbon atom with the empty $sp_xp_yd_{x^2-y^2}$ orbitals on the metal atom. The formation of π-bonds also takes place due to the overlap of the filled p_π-orbitals of the aryl ligand with empty orbitals on the metal and π-back-bonding from the filled orbitals of the metal to empty p_π^*-orbitals of the aryl ligand. The aryl complexes are generally more stable than the alkyl complexes due to the stronger π-back-bonding effects.[12,13]

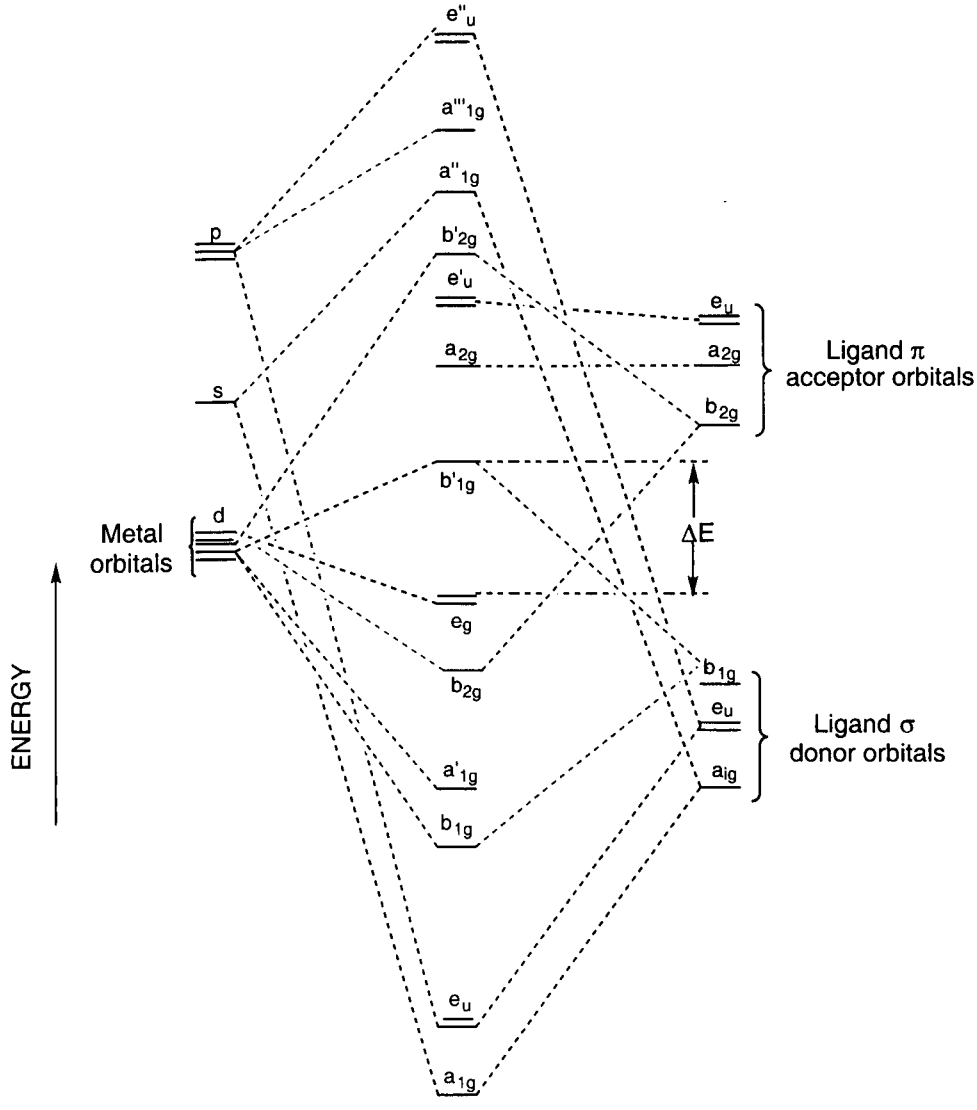

Fig.1.4: Energy level diagram of square planar Pd (II) or Pt (II) organometallic complex.

Section 1.1.3.6.2: Stability of carbon-palladium (II) and platinum (II) bonds.

The stability of metal complexes is often discussed in terms of the tendency to undergo reactions brought about by the influence of thermal, oxidative, hydrolytic or solvolytic factors.[14,15] Carbon bonds to palladium (II) are less stable to these factors than carbon bonds to platinum (II), though the nature of the ligand which forms the σ-carbon-metal bond is also

an important factor in the stability of the complex. It is more meaningful to discuss the stability of these complexes in terms of kinetics and thermodynamics. By heating these complexes, the σ-bonds undergo homolytic thermolysis, therefore the thermodynamic stability of these complexes depends on the relative energies of the metal-carbon σ-bond, the carbon-carbon bond and the carbon-hydrogen bond. Since it is known that the thermodynamic stability of the metal-carbon bond is 251 $kJmol^{-1}$, that of the carbon-carbon bond 347 $kJmol^{-1}$ and that of the carbon-hydrogen bond 364 $kJmol^{-1}$ the stability of the metal-carbon σ-bond is probably kinetic. This is exemplified by the thermal decomposition of the complex $[(PEt_3)_2Pd(CH_3)_2]$ which yields ethane and ethene as the major products, with only a small quantity of methane. This suggests that the complex decomposes by a mechanism involving the breaking of carbon-phosphorus and carbon-hydrogen σ–bonds rather than palladium (II)-carbon σ-bonds.[12] Metal-carbon σ-bonds decompose to give reactive products such as free radicals, or possibly a carbanion. This is an irreversible process, therefore the formation of stable compounds suggests that the metal-carbon σ-bond must have a high activation energy towards decomposition. The homolytic dissociation of the bond can come about by the promotion of an electron from the filled metal-carbon bonding orbital to the lowest unfilled orbital or by the promotion of an electron from the highest filled orbital to the metal carbon antibonding orbital, depending on which transition requires less energy. Therefore, to maximise the kinetic stability, these energy transitions should be as large as possible. The distance between the HOMO and LUMO orbitals is always greater for a square planar complex in which there is σ-bonding and π-back-bonding than in the case where there is simply σ-bonding. Complexes of the platinum group metals show the highest stability with the order increasing from $Ni^{II} < Pd^{II} < Pt^{II}$.[16,17] This is due to the crystal field stabilisation energy increasing in the same order, *i.e.* the energy gap between the HOMO's and LUMO's gets larger as the metals get heavier. The stability of aryl groups over alkyl groups forming metal carbon σ-bonds is due to the ability of this class of ligand to engage in π-back-bonding with the metal. This in turn increases the crystal field stabilisation energy of the complex or increases the energy gap between the HOMO and LUMO of the complex.

Section 1.1.4: *Cis* and *trans* influences and effects.

The properties of platinum (II) and palladium (II) four co-ordinate square planar complexes are known to be sensitive to the polarisability and geometrical distribution of the ligands bonded to the metal centre. Selectivity in reactivity has been observed for certain ligands in specific co-ordination environments.[18] Trends in the structure of the complexes have also been observed by diffraction methods and vibrational and NMR spectroscopies.[3] These trends arise because of the interaction of the donor electrons of a given ligand with the metal centre through σ-bonding and possibly π-back-bonding from the metal. It is important to note that this interaction occurs between every ligand in the complex and the metal centre. Therefore the influence of the bonding characteristics of each ligand is felt by every other ligand in the complex and this influence is mediated through the metal centre. These interactions are generally referred to as the *cis* and *trans* effects and influences.

Cis and *trans* influences are terms applied when discussing the ground state properties of a complex and *cis* or *trans* effects are used to describe the kinetic and thermodynamic behaviour of a complex with respect to the interaction of the ligands concerned through the metal centre. The reaction mechanism is the major influence on the kinetics of these complexes and therefore factors relating to the structure of its transition state are important. As a result the *cis* or *trans* influence which was present in the ground state may not correlate strongly with the *cis* or *trans* effect of the transition state. It is recognised that no absolute series for the *trans* or *cis* effect has been obtained (as the order is always dependent on the technique used to gauge the magnitude of the effect), depending on the mode of bonding for each of the ligands involved and whether the structure of the transition state resembles the complex in the ground state.

However, there are some trends which generally re-occur. The origin of these effects is fundamentally due to the bonding interactions which take place in the complex. A ligand which is highly polarisable can lose electron density through the σ-bonds to the ligand *trans* to it, weakening this bond and hence influencing the ground state properties of the bond. Alternatively the kinetic *trans* effect may arise from one ligand having a greater share of the empty p_σ orbital of the metal in the transition state, thus reducing the energy difference

between the two states. This theory is consistent with the observation that the more polarisable the metal, the stronger the *trans* effect, *i.e.* the *trans* effect at softer platinum (II) is greater than at the harder palladium (II).

A consequence of the *trans* effect is that soft ligands only bond *cis* to each other since the *trans* conformation is unstable: dialkyls of Au (III), and platinum (II) are always *cis* and a ligand such as ethylene makes the *trans* position of $[Pt(C_2H_4)Cl_3]^-$ susceptible to attack by hard ligands.[19,20]

The *trans* effect is very important in the preparation of specific isomeric forms of platinum (II) square planar complexes. However it is less useful for the preparation of palladium (II) complexes, due to greater lability of these species.[1,8,19,21]

Section 1.1.5.1: Cyclometallation.

Transition metals have been used regularly in the preparation of molecular and supramolecular materials because of the intermolecular interactions which can take place with these materials giving rise to desirable physical properties. Modification of the structures can be brought about by altering the transition metal or ligand used. Simple co-ordination chemistry suffers from the disadvantage of not always being completely selective towards the formation of the desired complex and secondly some complexes are quite labile leading to the formation of other structures by further reaction. The kinetic stability of the metal-carbon bond formed by cyclometallation reactions using platinum (II) and palladium (II) metal centres is a means to overcome this difficulty, generating kinetically stable molecular and supramolecular structures. This reaction allows the formation of species which will occupy just two of the co-ordination sites of the metal, leaving remaining sites vacant for further elaboration of the molecular structure.[22]

The first examples of cyclometallation using platinum (II) and palladium (II) were reported in 1965 by A. C. Cope.[23] He described a complex containing a covalent bond between a platinum (II) species and azobenzene. He also proved the metal was bonded at the *ortho*-position in the phenyl group of the azobenzene. Sodium tetrachloropalladate (II) was also found to react with azobenzene, but at a much faster rate forming the desired product in 95% yield in 2 hours at room temperature.[23]

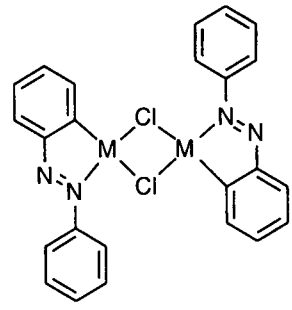

Fig.1.5: Cyclometallation of azobenzene using palladium (II) and platinum (II).

This marked the beginning of intense research into trends in cyclometallation reactions of platinum (II) and palladium (II) species due to potential applications in organic synthesis,[24] enantiomeric excess determination,[25] as carcinostatic agents[26] and novel metallomesogens.[27] Cyclopalladation reactions have successfully been carried out in solvents such as toluene,[28] methanol[29] or acetic acid[30] using either palladium acetate or sodium (or potassium) tetrachloropalladate (II) as a source of palladium (II).

Section 1.1.5.2: *Exo* versus *endo* cyclopalladation.

The cyclopalladation reaction has been widely applied to ligands such as azobenzenes, benzylidenanilines and N,N-dimethyl benzylamine derivatives due to ability of these ligands to donate a lone pair from nitrogen and subsequently bring about intramolecular C-H activation. The formation of a five membered *endo* metallocycle is the most favoured product in the cyclopalladation reaction. However, examples exist where *exo* metallocycles occur and where activation of aliphatic C-H bonds leads to more unusual metallocycles.

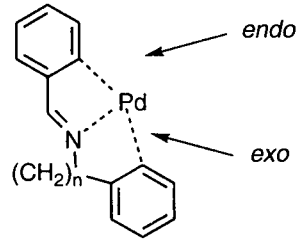

Fig. 1.6: Bonding modes for *exo* and *endo* palladacycles.

The table below ranks the order of stability of the final products of a given cyclometallation reaction in acetic acid.

Rank	Ring size	Nature of activated C-H bond	Class of Palladocycle
1	5 member	Aromatic	endo
2	6 member	Aliphatic	endo
3	5 member	Aromatic	exo
4	5 member	Aliphatic	exo
5	4 membered	Aromatic/Aliphatic	endo/exo

Table 1.1: Order of stability of final products for cyclopalladation in acetic acid.

An example of the selectivity of the cyclopalladation reaction towards five membered *endo* palladocycles is with the ligand bis(N-benzylidene)-1,4-phenylenediamine and palladium acetate in toluene, where five membered *endo* palladocycles have been produced. This leads to monopalladation of two different phenyl rings at either end of the molecule and shows the *endo* form to be the most favoured class of metallocycle for benzylidenes when undergoing the cyclopalladation reaction.[31] There is no dicylopalladation on the central ring observed as this would have required the formation of stable four membered *exo* metallocycles which studies have shown to be less favourable than the observed five membered *endo* species.

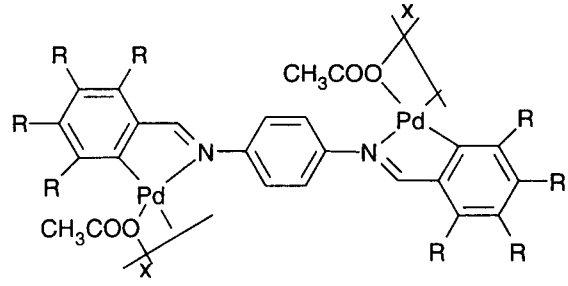

Fig.1.7: Cyclopalladation of bis(N-benzylidene)-1.4-phenylenediamine.

Results of studies in acetic acid show that cyclopalladation is thought to proceed through a highly ordered four centre transition state arising from the (Pd-acetato) and C-H bonds. The reaction is thought to be enhanced by the presence of protons, as the leaving group CH_3CO_2H is thought to accept a proton forming $CH_3CO_2H_2^+$.[30]

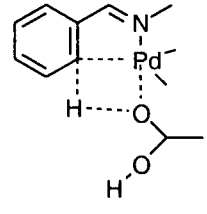

Fig.1.8: Highly ordered transition state for cyclopalladation of benzylidenes.

The order of selectivity of the cyclopalladation reaction is slightly different when using toluene as a solvent. This is thought to be because the reaction proceeds via the same highly ordered four membered transition state, but in this case the reaction is influenced by sterically bulky groups, thus making the formation of the transition state difficult. This can hinder the activation of a given C-H bond forcing the formation of an alternative metallocycle*. No 5 membered aliphatic *endo* metallocycles are observed.[28]

Rank	Ring size	Nature of activated C-H bond	Class of Palladocycle
1	5 member	Aromatic	endo
2	5 member	Aliphatic	exo*
3	6 member	Aliphatic	exo
4	4 member	Aromatic	exo

Table 1.2: Order of stability of final products for cyclopalladation in toluene.

Section 1.1.5.3: Mechanism of cyclopalladation.

Two steps are involved in the formation of the metallocycle.

1) The co-ordination of the imine to palladium acetate. This step is considered to be the fast step for the reaction and is not detectable.

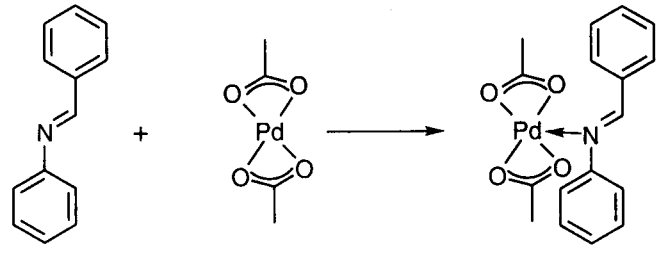

Fig. 1.9: Step 1: Co-ordination of benzylidene to palladium acetate.

2) The C-H activation leading to formation of the cyclopalladated product. This is the rate limiting step of the reaction and kinetic studies have been carried out to probe the transition state of the cyclopalladation reaction in acetic acid. It has been concluded on the basis of the thermal activation parameter and activation volumes that the transition state is highly ordered. These findings are supported by a crystal structure of the intermediates of the cyclopalladation of primary amines.

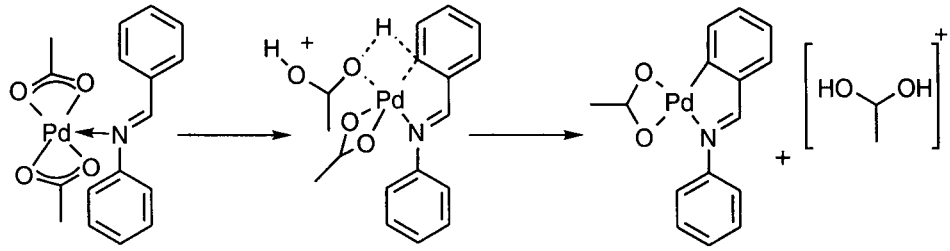

Fig. 1.10: Step 2: Activation of C-H bond leading to formation of metal carbon bond.

It is interesting to compare the conditions for cyclopalladation of benzylidenanilines with the reaction conditions for simple co-ordination of a benzylidenaniline ligand with palladium dichloride bis-benzonitrile. A simple ligand exchange reaction occurs when the benzylidenaniline and the palladium dichloride bis-benzonitrile are stirred in hexane.[32] This is because the non-polar nature of hexane does not facilitate the reaction.

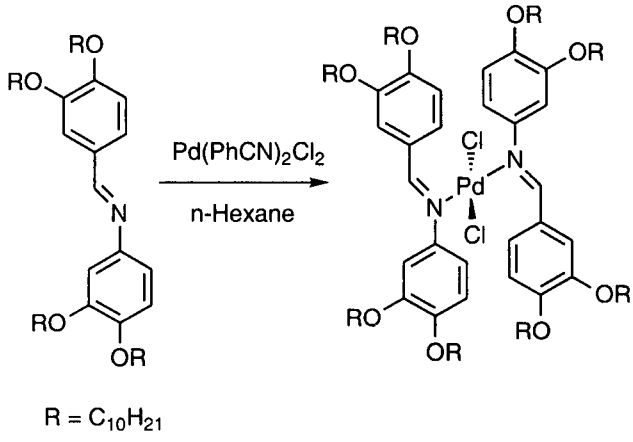

Fig. 1.11: Co-ordination complex of palladium (II) with η^1-benzylidenaniline.

Section 1.1.5.4: Regiospecificity on cyclopalladation.

The cyclopalladation of ligands such as azobenzenes, benzylidenanilines and N,N-dimethylbenzylamine derivatives is due to the ability of the lone pair from nitrogen to co-ordinate to the metal centre and subsequently bring about intramolecular C-H activation. Mechanistic studies on the cyclopalladation reaction have shown that the palladium acts an electrophile when methanol is used as a solvent, undergoing electrophilic aromatic substitution reactions.[10] Palladium (II) dichloride reacts with unsymmetrical azobenzene derivatives by attacking the aromatic ring with the greater electron density. In further studies Cope compared the reactions of *para*-methoxy and 3,5 dimethoxy-N,N-dimethylbenzylamine with lithium tetrachloropalladate (II) in methanol. This was found to give the di-μ-chloro-bis-(amine)dipalladium (II) *ortho*-palladated complexes in good yield. However, the *para*-nitro-

N,N-dimethylbenzylamine gave only a simple co-ordination complex and it was concluded that palladium (II) was a weak electrophile since in did not interact with the *para*-nitro-N,N-dimethylbenzylamine (a deactivated electron deficient aromatic system) due to the withdrawing effect of the *para*-nitro group.[29] A study of the electrophilic substitution of palladium (II) with *meta*-fluorinated azobenzene species shows selectivity towards the more negative positions on the aromatic ring when the cyclopalladation reaction is carried out in methanol.

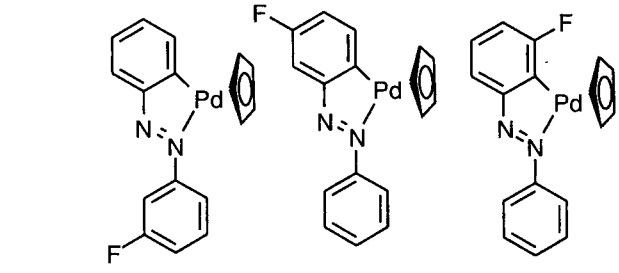

Yield %	80	20	<1
	A	B	C

Fig. 1.12: Cyclopalladation of *meta*-fluorinated azobenzene.

As expected the substantial product is the complex with *ortho*-palladation to the non-fluorinated ring. *Ortho*-palladation does occur on the fluorine substituted ring at the position *para* to the fluorine atom, as this is the position most favoured towards electrophilic attack on the fluorinated ring. However, there is only a trace amount of the third possible product C, since this is strongly deactivated towards electrophilic substitution due to the presence of the fluorine atom in the *meta* position relative to the carbon-nitrogen bond.[33]

Section 1.1.5.5: Ligand exchange reactions.

Selective cyclopalladation of aromatic rings with electron withdrawing substituents is possible by employing an alternative strategy: C-Pd activation.[34-36] The activation of the C-Pd bond occurs in the presence of acetic acid, facilitating a ligand exchange reaction whereby new a cyclopalladated system is formed from another N-donor ligand present in the reaction mixture.

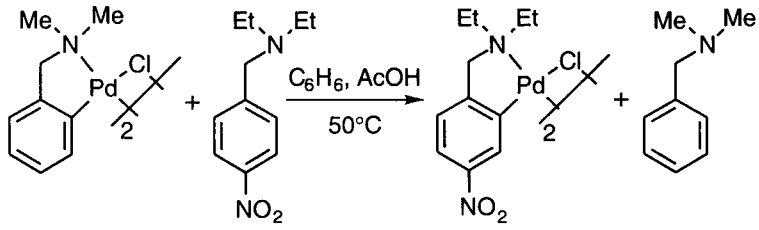

Fig. 1.13: Ligand exchange reaction from electron rich to electron deficient ring.

It is interesting to note that altering reaction conditions (*i.e.* the presence or absence of acetic acid) for the cyclopalladation of a ligand can bring about cyclopalladation at either an electron rich or an electron deficient aromatic ring in the same ligand. Transfer of the Pd-C bond from the electron rich aromatic ring to the electron deficient ring is also possible by heating the electron rich metallocycle in acetic acid. This suggests that if a cyclopalladation reaction is carried out in acetic acid, then the palladium (II) species is not behaving as an electrophile.

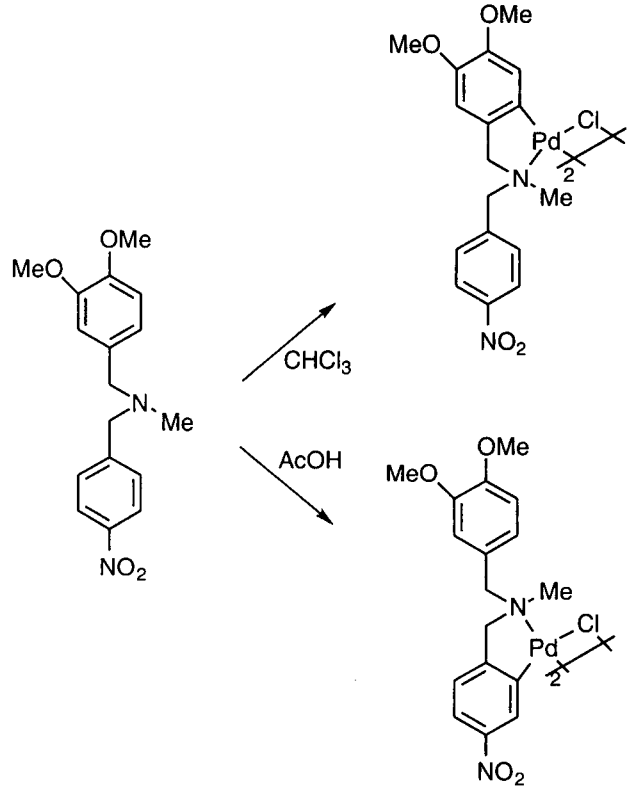

Fig. 1.14: Intramolecular cyclopalladation exchange from an electron rich to an electron deficient aromatic ring.

A mechanism for this ligand exchange reaction has been put forward[36] suggesting that ligand exchange occurs due to acidolysis of the initial cyclopalladated species in acetic acid. This proceeds by cleavage of the Pd-N bond followed by protonolysis of the Pd-C bond. The liberated palladium species proceeds to react with the electron deficient aromatic system. The

newly formed electron deficient palladocycle is less likely to undergo acidolysis and therefore equilibration of the system favours the formation of the electron deficient metallocycle.

Selectivity in the cyclopalladation reaction has been demonstrated by the previous example whereby the pathway of the cylcometallation reaction has been dictated by the reaction conditions used in conjunction with the directing effect that various aromatic substituents have on the route towards cyclopalladation. This has been defined as Regulated Cyclopalladation.[37] Selectivity can also be brought about to give the desired geometry by employing an alternative strategy: Enforced Cyclopalladation.[37]

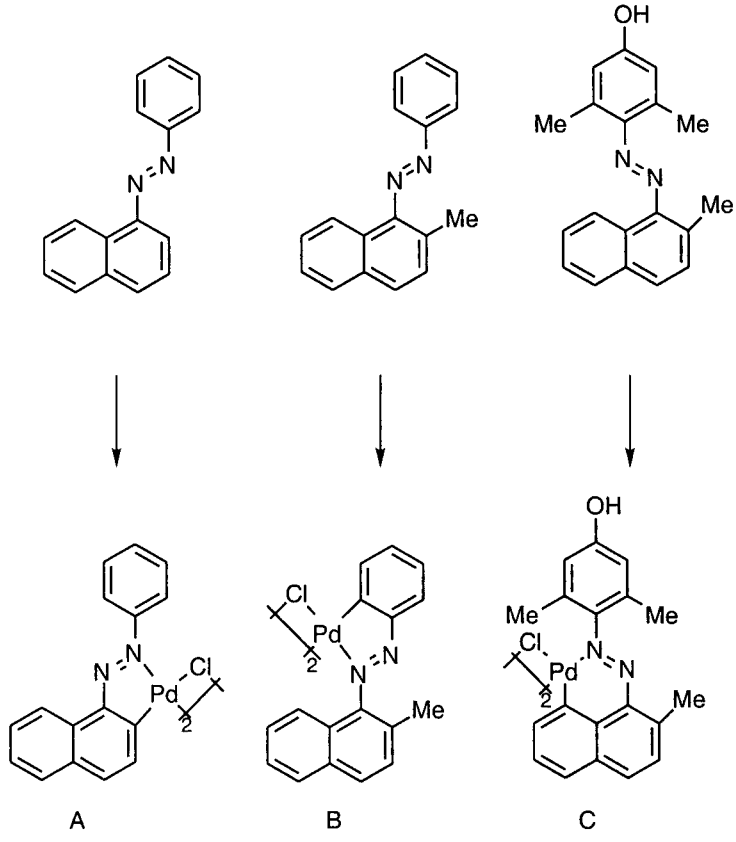

Fig. 1.15: Examples of Enforced Regioselectivity in cyclopalladation.

The position of cyclopalladation of a ligand is determined by the reactivity of various C-H bonds on the ligand which have the potential to be activated and subsequently undergo cyclopalladation. Selectivity using this approach relies on having a bias where one of the potential C-H bonds is strongly influenced by the presence of a strongly electron donating group (A) and/or by the strategic presence of substituents in the *ortho*-position of an aromatic ring (B or C), therefore protecting that position from formation of a Pd-C bond.

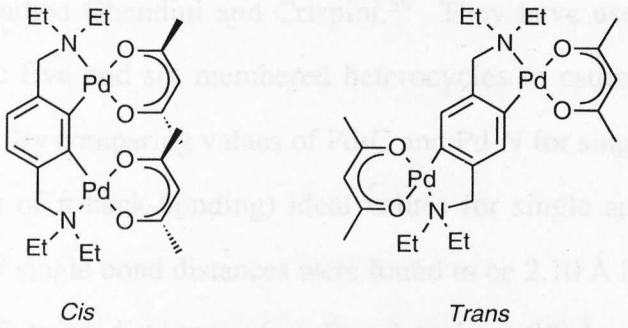

Fig. 1.16: Dicyclopalladated acetylacetonate complexes.

Trofimenko has prepared isomeric 1,3-diketonato complexes from the N,N,N',N'-tetraethyl-*p*-xylene-α,α'-diamine by reaction with sodium tetrachloropalladate as a source of palladium (II). The *cis* compound is of particular interest because the acetylacetonate rings are in a twisted conformation, giving rise to a chiral centre in the molecule. However, formation of the kinetic *trans* isomer is favoured over the thermodyamically favoured *cis* isomer. A desirable synthetic goal would therefore be to create conditions where the *cis* geometry could be achieved more efficiently.[38]

Section 1.1.5.6: Aromaticity in cyclopalladated systems.

Palladium (II) bonds with a square planar geometry when forming metallocycles. This tends to produce planar structures, particularly when the metallocycle formed is a five membered *endo* metallocycle. A sp^2 hybridised nitrogen atom as the N donor site is thought to enhance the formation of a five membered *endo* metallocycle as this system may be aromatic in nature. This is because it is a planar 4n+2 π-electron system (four electrons form the two π-orbitals from two conjugated double bonds in the ligand and a contribution of two π-electrons from a Pd orbital via π back-bonding achieves the required number of electrons delocalised in a planar ring).

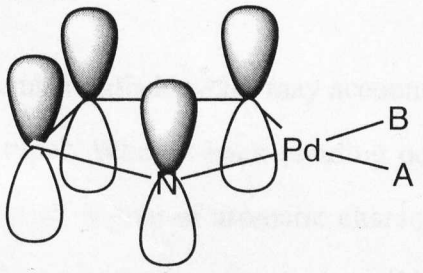

Fig. 1.17: Aromaticity in palladocycles.

The aromatic character of five membered palladocycles and how this is dependant on its

geometry has been studied Ghendini and Crispini.[39] They have used aromaticity indices developed for organic five and six membered heterocycles to estimate the bond order in cyclopalladated rings. By comparing values of Pd-C and Pd-N for single and "double" bonds (those involving a lot of π back-bonding) ideal values for single and double bonds were found. Pd-C and Pd-N single bond distances were found to be 2.10 Å in both cases while Pd-C and Pd-N "double" bond distances were found to be 1.90 Å each. They studied a population of structures examined in the Cambridge Structural Database which had its statistical distribution centred around palladocycles that had essentially a planar geometry. The study showed that a positive correlation exists between the deviation from planarity of a palladocycle and reduction in aromatic character.

The planarity of five membered palladocycles is related to the hybridisation of the nitrogen atom. It is notable that all the imine based metallocycles have near planar configurations and aromatic Pd-C bond distances. It is also generally the case that *endo* metallocycles are almost always formed instead of *exo* palladocycles and the Pd-C bond length is comparable with aromatic bond lengths. The greatest deviation from planarity are seen for metallocycles with a sp^3 hybridised nitrogen atom, where the nitrogen forms three single covalent bonds to other substituents and is also co-ordinated to the palladium bond.

The length of the Pd-N bond seems to dictate the degree of aromatic character in the palladocycle. Longer Pd-N bonds have weaker Pd-N π bond interactions and consequently reduced aromaticity and reduced planarity. A key factor influencing the length of the Pd-N bond is the ligand *trans* to it. Most palladocycles with reduced aromatic character have *trans* to the Pd-N bond, a Pd-P or Pd-S bond and generally the greater the π-acceptor ability of this ligand, the weaker the Pd-N π-bond.[39]

The aromatic character in 5 member palladocycles may account for the difference in reactivity of various complexes of this type. When π-back-bonding occurs to a large extent and the cyclometallated system has a high degree of aromatic character, this system is likely to be very stable and unlikely to undergo further reaction under mild conditions. A cyclopalladated system where there is little π-back-bonding, is more likely to undergo further reaction. This has direct consequences when designing molecular materials to perform specific functions:

high stability is desirable in a material which has applications in molecular electronics, while a more reactive palladocycle is desirable as an intermediate towards a target molecule.

A cyclopalladated system designed to be used as a metallomesogen is likely to benefit from enhanced intermolecular interactions. Therefore aromaticity and planarity in the molecular structure are key factors to be addressed in the design of these molecules. It is highly desirable to use a ligand which enhances the charge and shape anisotropy of the molecule, hence it is not surprising that many of the metallomesogenic systems are based on palladocycles with sp^2 hybridised nitrogen donor ligands adjacent to a phenyl ring, capable of forming five membered *endo* palladocycles which have a high degree of aromatic character.

Section 1.1.6: Summary.

Palladium and platinum (II) have been demonstrated to be suitable as platforms from which new metallomesogens can be developed. This is due to their propensity to bond in square planar based geometries - conferring planar structures on molecules - and forming extended linear systems giving molecules with enhanced shape anisotropy. The attachment of palladocycles to aromatic systems extends the planar surface and conjugation of a given molecule while increasing the polarisability of the delocalised core.

The ability of these metals to form stable bonds with variety of donor ligands has given rise to a wide variety of structural motifs from which many new materials can be developed. The facility to attach a ligand which confers specific properties on the molecule increases the scope for tailoring a molecule to the needs of a given application. Moreover, control of the molecular structure of the material is possible by regiospecific bonding between the metal centre and ligands achieved by the application of regulated cyclopalladation and enforced cyclopalladation strategies and through use of *cis* and *trans* bonding patterns around the metal.

The above considerations have been applied to prepare novel mesomorphic materials which are detailed in the following chapters.

Section 1.2: References.

1 J Chatt and R G Wilkins, *J. Chem. Soc.*, 1953, 70.

2 N N Greenwood and A Earnshaw *Chemistry of the Elements;* 1st ed.; Pergamon Press: Oxford, 1984.

3 F R Hartley *The Chemistry of Platinum and Palladium;* 1st ed.; Applied Science Publishers Ltd: London, 1973, pp 2.

4 J Chatt and F A Hart, *J. Chem. Soc.*, 1953, 2363.

5 T Boschi, B Crociani, L Toniolo and U Belluco, *Inorg. Chem.*, 1970, **9**, 532.

6 J Chatt, L A Duncanson and L M Venanzi, *J. Chem. Soc.*, 1955, 4461.

7 J Chatt and A A Williams, *J. Chem. Soc.*, 1951, 3061.

8 J Chatt and R G Wilkins, *J. Chem. Soc.*, 1952, 4300.

9 M J Baena, P Espinet, M B Ros and J L Serrano, *J. Mater. Chem.*, 1996, **6**, 1291.

10 M I Bruce, B L Goodall and F G A Stone, *J. Chem. Soc., Dalton Trans.*, 1978, 687.

11 F R Hartley *The Chemistry of Platinum and Palladium;* 1st ed.; Applied Science Publishers Ltd: London, 1973, pp 23.

12 G Calvin and G Coates, *J. Chem. Soc.*, 1960, 2008.

13 J Chatt and B L Shaw, *J. Chem. Soc.*, 1959, 705.

14 G Booth and J Chatt, *J. Chem. Soc. (A)*, 1966, 634.

15 S J Ashcroft and C T Mortimer, *J. Chem. Soc. (A)*, 1967, 930.

16 C M Harris, S E Livingstone and I H Reece, *J. Chem. Soc.*, 1959, 1505.

17 J Chatt, G A Gamlen and L E Orgel, *J. Chem. Soc.*, 1958, 486.

18 F R Hartley, *Chem. Soc. Rev.*, 1973, **2**, 167.

19 J Chatt and R G Wilkins, *J. Chem. Soc.*, 1956, 525.

20 R S Tobias, *Inorg. Chem.*, 1970, **9**, 1296.

21 G Faraone, V Ricevuto, R Romeo and M Trozzi, *J. Chem. Soc. (A)*, 1971, 1877.

22 R Carina, A Williams and G Bernardinelli, *J. Organomet. Chem.*, 1997, **548**, 45.

23 A C Cope and R W Siekman, *J. Am. Chem. Soc.*, 1965, **87**, 3272.

24 A D Ryabov, *Synthesis*, 1985, 233.

25 M Pabel, A C Wills and S B Wild, *Angew. Chem., Int. Ed. Engl.*, 1994, **33**, 1835.

26 R Navarro, J Garcia, E P Urriolabeitia, C Cativiela and M D Diaz-de-Villegas, *J.*

Organomet. Chem., 1995, **490**, 35.

27 B Heinrich, K Praefche and D Guillon, *J. Mater. Chem.*, 1997, **7**, 1363.

28 M Gomez, J Granell and M Martinez, *Organomets.*, 1997, **16**, 2539.

29 A C Cope and E C Friedrich, *J. Am. Chem. Soc.*, 1968, **90**, 909.

30 M Goméz, J Granell and M Martinéz, *J. Chem. Soc., Dalton Trans.*, 1998, 37.

31 J M Vila, M Gayoso, M T Pereira, M C Rodriguez, J M Ortigueira and M T Pett, *J. Organomet. Chem.*, 1992, **426**, 267.

32 M Lee, Y Yoo, M Choi and H Chang, *J. Mater. Chem.*, 1998, **8**, 277.

33 M I Bruce, B L Goodall and F G A Stone, *J. Chem. Soc., Chem. Commun.*, 1973, 558.

34 A D Ryabov and A K Yatsimirsky, *Inorg. Chem.*, 1984, **23**, 789.

35 A D Ryabov and G M Kazankov, *J. Organomet. Chem.*, 1984, **268**, 85.

36 A D Ryabov, *Inorg. Chem.*, 1987, **26**, 1252.

37 A D Ryabov, *Chem. Rev.*, 1990, **90**, 403.

38 S Trofimenko, *Inorg. Chem.*, 1973, **12**, 1215.

39 A Crispini and M Ghedini, *J. Chem. Soc., Dalton Trans.*, 1997, 75.

Chapter 2

Section 2.1.1: Introduction to liquid crystals.

Since their discovery in 1888, liquid crystals have posed some interesting questions about the behaviour of matter, requiring a more complete understanding of the forces which govern the transitions between the solid and liquid phase. Moreover, an understanding of these materials has allowed scientists and engineers to develop new materials with properties tailored for specific applications.

Liquid crystalline materials (or mesogenic materials as they are sometimes called) differ from other materials in that they exhibit an intermediate phase between the solid phase and the isotropic liquid phase. Such phases are called mesophases, meaning "*in between phase*". A material which exhibits this kind of behaviour is called a mesogen. Liquid crystalline behaviour can be exhibited by a material in two ways: (a) by heating the material to give a liquid crystal phase, (thermotropic liquid crystal) or (b) by dissolving the material in a suitable solvent (lyotropic liquid crystal) to give an ordered fluid. The ability of a material to show lyotropic liquid crystallinity does not necessarily mean that it will exhibit thermotropic liquid crystallinity, but it may; the converse is also true.

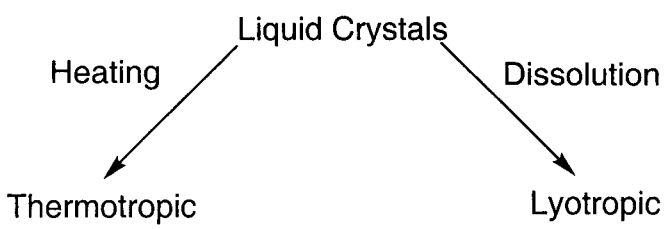

Fig. 2.1: Classification of liquid crystals.

In order to understand why these mesophases arise in certain materials, it is necessary to consider the changes which occur when a crystal melts (or dissolves) into a liquid phase. In a conventional material, this phase transition brings about the loss of positional and orientational order within the crystal lattice and gives a fluid which is completely disordered. However, this is not the case for liquid crystalline or mesogenic materials; for these materials the transition from the solid phase is achieved with the loss of only positional order in the crystal lattice, orientational order is to a large extent conserved. Molecules in such a phase

like to align or self-organise into ordered domains. A direct consequence of this is that we have a material which is fluid, like other conventional liquids, but with significant differences in some of the physical properties of the fluid phase in different directions. In other words the phase has anisotropic physical properties. By heating (or diluting further), the mesogenic behaviour is lost and an isotropic liquid is formed. Certain materials exhibit behaviour whereby on moving from the crystal phase to a fluid phase, loss of orientational order occurs, with conservation of positional order, which gives rise to a plastic crystal phase. There are two major types mesophases seen in thermotropic liquid crystals, calamitic phases, which are exhibited by rod-like molecules and columnar phases which are generally shown by disc-like molecules. A liquid crystal phase may be thermodynamically stable or enantiotropic, or it may be thermodynamically unstable in which case it is said to be monotropic. In an enantiotropic phase the mesogen shows the phase on heating and cooling, and so the process of moving from that phase to another phase is fully reversible. However, when the phase is monotropic, it will only appear on cooling.

Section 2.2.1: Calamitic mesophases.

Section 2.2.1.1: The nematic phase.

The order within a calamitic mesophase can vary considerably, giving rise to a number of distinct mesophases. The parameter known as the director (n) defines the net orientation of the molecules within the phase.[1] The most disordered phase, the nematic phase only has orientational order, brought about by the long axes of the molecules pointing on average in the same direction. It has no positional order at all.

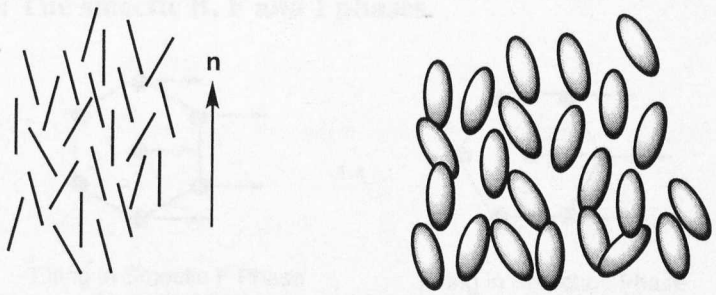

Fig. 2.2: Schematic representation of nematic phase.

The remaining phases (the smectic phases) all have some degree of positional order in addition to orientational order. The amount of positional order in each phase dictates the

order in which the phases maybe observed. In a hypothetical material which exhibits the nematic and all of the true smectic phases, the sequence will be observed as shown in the diagram.

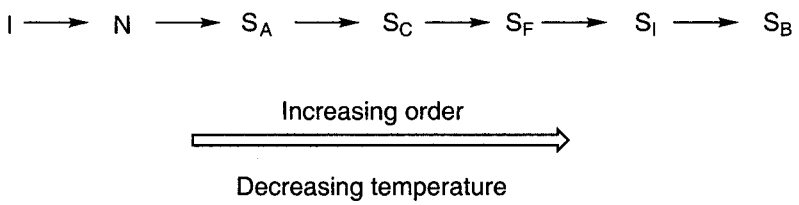

Fig. 2.3: Variation in positional order gives rise to a variety of phases.

Section 2.2.1.2: The smectic A phase.

The least ordered smectic phase, the smectic A phase, can be simply described as having the long axis of the molecules on average pointing in the same direction, with the association of the molecules into layers, where the director is perpendicular to the layer normal. This phase is still quite fluid, allowing diffusion between layers to occur. There is no positional order between the layers of this phase and the molecules are free to rotate about their long axes. This description is simplification of the true situation within each layer where the tilt direction varies randomly, averaging out over a number of layers. These layers themselves exist as a sinusoidal variation in the density of the phase.[2]

Section 2.2.1.3: The smectic C phase.

The smectic C phase arises from a greater degree of positional order. In this phase the molecules tilt at an angle to the layer normal and all the molecules have the same tilt direction within each layer.

Section 2.2.1.4: The smectic B, F and I phases.

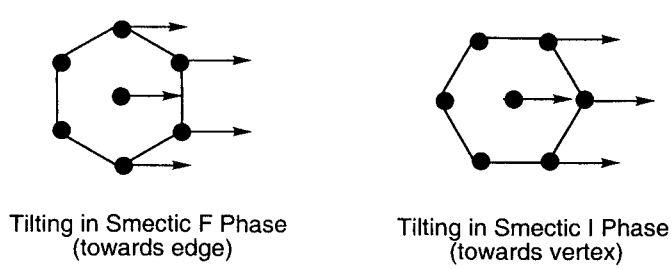

Fig. 2.4: Structure of smectic I and smectic F phases.

The order in a smectic phase can also be increased by introducing regular packing within the layers: hexagonal packing of the molecules gives rise to the smectic B phase. Tilting of this

phase can give rise to two other distinct smectic phases: the smectic F phase in which the tilt direction is towards the edge of the hexagon and the smectic I phase where the direction of tilt is towards the vertex of the hexagon.

Section 2.2.1.5: Crystal smectic phases.

Crystal smectic phases are the most ordered state between the true crystal state and the liquid crystal state; they show definite positional correlation between layers and in certain cases show the loss of rotational freedom, which is seen in all true smectic phases.[2]

Section 2.2.1.6: The smectic G and smectic J phases.

The smectic G phase is a layered phase with a high degree of inter-layer correlation, with an AAA--- monolayer stacking. The molecules within the layers have their long axes tilted with respect to the normal of the layer planes. The molecules have an average tilt angle of 25-30°, increasing slightly with decreasing temperature. This phase has a C-centred monoclinic cell, the molecules having a pseudo-hexagonal close packed structure at right angles to the tilt of the molecules. This pseudo hexagonal packing is too close to allow free rotation about the long axis of the molecules, however, neutron scattering studies have shown that co-operative motion occurs between the molecules. The smectic G phase is the correlated (or crystal) analogue of the smectic F phase, *i.e.* the tilt of the molecules is towards the edge of the hexagonal structure.

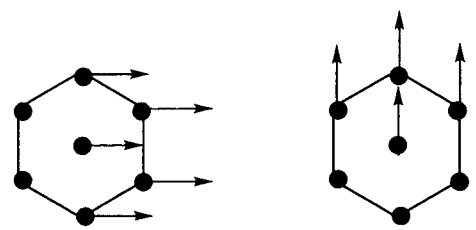

Fig. 2.5: Structure of smectic G and smectic J phases.

The correlated (or crystal) analogue of the smectic I phase is the smectic J phase. The smectic G phase and the smectic J phase have been proven to have separate identities from each other on the basis of miscibility studies. A crystal J to G phase transition has also been observed for the racemic material 4-(2'-methylbutyl)phenyl 4'-n-octylbiphenyl-4-carboxylate as in figure 2.6.[2]

$$I \longrightarrow N \longrightarrow S_A \longrightarrow S_C \longrightarrow S_I \longrightarrow S_J \longrightarrow S_G$$

Fig. 2.6: Phase behaviour of 4-(2'-methylbutyl)phenyl 4'-n-octylbiphenyl-4-carboxylate.

Section 2.2.1.7: Chiral mesophases.

Chiral modifications of the tilted phases (SmC*, SmF*, SmI*) can be obtained by resolving a racemic mixture of a mesogenic material or by addition of a chiral dopant. These phases have ferroelectric domains resulting from the low local symmetry in the phases (low local symmetry forces the transverse dipoles of the molecules to align perpendicular to the plane of tilting causing macroscopic polarisation within the smectic layer).[3,4] The chirality within the phase combined with other effects present causes precession between the layers, resulting in a net polarisation of zero due to the formation of a helix with its axis parallel to the smectic layer normal. The helix can be unwound by an applied external field or by surface stabilisation within a very thin cell. These cells can exhibit bistable switching, by reversing the sign of the applied electric field which can be exploited to give electro-optical effects.[4]

Chiral nematic phases also exist in which the director twists in a helicoidal array, having pitch length small enough to allow interaction with the visible region of the electromagnetic spectrum; this allows such phases to show iridescent colours. The pitch length varies with temperature, which in turn causes an observable colour change in the liquid crystal phase; this property makes liquid crystals useful as temperature sensors, which can then be processed to come in the form of a spray, a paint or encapsulated in a polymer film.[5]

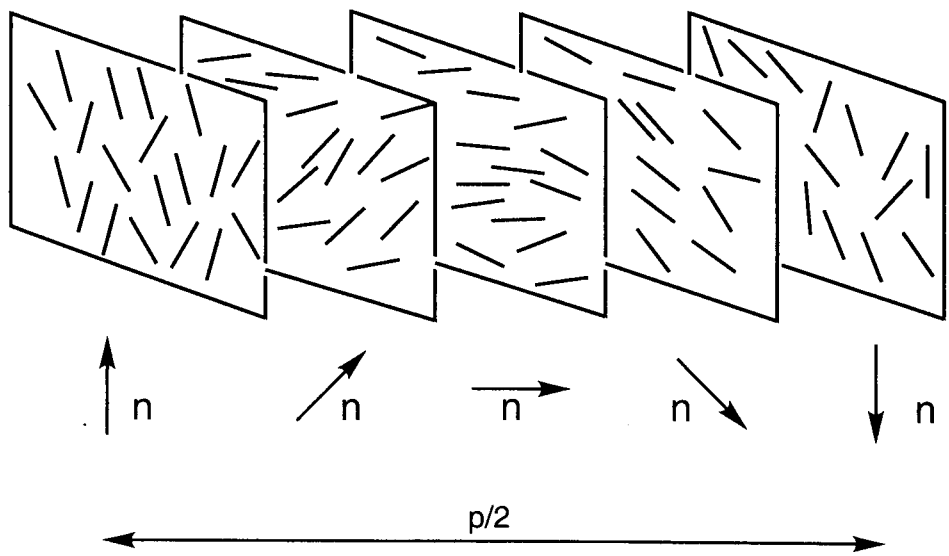

Fig. 2.7: Helical twisting of director in cholesteric phase.

Crystal phases of optically active mesogens do not possess the helicoid arrangement as the crystal-like structure suppresses this feature. Instead the formation of polydomains occurs causing the formation of individual ferroelectric domains; however, a macroscopic ferroelectric effect is not observed because of the random orientation of the polydomains. It is possible that an aligned crystal phase might show ferroelectric behaviour.

2.2.1.8: Molecular structure of calamitic mesophases.

The molecular structure of calamitic mesogens is essentially lath-like: highly conjugated moieties are joined by linkage groups, resulting in a flat planar centre known as the mesogenic core. This planar and linear geometry is enhanced by the attachment of alkyl or alkyloxy chains which increases the length to breadth ratio. A small polarisable group is sometimes used to promote intermolecular interactions; this is often located at a terminal position of the molecule. A lateral substituent may also be incorporated to modify the structure by twisting the molecular core, disrupting conjugation and hence changing the properties of the molecule.

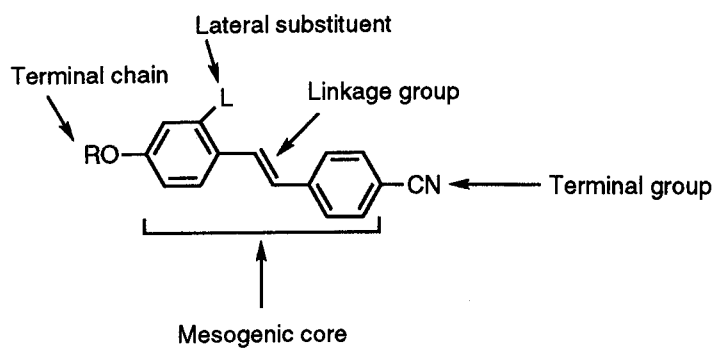

Fig. 2.8: Schematic representation of molecular structure of calamitic liquid crystals.

This general structure stems from the need for the molecules to meet following the requirements :

a) High shape anisotropy

b) Permanent dipole moment

c) High anisotropy of polarisability.

The forces at work within these molecular systems are due to the presence of polar groups capable of building up a distortion of the electron distribution. This creates an instantaneous dipole (aided by the presence of a highly delocalised core) leading to attractive intermolecular

and consequently this dictates the strength of the intermolecular forces. The highly anisotropic shape of the molecules combined with the anisotropic charge distribution leads to the formation of stable liquid crystal phases. Established structure-property relationships for calamitic mesogens state that nematic phases are seen generally seen in systems which have short alkyloxy or alkyl chains due to the dominant effect of the core and the molecules have more rigid character. As the length of the terminal chain is increased the nematic phase will be further stabilised, and smectic phases will begin to appear as a result of interactions of the terminal chains. Progressing to longer chain lengths can destabilise the nematic phase while making the smectic phase more stable.[3]

Section 2.2.2: Discotic mesogens.

Section 2.2.2.1: Structure of discotic mesogens.

Columnar phases were discovered in 1977 by Chandsrasekhar.[6] They have potential application in the area of conducting organic materials, by the transportation of charge through their columnar phases. The ability of discotic molecules to form mesophases arises from their ability to organise in arrays, along their short axes. As with calamitic mesogens, an analogous nematic discotic phase (N_D) exists, which is very fluid and shows only orientational order.

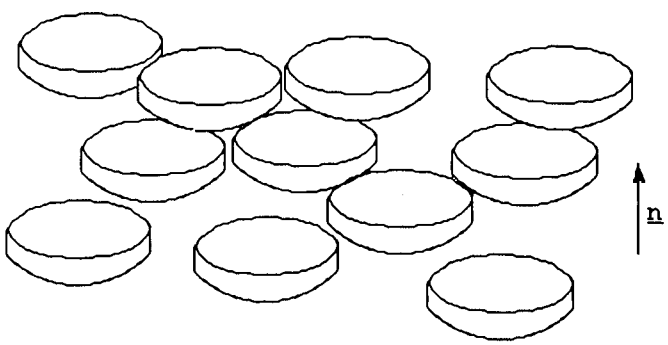

Fig. 2.9: Nematic discotic phase.

The more ordered columnar phases exhibited by these types of molecules are characterised by the symmetry of their side to side arrangements and the presence or absence of order within the columns. Examples of columnar phases include the disordered hexagonal (D_{hd}) phase and the ordered hexagonal (D_{ho}) phase, which are distinguished from each other by the packing of molecules within the columns. A disordered rectangular (D_{rd}) phase also exists in which the

rectangular symmetry is found; tilted and oblique discotic phases are also known. Phases which consist of nematic arrays in columnar stacks have also been observed, these are known as columnar nematic phases.[3]

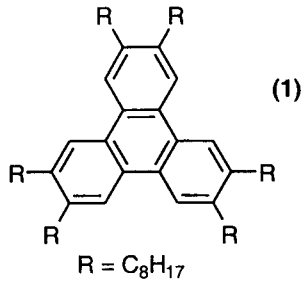

(1)

Fig. 2.10: Molecular structure of a discotic mesogen.

The molecular structure of these materials consists of a disc-like core which is usually an aromatic system (**1**), with six or eight alkyl chains radiating out from the edges of this aromatic core.

Section 2.2.3: Future prospects for liquid crystal technology.

While liquid crystalline display devices have been in service for over two decades now, providing optical displays which are cheap, reliable and have a low power consumption, interest is as keen as ever in searching for new materials which can meet the increasingly stringent demands in the electronics industry. A great deal of effort has been focused on the area of chiral liquid crystal phases, as these phases have the potential to switch on a microsecond time scale, which would be compatible with video and television frame rates. The storage of large amounts of information within a small area is also seen as one of the applications of greatest potential for liquid crystalline materials. Their ability to change colour with a change in temperature again shows their ability to give an optical signal. The ordering behaviour of mesogenic materials can be exploited as a dynamic or static effect to display information, making it a truly versatile molecular medium[7].

Section 2.3.0: Introduction to metallomesogens.

Interest in the field of liquid crystals has been focused on finding new ways to put to good use the properties of these materials. One approach is to incorporate the mesogenic material in a polymer, giving improved physical properties such as low water absorption, low thermal expansion, high mechanical strength, combined with better moulding characteristics and low melt viscosity to this class of hybrid plastics. Polymerisation of aligned liquid crystal phases

also presents the possibility of permanent stabilisation of the order within the mesophase.[8]

The elaboration of the structure of liquid crystals on the molecular level has also been examined for the past twenty years, by the systematic use of transition metals as co-ordination centres in the preparation of metallomesogens. Co-ordination chemistry when applied to mesogens has enabled new geometries to be explored, to determine their potential for molecular self-organisation. It introduces greater polarisability into certain organic ligands enhancing or indeed inducing mesogenic behaviour; judicious choice of the metal can also introduce magnetism and colour. The ability of dithiolenes to selectively absorb polarised light in a certain orientation has been utilised in host guest-display systems which effect contrast in the display by changing the orientation of the absorbing molecule from an absorbing to a non-absorbing orientation. This is brought about by dissolving a guest dye in a liquid crystal host which controls the orientation using its switching properties.[9] Transition metal complexes can form much more stable paramagnetic complexes than organic radical systems, therefore combining the magnetic properties of metals with liquid crystals would be attractive as it would enable the ordering of complexes in a magnetic field. The magnetic susceptibility of dinuclear copper (II) alkanoate has been observed to change moving from a crystal to discotic phase. This change has been attributed to a modification of the relative disposition of the dimers within the columns.[3]

The polarisability of electrons in metals can have a profound effect when co-ordinated to organic mesogens; the metal centre is capable of increasing the anisotropic polarisability of the ligand significantly, as a consequence promoting mesomorphic behaviour. The complex (M = Rh, Ir) **(2)** shows nematic and smectic A phases with phase ranges of 40°C, in contrast to a smectic B phase with a narrow phase range for the free ligand, the metal is acting as a very effective terminal polar group, similar to a cyano terminal group.[10]

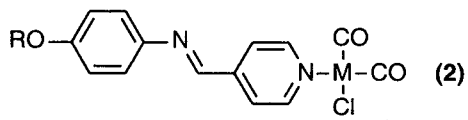

(2)

Fig. 2.11: *Cis*[$MCl(CO)_2L$].

The remainder of this chapter reviews important and recent work in the area of thermotropic metallomesogens. To discuss the topic of metallomesogens in a logical and ordered fashion

this review of the subject is broadly divided into three main sections listed below:

Section 2.3.1: Calamitic metallomesogens.

Section 2.3.2: Columnar metallomesogens.

Section 2.3.3: Polymeric metallomesogens.

These sections are then sub-divided in order to present the diverse range of materials in a logical manner, dictated primarily by the transition metal species present, but also by giving due consideration to the presence of specific molecular motifs.

Section 2.3.1: Calamitic metallomesogens.

The following sections outline previous research in calamitc metallomesogens. The compounds discussed are all from the d block transition metals series and are arranged within their respective groups in the periodic table.

Section 2.3.1.1: Group 6 calamitic metallomesogens.

In this group only chromium has been used to form calamitic metallomesogenic systems. Examples of metallomesogens formed from the two other members of the group (molybdenum and tungsten) are known, however these are columnar systems.[11,12]

Section 2.3.1.1.1: (η^6-arene)tricarbonyl chromium complexes.

These complexes (**3**) reported by Deschenaux *et al.*[13] have an octahedrally co-ordinated metal centre bonded to a mesogenic unit containing an elongated aromatic core comprising of five aromatic rings linked in a linear fashion through ester and imine functional groups to promote liquid crystalline behaviour. An important feature of these (η^6-arene)tricarbonyl chromium complexes is their ability to undergo ligand substitution reactions photochemically, enabling the mesomorphic properties of the material to be fine tuned by varying the substituents bonded to the metal. This series (as outlined in figure 2.12) shows nematic and smectic C phases for the first two analogues (n = 8,12), with the crystal to smectic C transitions at around 95°C and the smectic C to nematic phase transitions at 102°C and 110°C (for n = 8, 10 respectively) with clearing temperatures in the region of 141°C and 130°C respectively. The other two members of the series (n = 12, 14), show only smectic C phases between 92-118°C and 95-99°C respectively. The introduction of the metal tricarbonyl core to the ligand has lowered the temperature at which the melting points and clearing points occur, demonstrating

that the ability of the molecules to organise into ordered systems has been reduced by the bulky lateral metal substituent. The absence of columnar phases in the complexes compared to the hexagonal columnar phases and oblique lamello-columnar phase seen in the free ligands for n = 12 and 14 also illustrates the reduced ability to order in the (η^6-arene)tricarbonyl chromium complexes.

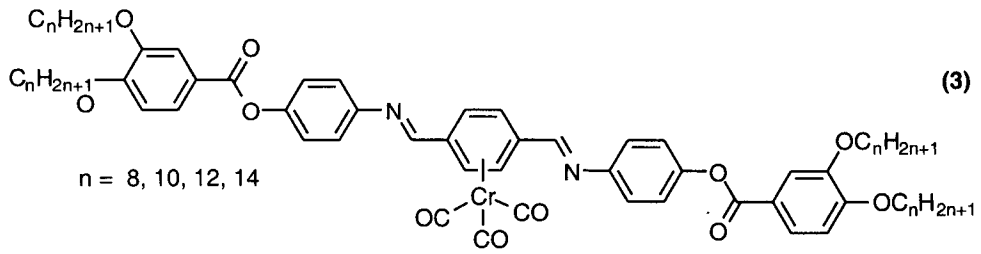

(3)

Fig. 2.12: Mesogenic (η^6-arene)tricarbonyl chromium complexes.

Section 2.3.1.2: Group 7 calamitic metallomesogens.

Calamitic mesogens for this group are known for manganese (I) and rhenium (I). These complexes are formed either *via* cyclometallation reactions or through co-ordination of metal carbonyl moieties to bipyridines or diazabutadienes. In all cases ligands with high structural anisotropy are necessary to produce mesogenic complexes, due to the bulky nature of the octahedral metal centre. Indeed, the suggestion is made that such systems should contain at least four rings plus a molecular core to induce mesogenic behaviour.[14]

Section 2.3.1.2.1: Octahedral manganese (I) complexes.

Bruce and Liu[15] have prepared high co-ordination number metallomesogens (**4**), using an octahedral manganese (I) metal centre bonded to a Schiff's base ligand which contains four ring systems in its mesogenic core. It has been shown by Bruce and Liu[15,16] that an elongated mesogenic core of this kind is critical to the formation of mesophases in high co-ordination complexes. The complexes show nematic phases between the temperatures of 120°C and 190°C, with some decomposition around the clearing point. The lateral substitution of the manganese centre has disrupted lateral interactions present in the parent ligand and as a consequence, the ordered smectic phases (G, J, I and C) are not observed in the mesomorphic behaviour of the complexes.

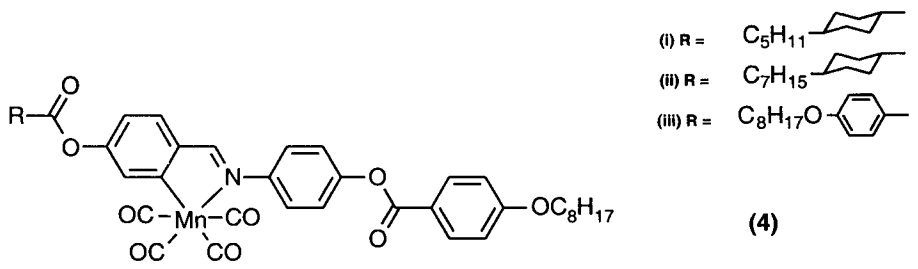

Fig 2.13: Liquid crystal complexes of octahedral manganese (I).

Section 2.3.1.2.2: Octahedral rhenium (I) complexes.

Rhenium (I) has been successfully co-ordinated to substituted 1,4-diazabutadienes with high shape anisotropy giving rise to *fac* complexes (**5**) which show mesogenic behaviour. The stability of the nematic phases of the rhenium complexes is greater than the parent ligands. The thermal stability of the complexes is also observed to be greater than the parent ligand. The octyloxy and decyloxy complexes (**5**) show nematic phases while the parent ligands also exhibit smectic C phases. The dodecyl analogue exhibits a smectic C phase. The exclusive formation of the nematic phase in the first two members of this series demonstrates the reduced anisotropy of the complex arising from its octahedral geometry. The clearing points of this class of complex are consistently greater than their parent 1,4-diazabutadiene ligands at values of 234°C (n = 8), 252°C (n = 10) and 220°C (n = 12). This is attributed to the loss of conformational freedom across the diazabutadiene linkage, giving rise to a more rigid molecular system.[17]

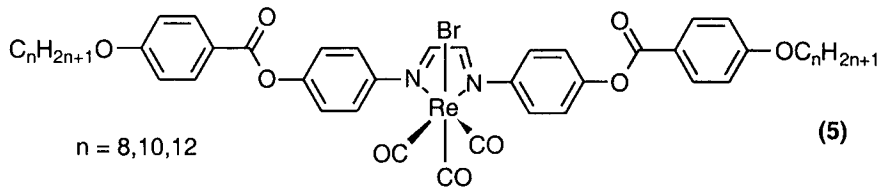

Fig. 2.14: Octahedral liquid crystal complexes of 1,4-diazabutadienes with rhenium (I).

Chloride, iodide and triflate analogues of the bromide complexes (**5**) have also been prepared in which nematic phases are seen for all the halide complexes. Lower transition temperatures are generally observed on increasing atomic mass of the halide. The dodecyl chloride analogue also shows a smectic C phase. In all iodide analogues the intermolecular order is disrupted significantly and only nematic phases with more modest phase ranges are observed. The triflate ions do not show any mesogenic behaviour at all, but consistently exhibit the lowest clearing points of all of this class of compound.[18]

By using a rigid 2,2'-bipyridine based mesogen the effect of co-ordination of the rhenium (I) fragment on transition temperatures has been further probed. For this series **(6)**, the first two members of the series show nematic phases only, between 275°C and 362°C (n = 4) and 224°C and 362°C (n = 8) , while the last member of the series shows a smectic C phase from 238°C to 267°C (n = 12) and then a nematic phase which clears at 296°C. These transition temperatures are also similar to those observed in the parent ligands. This is thought to be because the polarity of the rhenium bromide bond and the polarity of the cisoid α-diimine increase intermolecular interactions.[14]

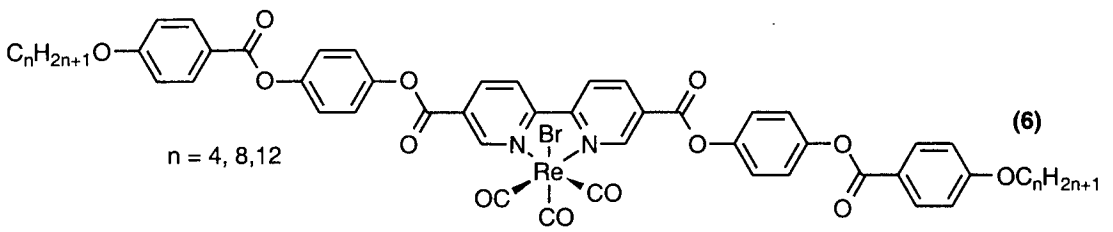

Fig. 2.15: Octahedral liquid crystal complexes of 2,2'-bipyridines with rhenium (I).

Fluoro substituted cyclometallated rhenium (I) complexes have also been prepared by Bruce *et al.*[19] It was hoped that fluorinated analogues of the parent ligand would enhance liquid crystalline behaviour of the rhenium (I) type complexes **(6)**. It has been reported that the tetra substituted complex (**7**) shows no liquid crystalline properties for n = 12 compared with a nematic phase between 131°C and 145°C for the unsubstituted rhenium (I) complex. In the octyloxy analogues, the tetra-fluorinated complex exhibits mesogenic behaviour with a nematic phase between 137°C and 160°C, compared with a nematic phase between 154°C and 176°C for the unfluorinated octyloxy complex.[20]

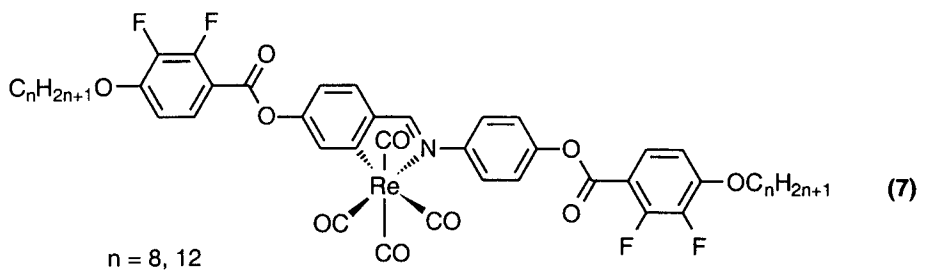

Fig. 2.16: Tetrafluoro-substituted rhenium (I) complexes.

Section 2.3.1.3: Group 8 calamitic metallomesogens.

Iron complexes dominate the literature of calamitic metallomesogens from this group. This is in part due to the extensive work carried out by investigating the utility of ferrocene as a

molecular building block for liquid crystalline materials. An example of a ruthenocene based material has also been reported.[21]

Section 2.3.1.3.1: Iron tricarbonyl complexes.

These complexes have been prepared and described by Ziminski and Malthête.[22] These materials lay the basis for a novel approach towards the development of ferroelectric liquid crystals, in which the chiral centre is rigidly constrained by its position in the conjugated backbone of the mesogenic core. Its close proximity to the iron tricarbonyl centre should combine the physical effects of these two components of the molecule, hopefully to give shorter switching times. The racemic butadiene complexes prepared by the authors showed nematic phases for the first series of compounds **(8)**, in the temperature region of 125-249°C, 125-220°C and 114-212°C for **(8i)**, **(8ii)** and **(8iii)** respectively. In the second series of compounds **(9)**, the phase behaviour of the series changed from a monotropic nematic phase or narrow ranged enantiotropic nematic phases to phases with increased thermodynamic stability and order, with the formation of enantiotropic nematic and smectic A phases and finally with the exclusive formation of smectic A phases with increasing chain length. The temperature range for these transitions is generally between 80-120°C.

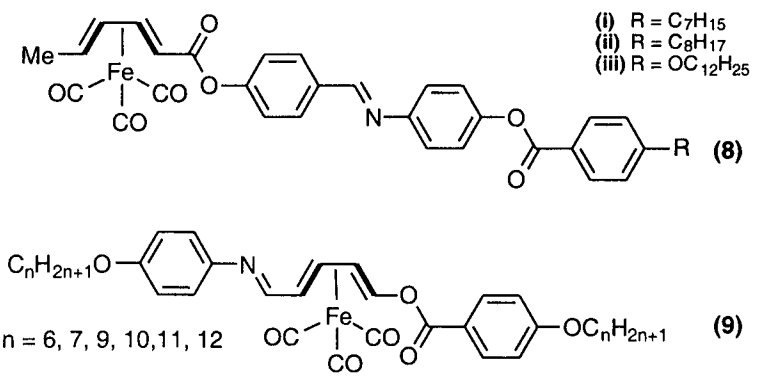

Fig. 2.17: Butadiene-irontricarbonyl metallomesogens.

Section 2.3.1.3.2: Ferrocene based complexes.

Ferrocene has been proven to be a useful building block in the development of novel mesogenic cores. The incorporation of ferrocene units into a mesogenic system is seen to be desirable due to their high thermal stability, high solubility in common organic solvents and because their molecular structure is clearly three dimensional in nature, considerable scope for the elaboration of the molecular structure is possible. The first example of ferrocene containing liquid crystals were a series of monosubstituted esters **(10)** prepared by Billard and

Malthête[23] which showed smectic phases.

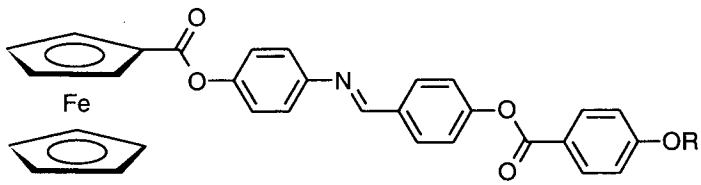

(10)

Fig. 2.18: First example of ferrocene containing liquid crystals.

This led to an intense and prolific study into the potential of the ferrocene moiety as a building block for liquid crystalline materials. A series of bis-(4-alkyloxy-4'-biphenyl)ferrocene 1, 1'-diesters (**11**), (alkyloxy chain lengths varying n = 4-11), were subsequently prepared. Two compounds in this series (n = 5, 6) showed monotropic smectic C phases in the region between 140°C and 129°C, while the last member of the series (n = 11) exhibited a monotropic smectic A phase. All compounds of this class are orange in colour.

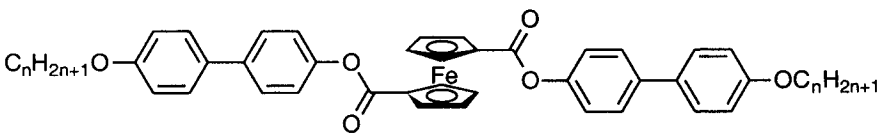

(11)

Fig. 2.19: Bis-(4-alkyloxy-4'-biphenyl)ferrocene 1, 1'-diesters.

The interruption of mesogenic behaviour in the middle of the series (n = 7-10) is accounted for by the inability of the isotropic state in each of these materials to supercool enough to form liquid crystal phases. The presence of only one benzoate group attached to the ferrocene unit does not induce liquid crystalline behaviour as this system has a smaller length to breadth ratio.[24]

Deschenaux and Marendaz[25] succeeded in producing a series of enantiotropic nematic phases with phase ranges of the order of 30-60°C using a 1,3 disubstituted ferrocene material (**12**). Significantly, the mesogenic core is built up from four phenyl rings in addition to the ferrocene unit to compensate for the bulky ferrocene unit. A series of 1, 1' disubstituted ferrocene derivatives (**13**) which are geometrical isomers of series (**12**) was also prepared. Only the first member of this series formed a mesophase, which was monotropic. The 1, 3 ferrocene derivatives form enantiotropic phases due to the extended linearity and planarity of the mesogenic core, while the unsubstituted cyclopentadienyl group helps to disrupt intermolecular forces, contributing to the formation of the nematic phase.

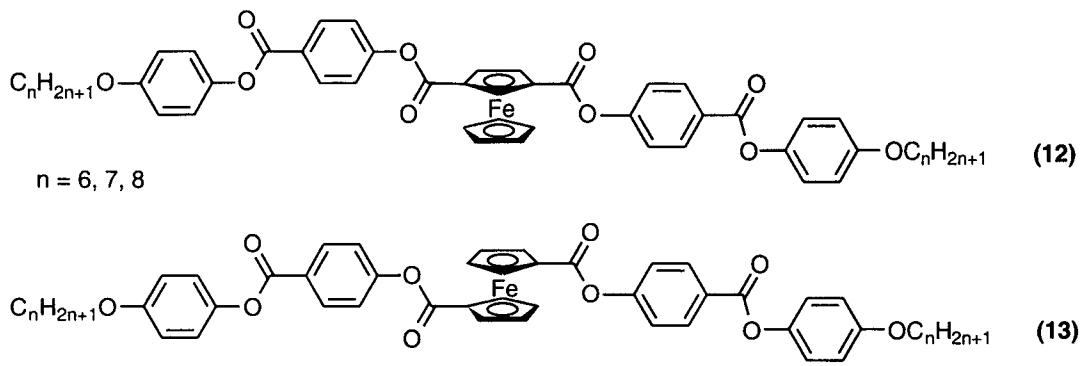

Fig. 2.20: 1, 3 and 1, 1' disubstituted ferrocenes.

The linearity of the 1, 1' disubstituted system while bridged by the ferrocenyl core, is nonetheless discontinuous, leading to a marked reduction in the ability of this isomer to self organise into a mesophase.

A further study of 1, 1' disubstituted ferrocenes by Deschenaux focused on the orientation of the ester group linkages in the mesogenic core of the molecules. This demonstrated that mesomeric and rotational effects arising from the connectivity of the ester linkages, in the 1, 1' ferrocenes shown in figure 2.21 greatly influences their ability to form enantiotropic mesophases. The ferrocene derivatives type **(14)** shown in figure 2.21 exhibit monotropic nematic phases for n = 1-6, while the second class of isomer **(15)** forms monotropic nematic phases for n = 1-6, with monotropic smectic A phases for n = 7, 8 and finally enantiotropic smectic A phases were observed for the remainder of the compounds in this series.[26]

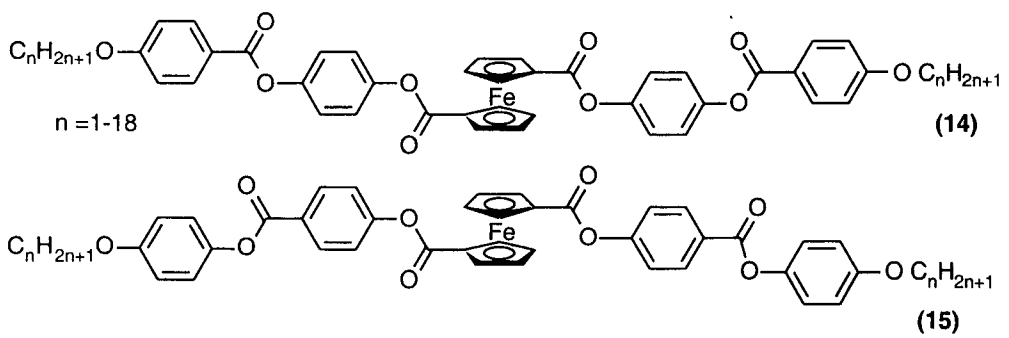

Fig. 2.21: 1, 1' disubstituted ferrocenes.

The 1, 1'-bis-(cholesteryloxycarbonyl)ferrocene derivative **(16)** shown in figure 2.22 exhibits mesomorphic behaviour, identified as a crystal smectic B phase between 247°C and 268°C. The formation of a phase with a high degree of positional order is attributed to the cholesteryl moieties which are non polar and have a propensity to form crystal smectic B phases.[27]

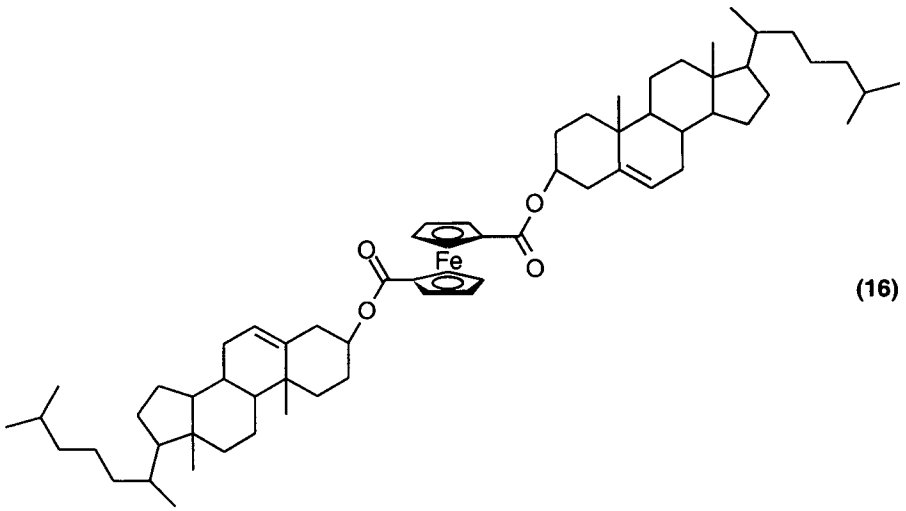

(16)

Fig. 2.22: 1, 1'-bis-(cholesteryloxycarbonyl)ferrocene derivative.

Tri-substitution of ferrocene has also been investigated as a means to develop novel mesogenic materials.[28] Three series of compounds **(17)**, **(18)**, **(19)** were prepared. In series **(17)**, the molecular structure of the material is based on three phenyl esters spanning the backbone of the mesogenic core. The broad width of the molecule (due to the pendant cyclopentadienyl group bonded through the iron metal centre) compared to its length results in these compounds melting directly from the crystal phase to the isotropic liquid. These transitions occur between 153°C and 161°C; only the last three members of the series (n = 12, 14, 16) showed mesomorphic behaviour - due to the extended linearity of these species - exhibiting monotropic smectic phases in each case. The second series of compounds **(18)** have increased linearity in that the ferrocene core is now tri-substituted and there are now three components with the ability to enhance intermolecular interactions. In this case the minimum requirement of three aromatic rings (and the Cp ring) has been fulfilled by distributing a single aromatic ring to each of the three substituents on the cyclopentadienyl rings. This also leads to monotropic mesogenic behaviour. The compounds in this series melt to the isotropic liquid from the crystal phase between 96°C and 102°C. On cooling, the first two members of the series (n = 12, 14) gave monotropic smectic A and smectic C phases, while the latter two members of the series simply gave monotropic smectic C phases. The presence of the third aromatic substituent has lead to the formation of mesophases in systems of more modest linearity (*i.e.* substituents with only one phenyl ester each).

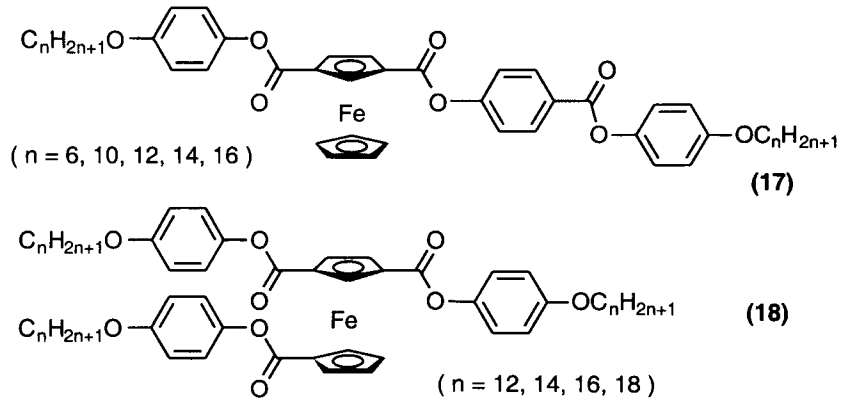

Fig. 2.23: Polysubstituted ferrocene derivatives.

The third type of compound examined in this study **(19)** has a 1,1', 3-tri-substituted ferrocene core with two phenyl groups and two ester functional groups on each substituent. This gives rigid linear structures extending from three points on the ferrocene core. The increased length to breadth ratio due to the extended aromatic conjugated system has promoted the linearity and rigidity of the system leading to the formation of enantiotropic mesophases for this class material. A smectic C phase forms at 167°C which then undergoes a transition to a smectic A phase at 244°C and finally clears to the isotropic liquid at 260°C. The presence of the third extended linear system has allowed stronger intermolecular interactions and greater ordering between the molecules.

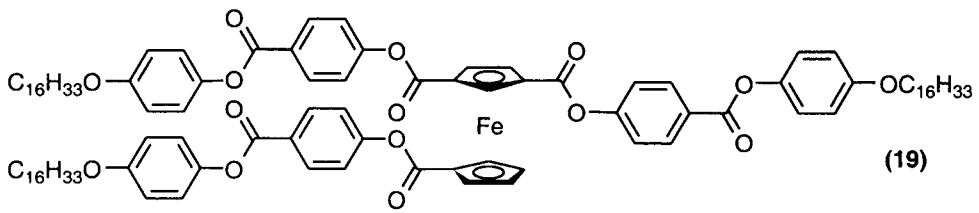

Fig. 2.24: Polysubstituted ferrocene derivatives.

Section 2.3.1.4: Group 9 calamitic metallomesogens.

It is not certain whether cobalt forms calamitic liquid crystals: 2, 2'-bipyridine based systems have been prepared as a means to achieve this goal, however, it has not been conclusively determined whether these compounds are mesomorphic.[29] Rhodium and iridium metallomesogens have been prepared from linear stilbazole derivatives and in the case of rhodium (III) from acetylide complexes.

Section 2.3.1.4.1: Rhodium (III) complexes.

A recent development has been the preparation of metallomesogens with an octahedral

geometry (**20**) by Rourke, Bruce and Marder in 1995, using a sufficiently large liquid crystalline ligand to overcome the perturbation in shape brought about by the metal centre with an octahedral geometry; smectic phases and nematic phases are observed as detailed below. This material is an example of a metallomesogen with a metal-hydride bond.[30]

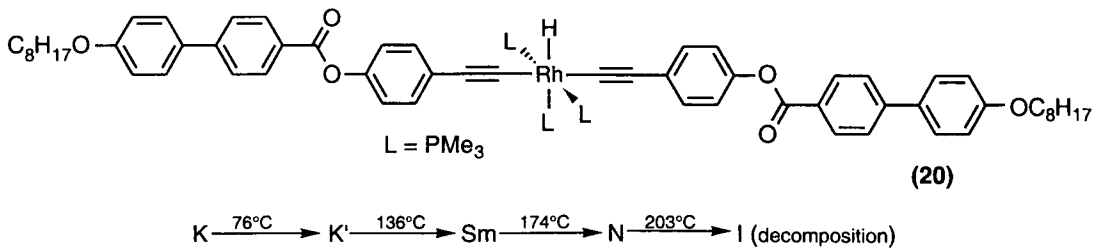

Fig. 2.25: Octahedral rhodium (III) metallomesogen.

Section 2.3.1.4.2: Iridium (I) and rhodium (I) stilbazole complexes.

The series of compounds prepared of type (**21**) show monotropic phases for materials with hexyloxy or heptyloxy terminal chains. The octyloxy member of the series (**21b**) shows an enantiotropic crystal to nematic transition at 68°C, clearing at 76°C and a monotropic nematic to smectic A transition on cooling at 66°C. The compounds in the series with longer alkyloxy terminal chains show enantiotropic smectic A phases between 64°C and 104°C.[10] The octyloxy rhodium complex shows a crystal to nematic transition at 79°C and a clearing point at 87°C, with a monotropic smectic A phase at 77°C.[31]

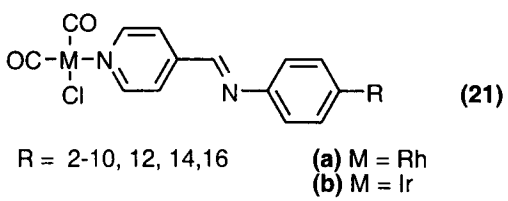

Fig. 2.26: Iridium (I) and rhodium (I) metallomesogens.

Section 2.3.1.5: Group 10 calamitic metallomesogens.

Metallomesogenic complexes based on palladium (II) and platinum (II) constitute a substantial number of compounds to the field due to their square planar geometry. They are also capable of bonding to various atoms from oxygen to carbon and they are able to undergo cyclometallation reactions, forming planar metallocycles, amenable to further structural elaboration. Materials of this type are outlined below.

Section 2.3.1.5.1: Palladium (II) and platinum (II) co-ordination complexes.

Three structural features are common to many examples of calamitic metallomesogens: they

contain a metal with a d^8-d^{10} electron configuration, they possess ligands which have the potential to co-ordinate to the metal giving a complex with a highly anisotropic shape and the ligands are bonded *trans* disposed to each other, through the metal. Co-ordination compounds of cyanobiphenyls with palladium and platinum are a good example of how such simple mesogenic systems can be assembled.

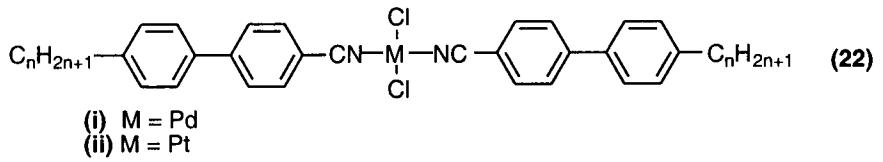

Fig. 2.27: Palladium (II) cyanobiphenyl complexes.

The parent ligands show nematic phases in the range 30-90°C for chain lengths $5 < n < 9$ and smectic A phases for chain lengths $8 < n < 12$. The palladium complexes **(22i)** show mesogenic behaviour in the region 170-200°C, with the appearance of smectic C phases, not seen in the original ligand.

By careful choice of ligands subtle modifications in the molecular structure of the complexes can be made, altering the phase behaviour observed. Platinum (II) complexes of alkyloxystilbazoles have little tendency to be mesomorphic, (long chains > C_9H_{19}, are required, with phases only seen above 200°C). The substitution of one of the alkyloxystilbazoles ligands for an alkene with a long alkyloxy chain gives the very versatile system **(23)** with mesogenic behaviour at lower temperatures.[32,33]

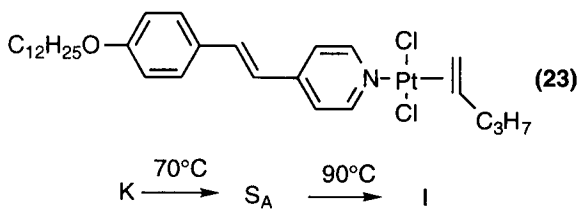

Fig. 2.28: Platinum (II) alkene mesogenic complexes.

Examples of an η^1 octa-alkyloxy substituted palladium (II) complexes **(24)** have been prepared showing monotropic calamitic smectic A phases, the transition temperatures of which are comparable to the crystal melting temperatures of the simple ligands. The complexes were prepared by stirring the benzylideneaniline ligands in the non polar solvent hexane to give simple co-ordination to the palladium (II) centre by displacing benzonitrile

from palladium dichloride bis benzonitrile. The decyloxy ligand melts at 80°C while its palladium complex shows a monotropic smectic A on cooling from 64°C to 55°C where it undergoes a transition to the crystal phase. A noteworthy point about this complex is that no metallocycle is formed allowing the aromatic groups a greater degree of freedom to move. The chlorine atoms are out of the plane of the aromatic core, hence a disordered and unstable liquid crystal phase is observed.[34]

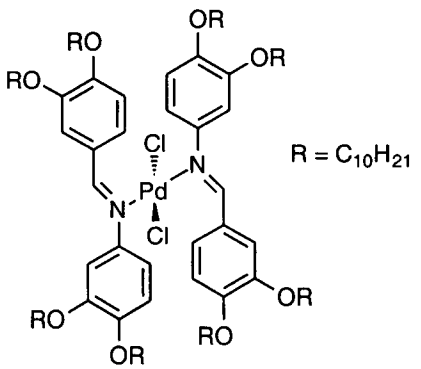

(24)

Fig. 2.29: η^1 octa-alkyloxy substituted palladium (II) complexes.

Section 2.3.1.5.2.1: Group 10 metallocycle based complexes.

The modification of the highly anisotropic shape of calamitic mesogens by cyclometallation and formation of dimeric bridged species is a convenient method of preparation of *ortho*-palladated metallomesogens (**25**); early studies of the role played by the bridging groups demonstrated the need to preserve planar geometries in a given complex to obtain metallomesogens.

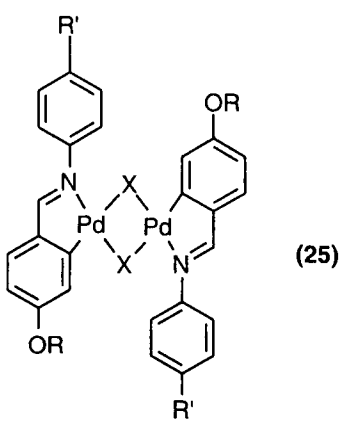

(25)

Fig. 2.30: Dimeric *ortho*-palladated Schiff's base.

In the late 1980s cyclopalladation of Schiff's bases with palladium acetate by Barberá yielded a dimeric *ortho*-palladated complex bridged by acetato species (X, figure 2.30), with an open

book conformation, in which each palladium atom occupies a square plane that is forced to a very closed dihedral angle resulting in a monotropic smectic A phase.[35]

$$R, R' = OC_{10}H_{21} : C \xrightarrow{102\ ^\circ C} S_C \xrightarrow{111\ ^\circ C} I$$

Phase behaviour of ligand.

$$R, R' = OC_{10}H_{21} : C \xrightarrow{170^\circ C} I \xrightarrow{160\ ^\circ C} S_A$$

Phase behaviour of Pd (II) acetato complex.

In the case of the acetato complexes, only the decyloxy member of the series is mesogenic, showing a monotropic smectic A phase, this demonstrates that the non-planar open book structure reduces the packing efficiency.

In contrast, the thiocyanato (**28**) and halide bridged analogues of these compounds show enantiotropic mesogenic behaviour as they each favour a planar bonding mode to bridge the two metal centres; in the case of the thiocyanato complex this is a strict planar geometry, in the halide bridged complexes the two metal centres are also co-planar. In the planar bridged molecules, the distance between the palladium centres and hence between the alkyl chains increases in the order Cl < Br < SCN, therefore minimising interactions in the case of the thiocyanato bridging ligand. Geometrical and linkage isomerism is possible within this series of complexes; the acetato ligands should show *cis* (**27**) and *trans* (**26**) isomers, though evidence from NMR suggests the *trans* isomer is the major isomer present.[36]

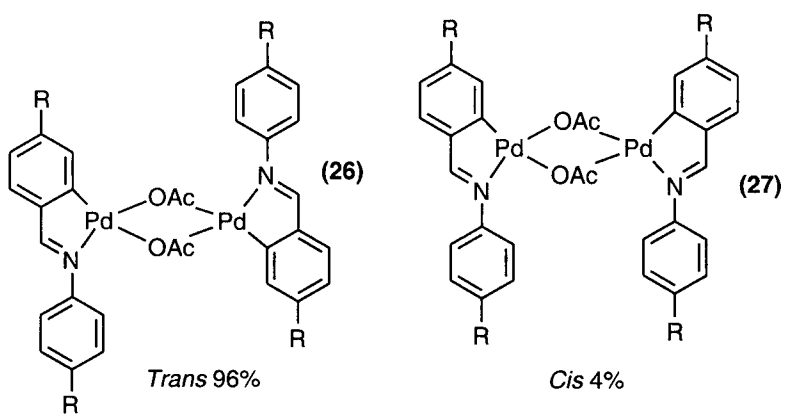

Fig. 2.31: *Cis* and *trans* isomerism in dimeric acetato complexes.

The thiocyanato ligand can produce linkage isomers also but it is thought that only the isomer (**28**) represented below in figure 2.32 is seen in substantial quantities.

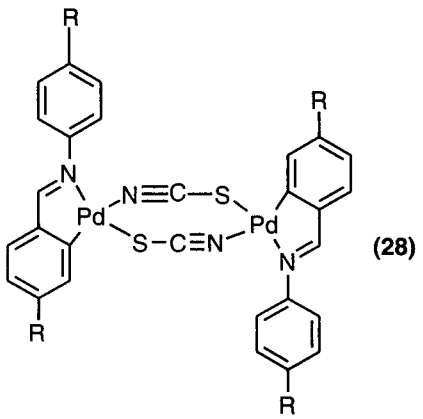

Fig. 2.32: Favoured isomer in thiocyanato bridged complexes.

Section 2.3.1.5.2.2: Long chain carboxylato bridged metallomesogens.

A further contribution by the Espinet group in 1990 was the preparation of carboxylato-bridged complexes which exhibit liquid crystalline behaviour, showing various phases, depending on the length of the carboxylato (**29**) chains present. A homologous series of such compounds has been synthesised by Espinet and Perez, the general structure of the compounds is shown in figure 2.33; the series consists of members n = 0-11,13,15,17. The complexes are based on an azine ligand with a substantially larger length to breadth ratio than the example cited in the above acetato complexes (**25**).

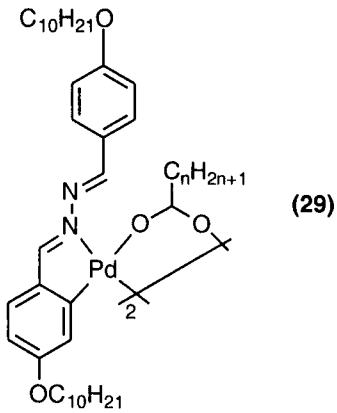

Fig. 2.33: Carboxylato bridged azine metallomesogens.

This improves the ability of the carboxylato complexes to become ordered in the fluid phase. The shortest and longest members of the series tend to give rise to the more ordered phases, while carboxylates of intermediate chain length tend to exhibit more disordered phases. This is due to the growth of the alkyl chain from the carboxylato bridge of the complex, making molecular ordering difficult: this counters the effect of the advantageous high length to breadth ratio of the molecules. This disruption continues until the branches are long enough

to orient themselves along the molecular axis, when the disruptive effect is lost. This series of materials show enantiotropic and monotropic nematic and smectic C phases, generally in the region of 90-150° C.[37]

Section 2.3.1.5.2.3: Mixed bridged dimeric metallomesogens.

In 1998 Espinet *et al.* reported a series of dinuclear cyclopalladated derivatives with mixed bridging ligands **(32)**, **(33)**. This work has enabled the study of isomerically pure *cis* bridged isomers of chloro-thiolate **(33)** and acetato-thiolate **(32)** complexes. This is in stark contrast to the exclusively *trans* isomers obtained for chloro bridged species and the mixture of *cis* (4%) **(27)** and *trans* (96%) **(26)** obtained for the acetato bridged isomers. The cycloplatinated analogues are also reported to be exclusively complexes with a *cis* orientation. The cyclopalladated chloro-thiolate isomers show smectic C and smectic A phases at temperatures generally between 100°C and 200°C, with some decomposition accompanying the transition to the clearing point.

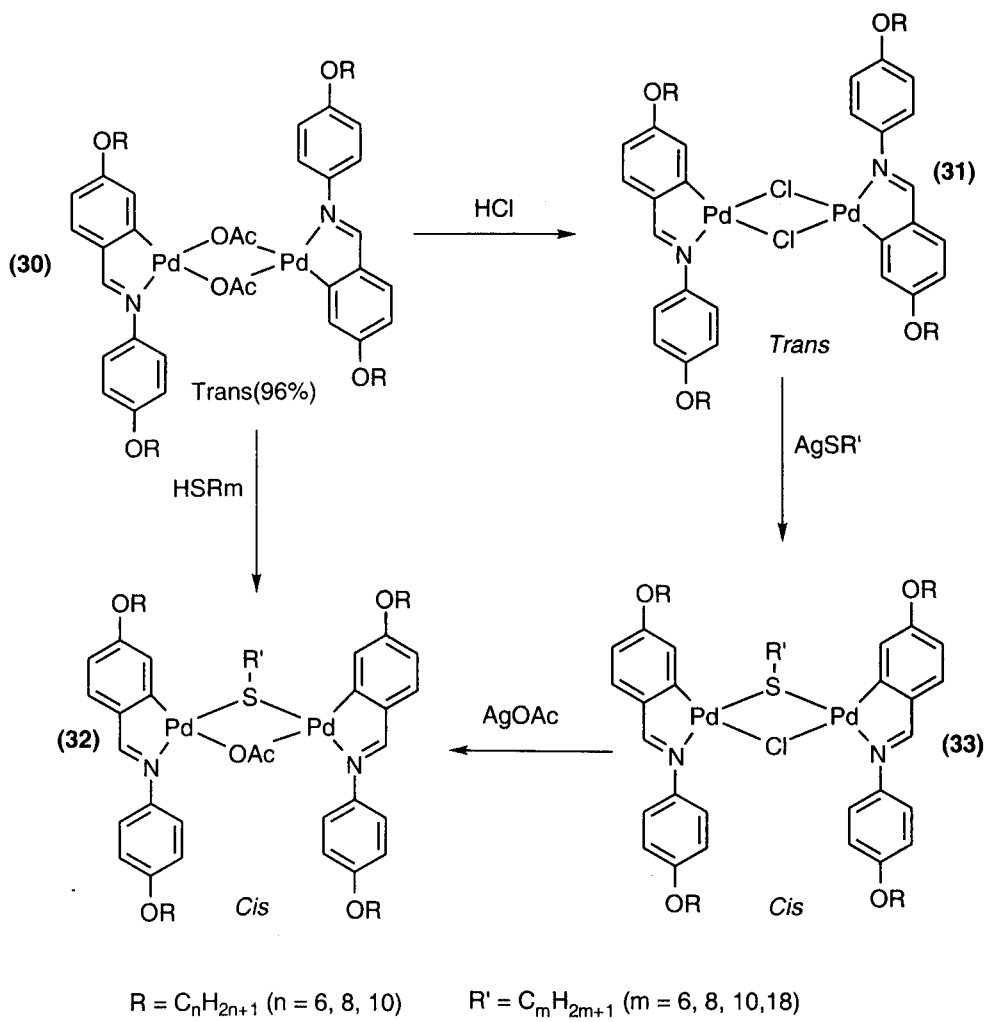

Fig. 2.34: Dinuclear chloro-thiolato and acetato-thiolato bridged complexes.

The acetato-thiolate **(32)** complexes show smectic A phases in all complexes and nematic phases for complexes with hexyloxy terminal chains (n = 6) on the Schiff's bases ligands. The transition temperatures that bring about formation of mesophases for this series are noticeably lower than for those of the chloro-thiolato series. Indeed, for the complex with the longest chain lengths (n = 10, m = 18), a smectic A phase is formed between 67°C and 137°C. These lower transition temperatures and formation of the less ordered nematic phases arises from less intermolecular interactions in the acetato-thiolato. This is because of the folded structure due to the acetato bridging ligand versus the planar structure arising from the chloro bridging ligand which allows more efficient packing of the molecules in the solid state and greater ordering of the mesophases.[36]

Section 2.3.1.5.2.4: *Ortho*-palladated azobenzene complexes.

In 1995 the structure of compound **(34)** was reported using both single crystal and low angle variable temperature X-ray diffraction to compare the structure of the material in the crystal and liquid crystal phases. It was observed that the chloro complex exhibited a nematic phase at 210°C, which gradually cleared on further heating with decomposition taking place above 235°C. The single crystal X-ray study showed that the crystals were monoclinic and that cyclometallation confers a roughly planar geometry spanning the breadth of the mesogenic core; slight twisting of the uncomplexed phenyl rings occurs due to the neighbouring chlorine atoms.

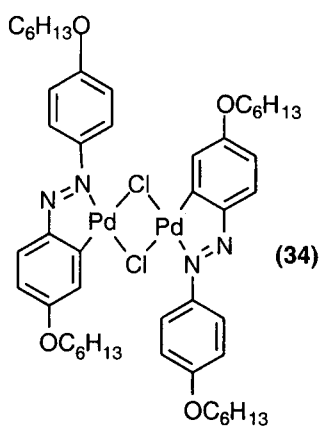

(34)

Fig. 2.35: Chloro bridged cyclopalladated azobenzene dimer.

A non bonded Pd-Pd interaction occurs within the crystal lattice which causes the centro-symmetrically related molecules to pair in the crystal structure, this causes a zig-zag pattern within the lattice. In the variable temperature X-ray study carried out, a nematic phase is

observed at 210°C, but at 220°C a mesophase is observed which is more characteristic of an ordered smectic phase; this may be a crystal E phase. The observed behaviour may be coupled to a dissociation of molecular pairs formed through the non-bonded Pd-Pd interactions discussed earlier, which would modify the short range positional order. [38] This is interesting as it may be evidence of metal-metal non-bonded interactions aiding the formation of a liquid crystal phase.

Section 2.3.1.5.2.5: Perturbing symmetry of metallomesogens.

The use of carboxylato anions as bridging ligands with Schiff's bases is restrictive in that it produces complexes which tend only to exhibit smectic A phase behaviour; it is thought that highly efficient packing of the molecules occurs, as these phases are generally seen in the region 130-200°C where decomposition can occur during long periods of study. To address this problem metallomesogens in which the molecular structure is less anisotropic and exhibit the more disordered nematic phase at lower temperatures have been prepared by Espinet. [39]

R	Transition	T[°C]
H	C-I	104.7
OC_2H_5	C+C'-C+N	99.1
	C+N-N	108.9
	N-I	117.8
OC_6H_{13}	C-S_A	84
	S_A-N	118.5
	N-I	124.8
$OC_{10}H_{21}$	C-S_A	74.3
	S_A-I	128

Table 2.1: Thermal behaviour of acetylacetonate complexes.

He achieved this by co-ordinating pentane-2,4-dione derivatives to the metallomesogenic core, producing complexes with single metal centres. These monomeric complexes (**35**), prepared in 1991, exhibited mesogenic behaviour in the range of 75-128°C; complexes where larger chain length showed smectic phases whilst shorter chains displayed nematic phases. This is typical of the behaviour seen when the terminal chain of a mesogen is extended.

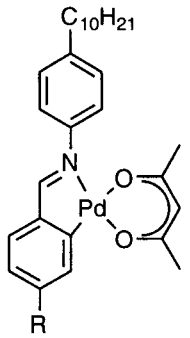

(35)

Fig. 2.36: Monomeric palladium (II) acetylacetonate metallomesogens.

These compounds can be taken repeatedly to the isotropic phase without decomposition, making them attractive for further study and processing.[39]

Section 2.3.1.5.2.6: Lateral-lateral fused mesogens.

Co-ordination of salicylidene with azobenzene based mesogens have been used to produce d^8 palladium **(36)** metallomesogens, the metal acting as a spacer between the two elongated rod-like moieties. The spacer distance imposes constraints on the packing ability of these types of complexes, by causing the aliphatic chains to fold and pack in a distorted fashion in the complex **(36)**.[40]

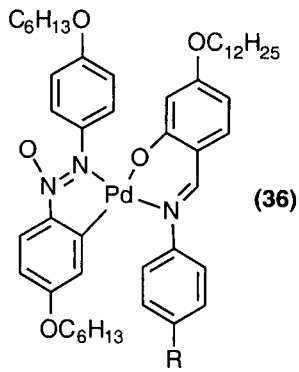

(36)

Fig. 2.37: *Trans* isomer of lateral-lateral fused complexes.

Ghedini prepared these lateral-lateral fused mesogenic complexes as a mixture of *cis* and *trans* isomers in which monotropic nematic and smectic A phases were generally observed in odd members of the series (n = 3-8). The even members showed enantiotropic nematic (n = 4) and smectic phases (n = 6, 8). These mesophases were observed in the range 120-144°C. X-ray data for the complexes suggest the *cis* compounds have a molecular length of 36 Å versus 35 Å for the *trans* isomers, which is roughly constant for the whole series of compounds, suggesting intramolecular packing and distortion of the chain.

Section 2.3.1.5.2.7: Cyclopalladated pyrimidine complexes.

Neumann *et al.*[41] have prepared novel macrocyclic metallomesogens. These materials consist of two distinct components which are joined by spacer groups: a 2-phenylpyrimidine unit (which can undergo cyclopalladation) and a biphenyl unit which encourages a rigid planar structure in the ligand. The smaller ligand **(i)**, melts at 172°C and shows a monotropic nematic phase, clearing at 142°C. The larger ligand **(ii)**, with an extra methylene unit shows simply a melting transition to the isotropic phase at 87°C. The additional flexibility in the spacer group has disrupted the rigidity of the macrocycle rendering it incapable of self organising in the fluid phase.

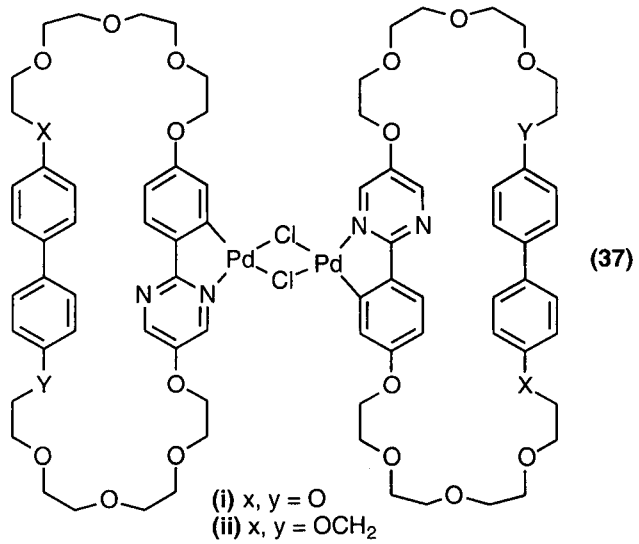

(37)

Fig. 2.38: Binuclear cyclopalladated cyclophanes.

Cyclopalladation leads to the formation of a dimeric chloro-bridged structure which has a rigid metallomesogenic core **(37)**, while the biphenyl units enhance this order and the molecules have a highly anisotropic shape, which gives rise to stabilisation of mesophases. The cyclopalladated complexes both exhibit liquid crystalline behaviour. The complex of the more rigid ligand **(37i)** melts at 168°C to form a smectic A phase and then undergoes a transition to the nematic phase at 208°C before finally clearing at 226°C with some decomposition. The complex of the more flexible macrocycle **(37ii)** melts into the isotropic phase at 118°C but shows a monotropic nematic phase which clears at 91°C. Ghedini *et al.*[42] prepared mononuclear metallomesogens based on a pyrimidine ligand **(38)**. The material in figure 2.39 melts at 83°C and shows a monotropic smectic A phase between 40°C and 68°C.

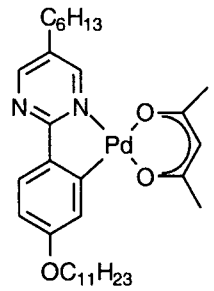

(38)

Fig. 2.39: Cyclopalladated pyrimidine complexes.

The bipyridine complex, shown below (**39**) exhibits a enantiotropic nematic phase between 146°C and 158°C.

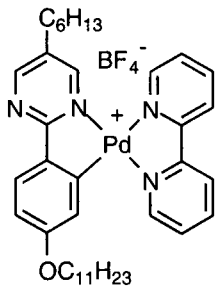

(39)

Fig. 2.40: Cyclopalladated pyrimidine bipyridine complexes.

Bipyridine ligands with long terminal alkyloxy chains have given rise to liquid crystal behaviour by co-ordination to a cyclometallated species yielding (**40**) shown in figure 2.41. The presence of an alkyl sulfate enhances the stability of these materials relative to the tetrafluoroborate salt.

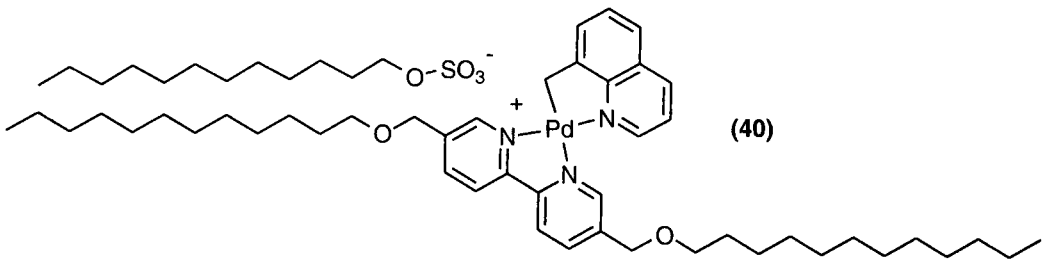

(40)

Fig. 2.41: Palladium bipyridine alkylsulfate metallomesogen.

Two transitions are observed using DSC which have been assigned as transitions from the crystal phase to a columnar phase at 131°C and from this phase to a smectic A phase at 168°C. This unusual combination of both calamitic and columnar phases has been confirmed by X-ray diffraction. The X-ray study shows the columnar phase to comprise of an assembly of aromatic cores stacked in columns which give rise to layered structures.[43] The transition

from the crystal to the columnar phase causes a small increase in the *a* lattice period, which reflects the loss of positional order within the crystal lattice.

Section 2.3.1.5.2.8: Palladium (II) cyclopentadienyl complexes.

In 1996 Ghedini reported the co-ordination of cyclopentadiene rings to an azobenezene cyclopalladated species **(42)**, yielding compounds with bulky lateral substituents which favour lower melting and clearing points than analogous acetylacetonate complexes; this is thought to be as result of the inability of the half sandwich complexes to pack as efficiently as the acetylacetonate complexes as crystals and in the mesophases.[44]

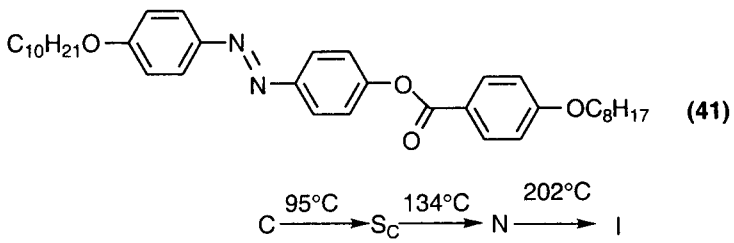

Fig. 2.42: Phase behaviour of unsymmetrical ligand.

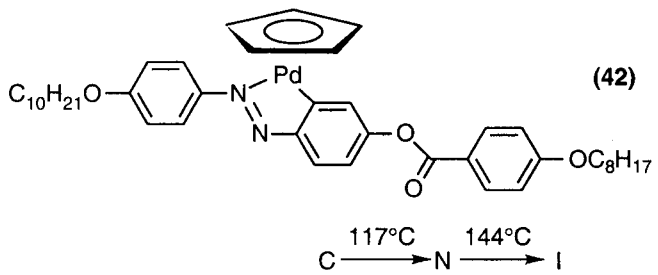

Fig. 2.43: Phase behaviour of half sandwich palladium (II) metallomesogen.

A complicating factor in the evaluation of the mesomorphic behaviour of these materials **(42)** is that the cyclopalladation reaction for this particular system is not regiospecific to one phenyl ring, ultimately leading to a mixture of two isomeric half sandwich palladium complexes. As a consequence of this, Ghedini *et al.*[45] prepared analogous symmetrical compounds for both palladium and platinum, with more conclusive results on the mesogenic behaviour of these materials. The palladium (II) analogue of the system **(43a)** shows a nematic phase between 143°C and 226°C, identified by a marbled texture observed on heating together with a schlieren texture observed on cooling. The platinum (II) analogue **(43b)** shows transitions at temperatures about 20°C higher than the palladium (II) analogue due to the increased polarisability and increased molecular mass of the platinum (II) metal centre.

This nematic phase has a range from 160°-250°C with decomposition observed at the clearing point. The high tendency to form nematic phases results from the large lateral palladium cyclopentadienyl fragment in the centre of the molecule which disrupts lateral intermolecular interactions.

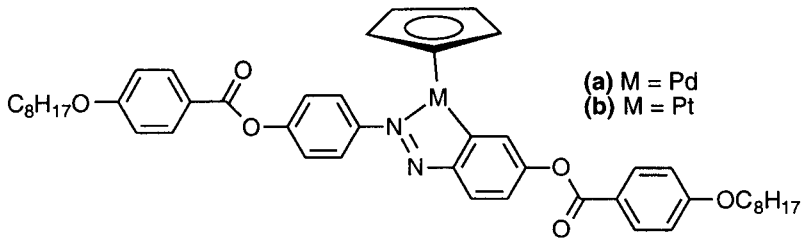

(43)

Fig. 2.44: Half sandwich metallomesogens.

Section 2.3.1.5.2.9: Chiral monomeric complexes.

Espinet has reported the monomeric metallomesogen **(44)** which exhibits a monotropic chiral smectic C phase in the temperature at 111°C. This compound was obtained by co-ordination of a β-diketonate derivative to the metallomesogenic core. The chiral centre is present on the terminal alkyloxy chain and gives rise to optical switching on a millisecond time scale.[46]

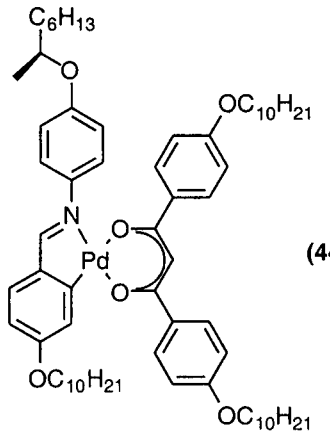

(44)

Fig. 2.45: Phenyl alkyloxy substituted β-diketonate with chiral terminal chain.

Section 2.3.1.5.2.10: Chiral palladium (II) amino acid based complexes.

Another approach toward the preparation of chiral metallomesogens was the preparation of a series of l-amino acid chelated cyclopalladated complexes **(45)**. All of the complexes prepared in this investigation produced smectic phases, due to the long alkyloxy chains in the cyclopalladated ligand. For the series of compounds shown in figure 2.46, the l-valine, the l-leucine and the l-phenylalanine complex showed the smectic A phase whereas the alanine complex showed the smectic C phase.

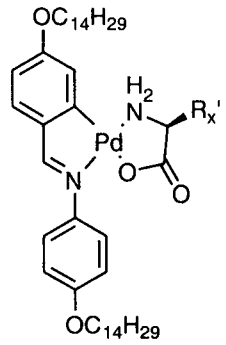

$R_1' = CH_3$
$R_2' = CH_2Ph$
$R_3' = CH(CH_3)_2$
$R_4' = CH_2CH(CH_3)_2$

(45)

Fig. 2.46: Amino acid chelated cyclopalladated metallomesogens.

It is also worth noting that this alanine complex has the second largest mesogenic range in this series of compounds (81°C-174°C), showing mesophase behaviour at higher temperatures than the l-leucine (74°C-120°C) or l-valine (101°C-136°C) complexes, suggesting that the steric bulk of these analogues is reducing intermolecular interactions. The steric bulk of these analogues only succeed in lowering the melting point of the l-leucine analogue and the l-phenylalanine analogue (64°C-212°C). The low melting point of the l-phenylalanine complex can be explained by disruption of the packing crystal phase while the higher clearing point is due an increase in intermolecular interactions arising from the phenyl ring, stabilising the mesophase at higher temperatures. Analogous palladium (II) alanine complexes using azobenzene and azine ligands have also been prepared which all show smectic C phases. Therefore it may be concluded that the co-ordination of alanine to palladocycles of this kind gives rise to intermolecular interactions which favour the formation of smectic C phases.[47]

Section 2.3.1.5.2.11: Bridged dimeric chiral palladium (II) complexes.

Another novel class of organometallic liquid crystals **(47)** displaying chiral phases was reported by Espinet in 1993.[48] These complexes were prepared as outlined in figure 2.47, the chloro-substituted carboxylato-bridged dimer was obtained in a *cis/trans* mixture and showed double melting behaviour. This complex exhibits mesogenic behaviour despite the fact that the dimeric species possesses the open book structure. It is thought that the occurrence of this behaviour is a direct result of presence of the dipole in the C-Cl bond, improving intermolecular interactions. The final product is bridged by carboxylato and thiolato groups exclusively in a *cis* arrangement.

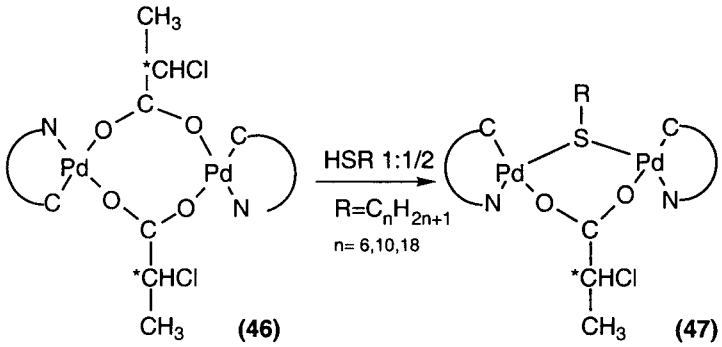

Cis and Trans isomers

Transition	T[° C]
K-S_A	152
S_A-I	186
I-S_A'	203
S_A'-I'	224

Cis isomer only

Transition	T[°C]
K-S_A	92
S_A-Ch	128
Ch-I	132

Fig. 2.47: Bridged dimeric chiral palladium (II) complexes.

Section 2.3.1.5.2.12: Bridged dimeric chiral platinum (II) complexes.

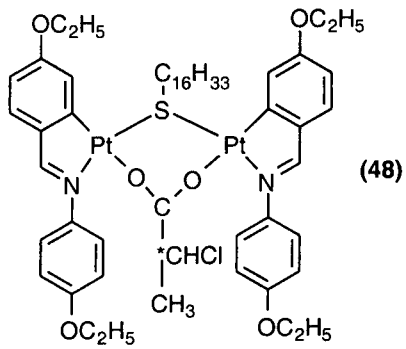

Fig. 2.48: Chiral platinum metallomesogen exhibiting an optical storage effect.

The chiral platinum complex (**48**) has a cholesteric phase between 120°C and 133°C. This cholesteric phase can be stored by cooling to a glassy state, which sustains order in the material for at least a year. The material has been shown to exhibit an optical storage effect arising from an alignment effect on the director caused by the exposure of the chiral nematic phase to an argon laser. A notable advantage of this compound is the intrinsic absorption of visible light in the blue-green wavelength range by the coloured platinum compound, precluding the need for a dye additive, which is required for other calamitic materials showing this effect.[49]

Section 2.3.1.5.2.13: Properties of metallomesogens with chiral terminal chains.

Baena *et al.* conducted a study in 1994 of how ferroelectric behaviour of a chiral smectic C phase is influenced by varying the structure of the metallomesogen as outlined below:

(i) length of the achiral terminal chain, (ii) position of the chiral tail and (iii) the number of chiral tails per molecule. He conclude the following:

1) *ortho*-palladation of the ligands facilitated the formation of mesogenic materials.

2) The broadest enantiotropic chiral smectic C phases are obtained when the chiral chain is attached to the *ortho*-palladated ring and the other phenyl group present has a terminal chain length of 8 carbons.

3) The highest polarisation values (P_S) are obtained when the chiral chain is locked by *ortho*-palladation of the aldehydic ring, this facilitates better coupling of the dipoles associated with the chiral chain.

4) The molecules with 4 chiral chains present have dramatically decreased mesophase stability, but low melting points (90° C).[46]

Section 2.3.1.6: Group 11 calamitic metallomesogens.

Examples of metallomesogens from this group are known for paramagnetic copper (II) complexes[50-52] and the diamagnetic copper (I) metal centre.[53] A rich variety of gold (I) complexes have also been prepared by bonding to stilbazole,[54] acetylides[55] and through the formation of gold (I) carbene[56] complexes. The ability of silver to form linear dimers with stilbazoles has also led to the development of ionic metallomesogens which exhibit nematic phases.[57]

Section 2.3.1.6.1: Copper (II) complexes

Liquid crystalline N-salicylideneaniline complexes have been prepared using copper (II) as a metal centre (**49**).

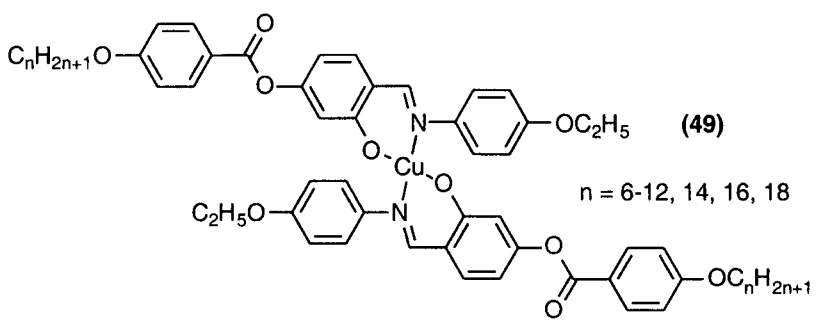

Fig. 2.49: Copper (II) complexes of N-salicylideneaniline derivatives.

These square planar complexes show smectic C and nematic phases. The free ligand in this instance exhibits only nematic phases (except for when n = 18, where a smectic C phase is

also observed). The co-ordination of two of ligand molecules gives rise to a system of higher symmetry and planarity, enhancing the formation of smectic C phases exhibited in the latter half of the series (n = 11, 12, 14, 16, 18).[50]

5-substituted tropolones have been co-ordinated to copper (II) forming a new class of metallomesogens (**50**) which exhibit enantiotropic and monotropic mesophase behaviour. The rigid, linear, square planar bonded systems favour the formation of enantiotropic tilted smectic C phases (n =12, 14) and also the more ordered smectic B (n = 10, 12, 14 16,) and crystal B (n = 12, 14) phase.

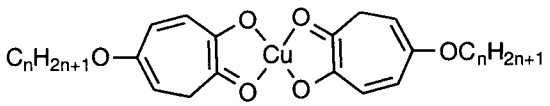

(50)

n = 8, 10, 12, 14, 15, 16

Fig. 2.50: Mesogenic copper (II) tropolone complexes.

Increasing chain length to a hexadecyloxy terminal chain leads to the loss of the smectic C phase observed in earlier analogues and instead shows a monotropic smectic B phase. A plastic crystal phase was also observed to which no definite assignment has been made although a G or J phase has been suggested. Transition temperatures for the series are quite high between 230° and 250°C, reflecting the high intermolecular interactions between the molecules in both the crystal and liquid crystal phases.[52] This work has in part been repeated and published by Vill *et al.*[51] with more extensive thermal analysis data presented stating that in two cases (n = 12,16) the smectic B phases and smectic G/J phase formed is actually enantiotropic and not monotropic as claimed by Chipperfield *et al.* Vill *et al.* have carried out X-ray analysis studies which indicate the packing of the smectic B phase at 220°C, with the formation of an interdigitated layered structure. At lower temperatures (180°C) the formation of a tilted hexatic phase is indicated by the shortening of the smectic layer spacing.[51]

Section 2.3.1.6.2: Chiral paramagnetic complexes.

Chiral paramagnetic metallomesogens have been prepared by Marcos *et al.*[58] These materials (**51**) exhibit chiral smectic C* and smectic A phases, with a similar pattern of mesomorphism shown in the parent ligand but at lower temperatures. Melting to the smectic C* phase occurs at 52°C and the transition to the smectic A phase occurs at 92°C with the isotropic liquid

forming at 114°C. The phase behaviour of the complexes is shown in figure 2.51; complex formation leads to broader smectic A phases at elevated temperatures while the smectic C* phases, also at high temperatures have diminished phase ranges. This reduction in smectic C range (of about 30°C in both cases) and increase in smectic A phase ranges may be linked to broader planarity of the complexes, compared with the free ligand, favouring lateral intermolecular interactions giving rise to smectic A phases rather than the helical type arrangement of the smectic C* phase. The co-ordination of the metals to this ligand combines the chiral mesomorphic behaviour of the ligand with the paramagnetic properties of the chosen metal. This allows an application where a magnetic field may be used to align the materials, in order to manipulate the self ordering properties of the system.

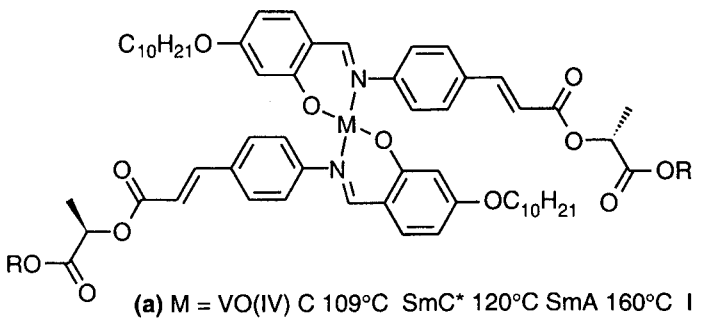

(51)

(a) M = VO(IV) C 109°C SmC* 120°C SmA 160°C I
(b) M = Cu(II) C 125°C SmC* 137°C SmA 178°C I

Fig. 2.51: Paramagnetic chiral N-salicylicylideneaniline derivatives.

Section 2.3.1.6.3: Gold (I) acetylide complexes.

The formation of gold-acetylides giving rise to a linear geometry was demonstrated to be useful as a structural motif for the preparation of novel metallomesogens as shown in figure 2.52 by the Japanese group of Takahashi *et al.*[55] This was achieved by preparing (isonitrile)gold (I) acetylide complexes, facilitating the formation of an extended linear system through the attachment of the isonitrile group to the gold metal centre. Two gold-acetylide complexes of type **(52)** have been prepared: **(52i)** which melts to form a smectic A phase at 142°C with some decomposition and **(52ii)** which melts to form a nematic phase at 88°C which then begins to decompose at 130°C. The second series **(53)** has poor stability showing thermal decomposition above 100°C. The presence of a lateral substituent (such as an ethoxy group) at the aromatic nucleus of the isonitrile ligand lowers the intermolecular interactions for these materials. For compound **(53)** with m = 2 and n = 4, an enantiotropic smectic A phase is formed from 79°C to 96°C. Complexes of type **(54)** were also prepared,

which contain aliphatic isonitrile groups. These complexes exhibit significantly higher thermal stability. The n-octyl isomer (**54iii**) shows a nematic phase from 113°C to 164°C with some decomposition. To lower the melting point and clearing point of these materials branched octyl isonitrile complexes were prepared, with a n-dodecyloxy group attached to the phenyl ester. A nematic phase of similarly broad range (110°-156°C) is seen for (**54iv**), again with some decomposition. The introduction of branching at the α position of the aliphatic isonitrile causes destabilisation of the mesophase, with this material melting into the isotropic liquid at 101°C, and forming a monotropic nematic phase below 69°C. When the branching occurs in the β position, an enantiotropic nematic phase is observed between 87°C and 116°C.

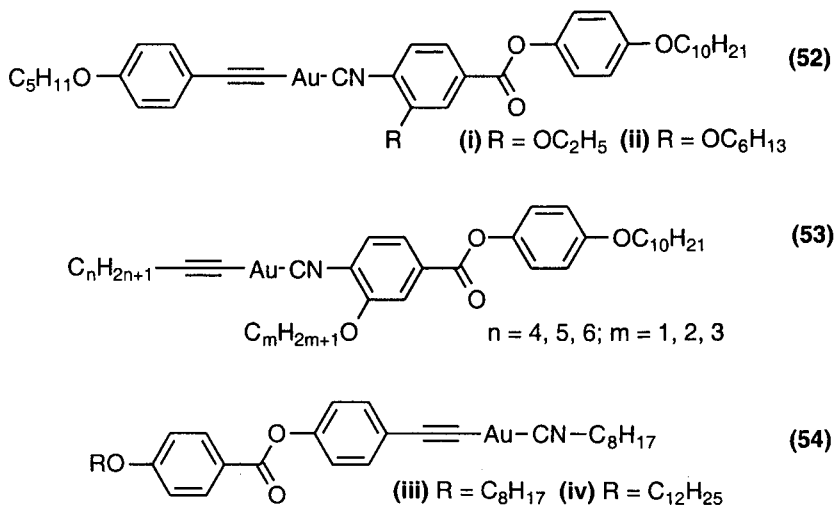

Fig. 2.52: (Isonitrile)gold (I) acetylide complexes.

Section 2.3.1.6.4: Gold (I) carbene complexes.

Novel gold carbene metallomesogens (**55**) have been prepared by Takahashi *et al.*[56], from gold isonitrile complexes by nucleophilic addition of alcohols.

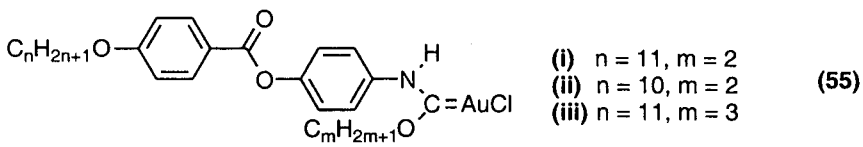

Fig. 2.53: Gold (I) carbene metallomesogens.

The product is obtained as two isomers (Z and E) which are isolated from each other by fractional recrystallisation and are stable in the solid state but interconvert in chloroform solution.

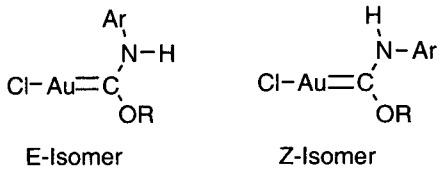

Fig. 2.54: Isomers of gold (I) carbene complex.

The phase behaviour of these materials **(55)** is complex, in that each separate isomer exhibits slightly different phase behaviour. The two component mixture of the two isomers arising from isomerisation of a pure isomer formed in the molten state yields the E and Z isomers in a 3:1 ratio respectively, which also exhibits slightly different phase behaviour. This series of compounds in what ever form (E, Z) exclusively show smectic A phases. The largest phase range exists for what originally begins as the pure E-isomer of the compound **(55i)** with a smectic A phase range of 142-160°C. The phase range for the Z-isomer of this compound is from 149-160°C. Similar behaviour is seen for compound **(55ii)** with phase ranges of 143-158°C (E-isomer) and 152-158°C. The final member of the series listed **(55iii)** has a propyloxy side group which reduces intermolecular interactions and as a result a lower melting point (116°C) and clearing point (128°C) is observed for this material.

Section 2.3.1.6.5: Gold (I) stilbazole complexes.

This series of complexes **(56)** was reported by Bruce *et al.*[54] These complexes are brightly coloured and exhibit mesophases between 120°C and 200°C with some decomposition at the clearing point.

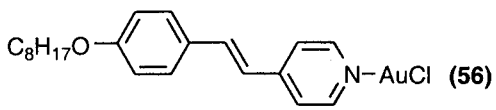

(56)

Fig. 2.55: Gold (I) stilbazole complex.

Section 2.3.1.7: Group 12 calamitic metallomesogens.

The first reported metallomesogen was prepared by Vorländer[59] in 1923. It was a mercury (II) complex. Mercury also undergoes cyclometallation reactions and this feature has been exploited to produce liquid crystalline materials.[60] The zinc (II) metal centre has been co-ordinated to 5,15-substituted porphyrin systems which have high linear anisotropy, resulting in calamitic liquid crystals.[61]

Section 2.3.1.7.1: Zinc (II) complexes.

Metalloporphyrins have potential materials applications in fields such as non-linear optics, photoelectronics and organic semi-conductors. The ability to order these materials is often critical to them achieving an optimised level of performance. This can be achieved quite effectively by incorporating liquid crystalline properties into a porphyrin material. Bruce *et al.* have reported a number of porphyrin based metallomesogens such as **(57)** which show highly ordered crystal smectic B and E mesophases.[61]

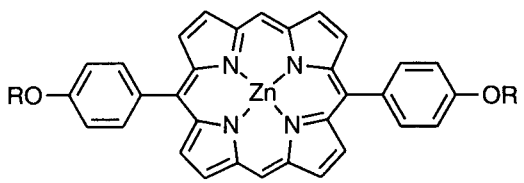

(57)

Fig. 2.56: Calamitic Zn (II) complexes of 5,15-disubstituted porphyrins.

Systems which exhibit fluid liquid crystal phases, *i.e.* smectic A and nematic phases have also been prepared using 5,15 disubstituted porphyrins. These systems -**(58i)** and **(58ii)**- have mesogenic cores consisting of a larger number of six membered rings which extend the planarity and linearity of the system, in addition to providing extra components which can generate more dipolar interactions. Porphyrin **(58i)** with a cyclohexyl group exhibits a smectic A phase between 330°C and 384°C while the phenyl analogue **(58ii)** shows a broad range nematic phase from 309°C to 433°C.[62]

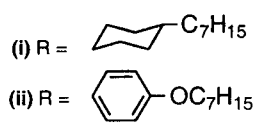

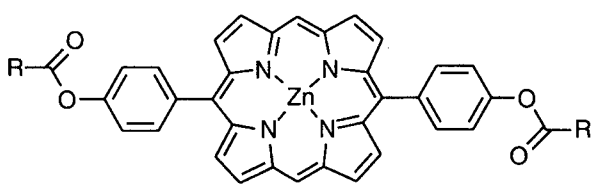

(58)

Fig. 2.57: Calamitic mesophases from Zn (II) complexes of 5,15-disubstituted porphyrins.

These materials are prone to decomposition due to their high transition temperatures. In response to this, low melting systems have been developed by disrupting intermolecular interactions or aggregation arising from the π-π interactions between adjacent rings. To this end, additional alkyloxy chains were introduced to the inner phenyl ring of the porphyrin

based aromatic core of these systems, as illustrated in figure 2.58, to lubricate the whole system. Compound **(59i)** shows no enantiotropic liquid crystalline behaviour though it undergoes crystal transition at 129°C before clearing at 178°C. A monotropic nematic to isotropic transition is observed at 138°C. The second member of the series **(59ii)** shows an enantiotropic nematic phase between 114°C and 177°C for the α,β-atropisomer and a simple clearing from the crystal phase to the isotropic liquid at 192°C for the α,α-atropisomer. The third member of the series **(59iii)** shows an enantiotropic nematic phase between 122°C and 160°C for the α,β-atropisomer and again a simple clearing from the crystal phase to the isotropic liquid at 177°C for the α,α-atropisomer. Therefore this strategy has succeeded in producing porphyrin metallomesogens with lower transition temperatures, making them easier to process and also enabling in depth analysis to be carried out. However, the range of these materials is narrow compared to the above compound **(58)** which has a phase range of over 100°C.

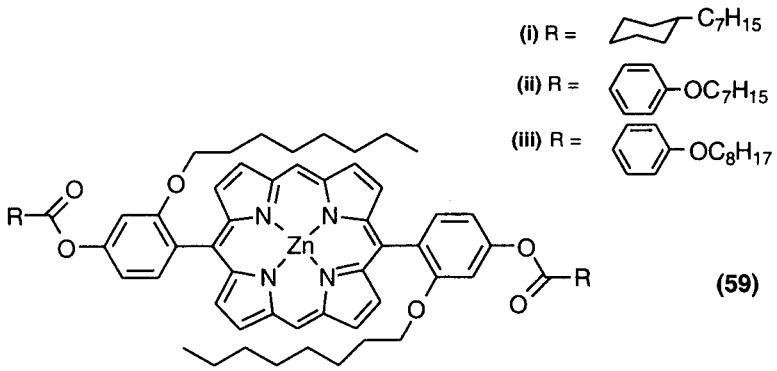

Fig. 2.58: Low melting calamitic mesophases from Zn (II) porphyrins.

Further improvements on the mesogenic behaviour of this class of metallomesogens came in the form of a hexacatenar metalloporphyrin with nine constituent aromatic rings.

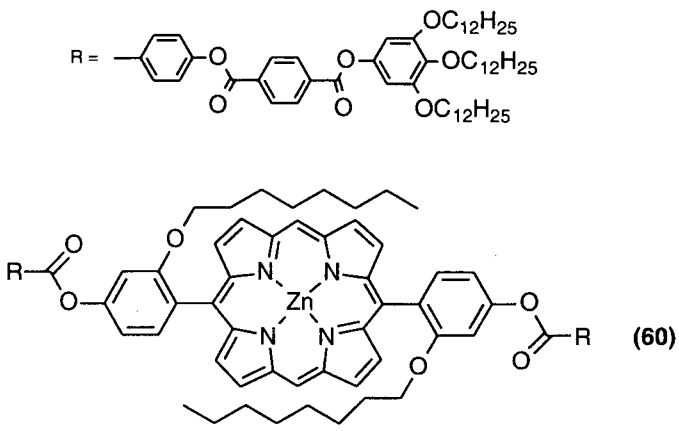

Fig. 2.59: Low melting calamitic mesophases from polycatenar metalloporphyrins.

This material **(60)** displayed a broad nematic phase between 50°C and 153°C. This is a considerable drop in transition temperature from 300°C seen for the earlier metalloporphyrin based metallomesogen systems.[63]

Section 2.3.1.7.1: Mercury (II) complexes.

This material **(61)**, prepared in 1923 was reported to exhibit smectic phases.[59] It was the first example of a liquid crystal containing a metal-carbon bond.

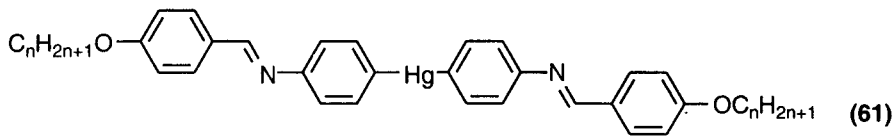

(61)

Fig. 2.60: The first organometallic liquid crystal: Mercury (II) bis-4-(4'-alkyloxy)benzylidene.

Mercury (II) has also been used in cyclometallation reactions to form chiral metallomesogens exhibiting the chiral smectic C phase at room temperature. These complexes **(62)** form a 1:1 mixture of isomers due to the asymmetry of the parent ligand, one of the isomers is shown in fig. 2.61. The clearing point of the mixture of the hexyloxy isomer is 58°C and that of the decyloxy isomer is 63°C.[60]

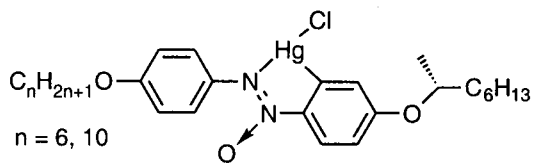

(62)

Fig. 2.61: *Ortho*-cyclolmetallated mercury (II) complex.

Section 2.3.2: Columnar metallomesogens.

The ability of molecular materials to form columnar assemblies is usually associated with molecular geometries which are obviously discotic in nature. However, an increasingly popular approach to the design of columnar mesophases is the use of non-discotic or sub-discotic molecular fragments which give supramolecular columnar structures. Co-ordination chemistry has been at the forefront of developing such structures. The aim of this activity is not simply to produce self organising systems from obscure origins, but to build new materials which incorporate physical properties such as ferroelectricity,[12] helical superstructure,[53] and photoconductivity[64] which can be directly attributed to the presence of the metal centre in the material.

Section 2.3.2.1: Group 4 columnar metallomesogens.

A recent development in the field of metallomesogens has been the preparation of oxotitanium based systems. No examples of hafnium or zirconium columnar metallomesogens are known.

Section 2.3.2.1.1: Oxotitanium complexes.

The first example of a oxotitanium discotic metallomesogen (**63**) was reported in 1998 by Shimizu *et al.*[64] It is based on a (octadecylthio)phthalocyanine system. The material shows a hexatic phase between 59°C and 68°C and a disordered hexatic phase between 68°C and 292°C. The mesophase was detected in the first instance by DSC analysis and the mesophase was then identified by X-ray diffraction. This class of metallomesogen has a potential use as a photoconductive material due to the phthalocyaninatooxotitanium core.

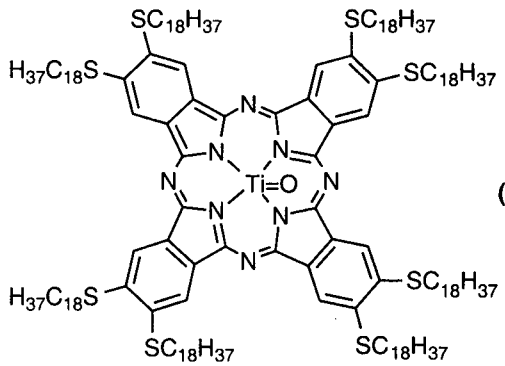

(63)

Fig. 2.62: Phthalocyaninatooxotitanium columnar liquid crystal.

Section 2.3.2.2: Group 6 columnar metallomesogens.

Chromium, molybdenum and tungsten have all been successfully employed to produce metallomesogenic materials. This has been achieved for chromium in a number of systems ranging from carboxylic acid to alkyloxy substituted tris(1,3-diphenyl-1,3-propandionate) complexes. Examples of these systems are given below.

Section 2.3.2.2.1: Chromium (III) complexes.

The chromium (III) (**64**) complex shown in figure 2.63 exhibits two mesophases. The first, termed a disordered octahedral rectangular phase, exists from room temperature to 62°C where the second phase, a disordered octahedral hexagonal phase forms. This phase clears to the isotropic state at 109°C.[65]

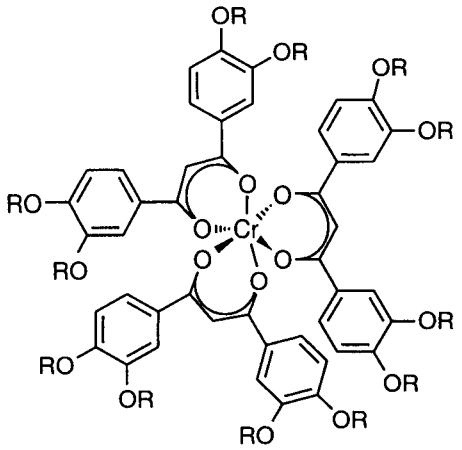

(64)

$R = C_{12}H_{25}$

Fig. 2.63: Chromium (III) tris(1,3-diphenyl-1,3-propandionate) complexes.

Section 2.3.2.2.2: Molybdenum (IV) complexes.

A series of dimetal tetracarboxylates **(65)**, (where n = 1-11, 16), containing quadruple metal-metal bonds has been prepared which may have interesting electronic, magnetic and photophysical properties. The series was examined using DSC and polarising optical microscopy. Compounds co-ordinated with n-pentanoic acid or carboxylic acids with longer chains form discotic liquid crystal phases. The n-pentanoic acid derivative exhibits a mesophase between 152°C and 174°C. The next member of the series melts into a discotic phase at 108°C and clears at 172°C. The liquid crystalline nature of the phase was confirmed by studies of the optical texture of the octanoate derivative which showed fan like domains greater than 200 μm in length, leading to the assignment of phase as being discotic. For the rest of the series the onset temperature varies only slightly while the clearing points of the materials steadily decrease until simple melting from the crystal to the isotropic phase occurs for the n-dodecanoate analogue.[66]

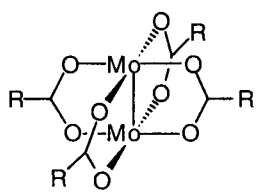

$R = CH_3(CH_2)_n$ **(65)**

n = 1-11, 16

Fig. 2 64: Molybdenum alkanoate liquid crystals.

Section 2.3.2.2.3: Tungsten-oxo (VI) complexes.

Tungsten-oxocalix[4]arenes **(66)**, have been reported by Swager *et al.* which show mesogenic behaviour. These bowlic materials assemble in a head to tail manner, mediated by the

occupation of the calixarene cavity by the tungsten oxide head of the nearest-neighbouring molecule. The material **(66)** has been identified as having a hexagonal disordered bowlic phase (D_{ho}) between 77°C and 267°C; this is preceded by a slightly more ordered phase between 54°C and 77°C. The structure of this phase is thought to be closely related to the mesophase at higher temperatures, since the transition between the two phases has a low enthalpy value (2.5 $kJmol^{-1}$).[12]

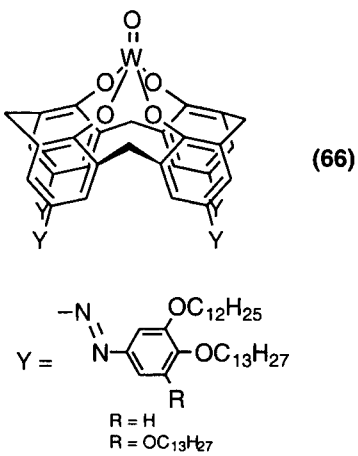

Fig. 2 65: Tungsten-oxocalix[4]arene liquid crystals.

Section 2.3.2.3: Group 10 columnar metallomesogens.

Section 2.3.2.3.1: Palladium(II) cyclometallated complexes.

Cyclopalladation of bis(N-benzylidene)-1,4,-phenylenediamines with aliphatic peripheral chains **(67)** has given rise to tetrapalladium species which show columnar liquid crystalline behaviour.

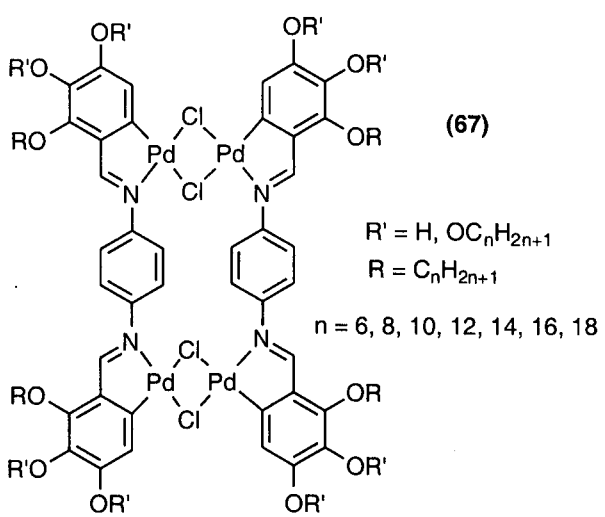

Fig. 2.66: Tetranuclear cyclopalladated columnar liquid crystals.

Various patterns of substitution of the terminal alkyloxy groups on the of the N-benzylidene

ring have been explored such as *ortho* plus *meta* (n-23), *ortho* plus *para* (n-24) and *ortho* plus *para* plus *meta* (n-234). This series materials shows four columnar phases which are distinguished as being three phases showing no long range order between the position of the flat cores of the molecules (termed disordered columnar phases) and one phase in which the flat cores of the molecules retain positional order (termed an ordered columnar phase), this having been gauged from X-ray studies. The transition temperatures for these materials ranges from 100°C to about 250°C.[67]

Section 2.3.2.3.2: Chiral palladium (II) β-diketonate complexes.

Oxovanadium (IV), copper (II) and palladium (II) β-diketonate complexes with ten chiral centres (**68a-c**) have been prepared by Barberá *et al.* which show room temperature columnar phases and undergo ferroelectric switching. The mesophase was conclusively identified as a rectangular columnar phase by X-ray diffraction studies. The unsymmetrical nature of the β-diketonate ligands employed gives rise to *cis* and *trans* isomeric complexes in a 1:1 ratio as proven by proton NMR studies of the palladium complexes (**68b**). The copper (**68a**) and vanadium (**68c**) analogues are assumed to form the *cis* and *trans* isomers in a similar fashion.[68]

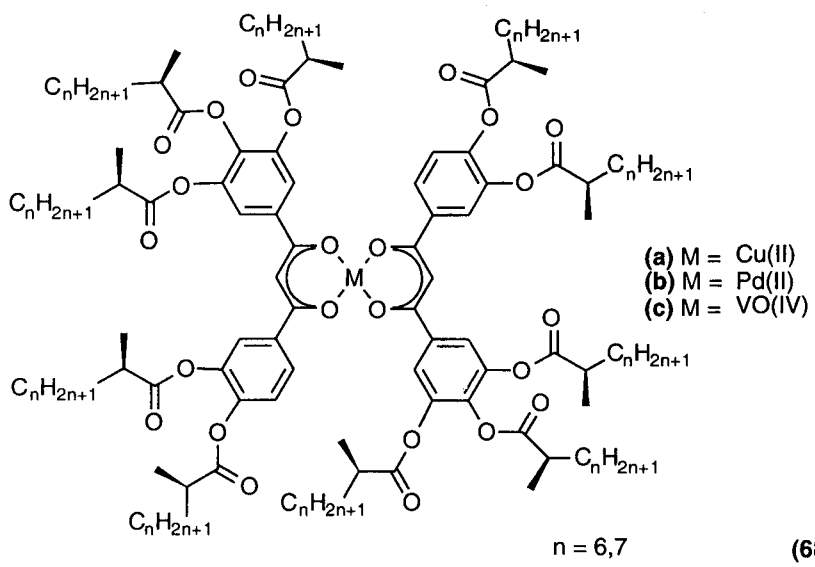

Fig. 2.67: *Trans* chiral β-diketonate complexes exhibiting helical self-assembly.

The *trans* isomer is shown in figure 2.67, where the di-substituted phenyl groups are *trans* to each other and the tri-substituted phenyl groups are *trans* to each other. The compounds clear into the isotropic phase in the region of 125°C for the vanadium (IV) complexes, 130°C for

the copper (II) complexes and 149°C for the palladium complexes. None of these materials shows any sign of undergoing a phase transition to a crystal phase on cooling to -20°C. The paramagnetic complexes display dendritic mesophase textures and form slowly on cooling from the isotropic liquid, while the palladium complexes are more viscous and exhibit more crystalline textures and are formed very quickly on cooling from the isotropic melt. When the mesophases are allowed to form at a very slow rate or by annealing at 100°C for several hours, a texture with a maltese cross appears. The X-ray studies show that a rectangular columnar structure is formed by these materials. The X-ray analysis suggests that the intracolumnar metal-metal distances in the palladium complexes is quite short relative to the other two metal analogues. The stacking order within the columns also extends over longer distances for the palladium complexes than for those of the paramagnetic materials, indicating that the palladium complexes are more ordered. This is borne out by the fact that the palladium complexes are more viscous materials.

Circular Dichroism studies of the heptyloxy oxovanadium (IV) complex in a THF solution, as a freshly prepared thin film and after annealing the thin film have been performed. The lack of a CD signal in the THF solution and the presence of strong CD signals for the treated and untreated thin film samples, suggests that the optical activity arises from the columnar structures and not from the stereogenic centres. A positive exciton splitting in the CD spectrum of the thin film demonstrates the presence of a right handed helix along the length of the column. The CD spectra of the annealed materials show higher optical activity, possibly due to a chiral rearrangement of the structure of the mesophase to give a chiral superstructure. Broadband Dielectric Spectroscopy of these materials also demonstrates the presence of a helical structure due the presence of a low frequency mode similar to the Goldstone mode of the smectic C* phase.[68]

Section 2.3.2.4: Group 11 columnar metallomesogens.

Metallomesogens arising from this group generally contain either copper (II) or gold (I) metal atoms, since these materials co-ordinate in planar or linear geometry. An example of a copper (I) metallomesogen has been recently prepared which arises from a non mesogenic 2,2'-bipyridine ligand. It is an interesting complex, not least because of the apparent non linearity of the co-ordinating ligand. No silver compounds have been prepared exhibiting conventional

columnar phases, however Baena *et al.* have reported thermotropic metallomesogenic covalent silver thiolate "soaps" which exhibit a micellular mesophase with a hexagonal columnar packing structures.[69]

Section 2.3.2.4.1: Copper (I) complexes.

Ziessel *et al.* have reported the first columnar liquid crystal displaying macroscopic ordering to form a metallohelicate structure **(69)**. The columnar phase is present between 25°C and 181°C. The phase displays a pseudo focal conic texture and the columnar structure was confirmed by X-ray analysis.

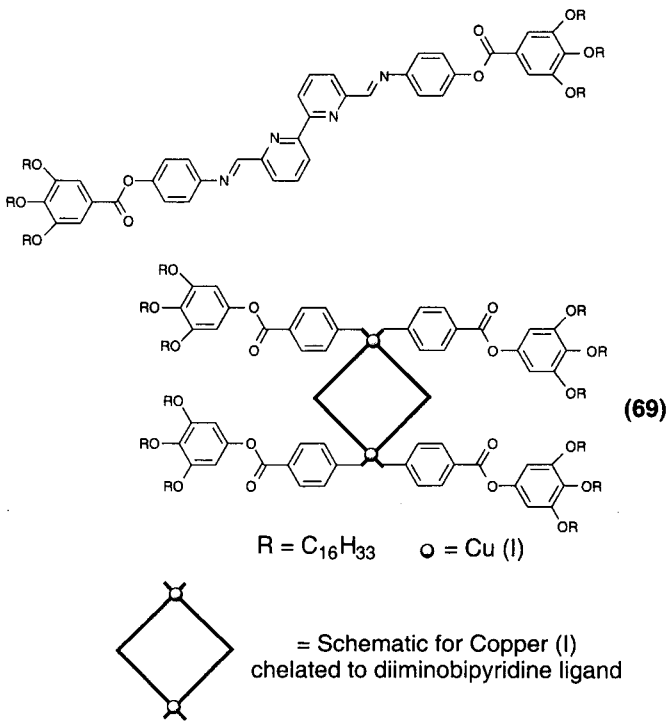

Fig. 2.68: Copper (I) metallohelicate columnar liquid crystal.

The phase behaviour of this deep green coloured material is attributed to the ordering ability of the copper (I) metal centres, mediated through the helical structure in a delicate balance with the disordered structure of the long alkyl chains. The diiminobipyridine ligand does not display any mesomorphic behaviour by itself, underlining the contribution made by the metal centre in generating a well defined geometrical structure capable of strong intermolecular interactions.[53]

Section 2.3.2.4.2: Copper (II) complexes.

An example of a paramagnetic discotic system is the bis(β-diketonato)-copper(II) complex shown **(70)** in figure 2.69.

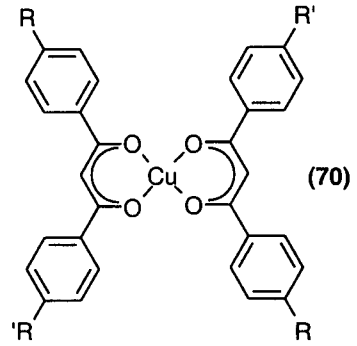

(70)

Fig. 2.69: d^9 Copper (II) discotic metallomesogen.

These complexes (**70**) show mesophases with very ordered columnar phases from 85-128°C (R, R'= $C_{10}H_{21}$), or for unsymmetrical complexes (R= C_7H_{15}, R'=$C_{13}H_{27}$) melting and clearing has been observed between 71°C and 122°C.[1]

Bis(β,δ-triketonato)copper (II) complexes have been prepared which exhibit columnar disordered hexagonal phases from temperatures as low as 76°C ((**71i**), n = 14) and with phase ranges as broad as 140°C ((**71ii**), n = 7, 8). Examination of these materials using polarised optical microscopy showed pseudo-focal conic textures with mosaic regions and linear birefringent defects, which suggest hexagonal columnar structures. X-ray analysis confirmed these assertions showing a diffraction pattern characteristic of a columnar disordered phase.[70]

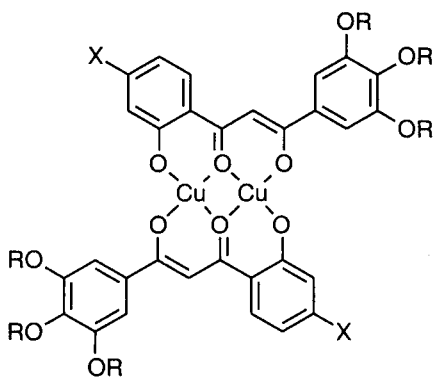

$R = (CH_2)_{n-1}CH_3$
(i) X = H, n = 5-8, 10, 12, 14
(ii) X = OR n = 6-8, 10

(71)

Fig. 2.70: Columnar phases from bis(β,δ-triketonato)copper(II) complexes.

Section 2.3.2.4.3: Gold (I) pyrazolate complexes.

Trinuclear gold complexes which form cyclic co-ordination complexes (**72i, 72ii**) have been prepared by Serrano *et al.*[71,72] Specifically, the material described in figure 2.71 as (**72ii**) exhibits a hexagonal columnar phase between 36°C and 59°C and (**72i**) also exhibits a hexagonal phase between 59°C and 64°C. Both compounds can be supercooled to -30°C before crystallisation occurs. If left to stand at room temperature, (**72i**) crystallises after a few

hours, while for **(72ii)** the crystallisation process takes several weeks to occur. X-ray studies carried out on both compounds showed the absence of any periodicity in the columns of the mesophases allowing the phases to be assigned unequivocally as disordered hexagonal phases.

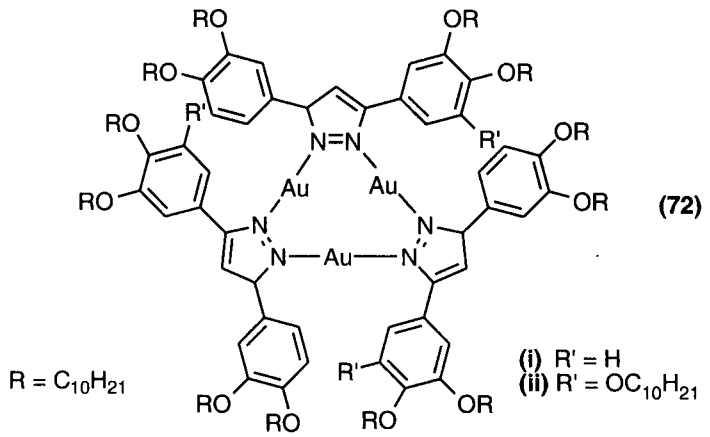

Fig. 2.71: Trinuclear gold pyrazolate complexes.

Section 2.3.2.5: Group 12 columnar metallomesogens.

Zinc and cadmium form co-ordination complexes with porphyrins, displaying columnar phases. Mercury has not been used to form columnar mesophases.

Section 2.3.2.5.1: Zinc (II) complexes.

A series of octaethanolporphyrin derivatives **(73)** has been prepared by Bard *et al.*[73] in which single columnar phases were observed. The basic series in this study consisted of the n-butyl, n-hexyl, n-octyl and n-decyl derivatives **(73ai-73aiv)** of the octaethanolporphyrin core. These materials all have simple melting from the crystal phase to the isotropic phase (decreasing monotonically from 154°C for the n-butyl member to 69°C for the n-decyl derivative) except for the octyl derivative which showed a discotic phase between 84°C and 89°C. The co-ordination of the zinc (II) metal centre **(73b)** into the porphyrin radically improves the mesogenic characteristics of the series. All of these materials exhibit liquid crystalline behaviour, with the discotic phase occurring at 159-164°C for the n-butyl analogue **(73bi)**. A decrease in crystal to discotic transition temperatures occurs for the rest of the series, with the n-decyl member of the series **(73biv)** having a discotic phase between 86-142°C. The broadest phase range for the series is for the n-hexyl compound **(73bii)** which shows a discotic phase between 114-181°C. Further variety in structure of these materials was achieved by varying the metal used to co-ordinate to the porphyrin ring. The n-octyl

porphyrin was commonly used for all of these metal species (**73aiii-73eiii**) and the metals have been observed to also induce a single discotic phase at various temperatures below the zinc (II) analogue (*i. e.* crystal to discotic phase transitions occur between 84°C and 103°C). The mesophase range for these compounds was typically around 40°C.

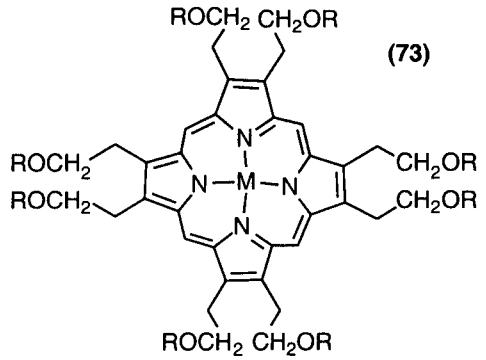

(73)

(i) R = n-Butyl
(ii) R = n-Hexyl
(iii) R = n-Octyl
(iv) R = n-Decyl

(a) M = 2H
(b) M = Zn
(c) M = Cu
(d) M = Pd
(e) M = Cd

Fig. 2.72: Columnar octaethanoporphyrin ether derivatives.

A previous study by the same authors[74] was conducted in which a series of ester derivatives of octaethanol porphyrin (**74**) were prepared. The free base compounds of this series (**74ai-74aiii**) all showed at least one discotic phase. Similarities in the properties of these materials were dependant on the chain length of the ester rather than on presence or absence of a zinc metal centre in the porphyrin. The butyl esters (**74i**) each showed one discotic phase, the crystal to discotic phase being around 180°C in each case. The stability of the phase was enhanced for the co-ordinated porphyrin, which had a clearing temperature of 273°C, -some 50°C above that of the unco-ordinated porphyrin species. The n-hexyl (**74ii**) esters have dramatically lower crystal to discotic transition temperatures, both around 60°C for the free and co-ordinated porphyrins. Two phases are observed for each of these materials, with similar transition temperatures for each transition but again the metalloporphyrin has the higher clearing point, by 12°C in this case (220°C versus 232°C). The n-octyl esters (**74iii**) have crystal to discotic transition temperatures of 91°C (**74aiii**) and 96°C (**74biii**) followed closely by a discotic to discotic transition in each of the materials around 100°C. The isotropic liquid is reached for the free porphyrin at 166°C while again the discotic phase has attained a higher thermal stability when the zinc (II) metal centre is co-ordinated to it with a clearing point of 208°C. Clearly the ester linkages in the porphyrin have augmented the ability of this system to self organise with the appearance of multiple phase bearing materials in co-ordinated and free ester derivatives of octaethanolporphyrin. The presence of the metal

centre extends the range of the discotic phases by increasing intermolecular interactions between porphyrin rings.

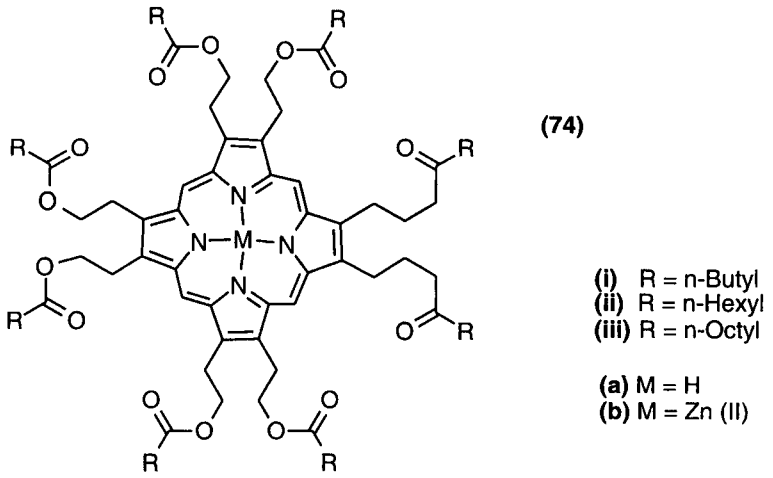

Fig. 2.73: Columnar octaethanoporphyrin ester derivatives.

Section 2.3.3: Polymeric metallomesogens.

The combination of metallomesogens with polymer materials is desirable as it allows greater control over the mechanical properties which these materials will show, with better processability and gives rise to useful composite materials with a larger range of applications.[8,75] Examples of main chain, side chain and cross-linked polymeric metallomesogens are outlined in this section.

Section 2.3.3.1: Main chain metallomesogenic polymers.

The polymer shown below (**75**) is an example of a thermotropic organometallic liquid crystalline polymer. It shows a nematic phase above 160°C identified by the schlieren texture observed using optical microscopy as well as the absence of any X-ray reflections for this ordered phase. This phase remains until above 250°C where decomposition begins to occur.

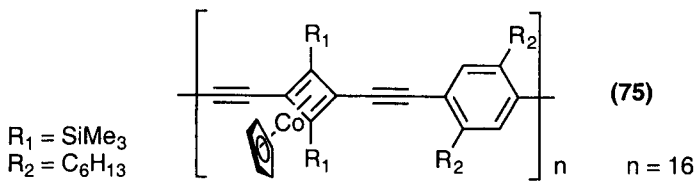

Fig. 2.74: Mesogenic cobalt cyclopentadienylide cyclobutadiene acetylene co-polymer.

The rigidity within this system arises from the conjugated backbone of the polymer, while the lateral hexyl chains, trimethyl silyl groups and cobalt cyclopentadienylide groups disrupt packing between polymer chains enabling the formation of the nematic phase at temperatures at which the materials are thermally stable. This polymer is an example of a main chain

liquid crystal polymer.[76]

Section 2.3.3.2: Side chain metallomesogenic polymers.

An example of a side chain liquid crystalline polymer **(76)**, based on a ferrocene monomer and an azobenzene mesogenic unit has recently been prepared. Ferrocene has great potential as building block in such materials as it has high thermal stability, tuneable redox characteristics and great versatility in terms of the reactions it can undergo, allowing the potential for variety in its structure.

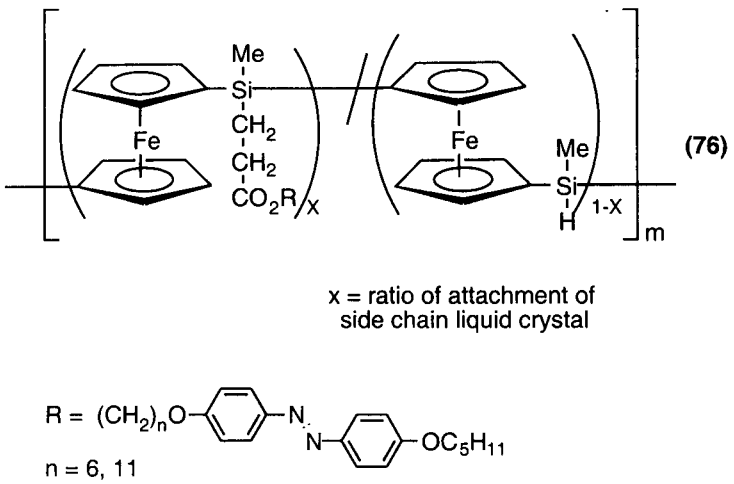

Fig. 2.75: Calamitic side chain liquid crystals on a poly(ferrocenylsilane)backbone.

This material is especially of interest as it has the ferrocene units in very close proximity to each other allowing scope for iron-iron interactions to take place. Synthesis of this polymer was achieved by ring opening polymerisation of a ferrocenophane precursor and subsequent functionalisation of the hydrosilyl group, yielding over 80% conversion of these sites. A nematic phase was observed for the polymer with the hexyloxy spacer from 36°C and remained until 250°C when decomposition set in. The polymer with the undecyloxy spacer melted at 53°C also giving a nematic phase. The influence of the polymer becomes less as the side chain lengthens, hence the increase in the transition temperature observed for the undecyloxy side chain material. Glass transition temperatures for the two polymers were observed at 30°C (hexyloxy spacer), and 35°C (undecyloxy spacer) while the unfunctionalised poly(ferrocenylmethylsilane) has a glass transition temperature of 9°C.[77]

Section 2.3.3.3: Spinal metallomesogenic polymers.

The polymeric phthalocyanine system (**77**), in which the cobalt metal centres are linked through cyano bridges is a blue waxy material. It shows mesogenic behaviour identified by DSC measurements and by optical polarised microscopy, however the identity of the phase has not been determined conclusively.[78]

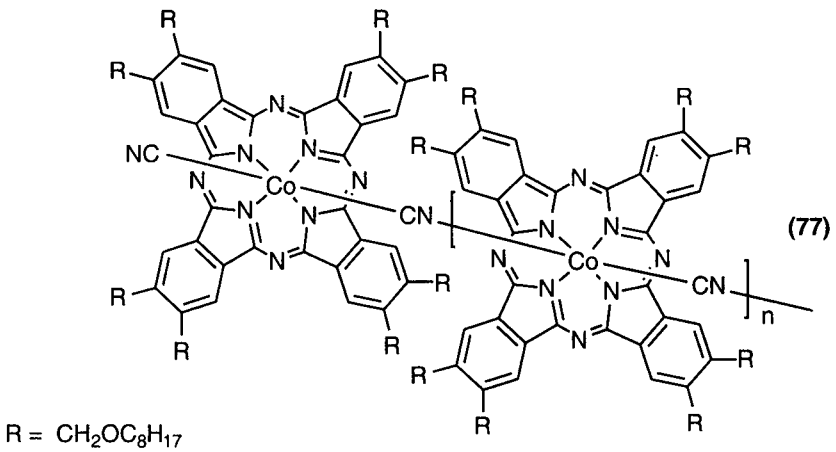

Fig. 2.76: Cobalt phthalocyanine columnar liquid crystals.

An example of the spinal metallomesogenic polymer has also been prepared using tin (IV) systems (**78**) with oxygen acting as a bridging ligand.[79] The phase is formed by the heating of the monomer from the crystal through an unidentified mesophase (95-114°C) and into the isotropic state where a condensation type reaction occurs transforming the isotropic mass to a viscous anisotropic mass. Infra red analysis of the oxystannyl polymers is presented in support of this reaction. The birefringence is lost by heating these newly formed polymers above 290°C where an isotropic state exists.[79]

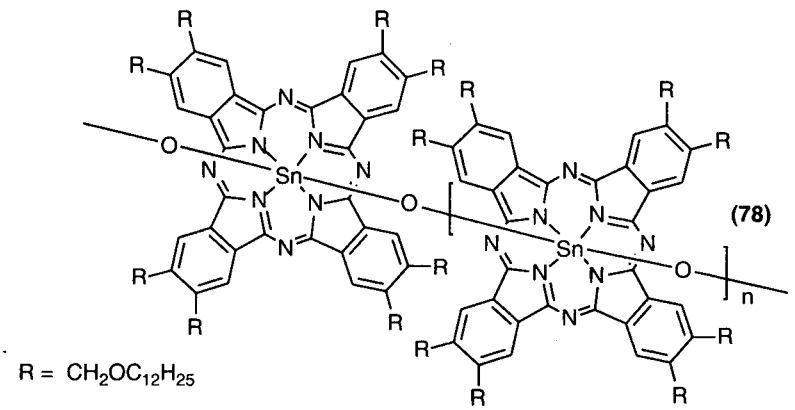

Fig. 2.77: Oxystannyl polymeric phthalocyanine columnar liquid crystals.

Structurally similar metalloid oligosiloxane materials have also been prepared showing

lamellar order below 60°C.[80]

Section 2.3.3.4: Cross-linked metallomesogenic polymers.

Serrano *et al.*[81] have prepared cross-linked metallomesogens **(79)** which enhance the melt processability and mechanical properties of aniotropic fibres. Using the semiflexible thermotropic liquid crystal polymer **(P)** cross-linking can be tailored by limiting the percentage of metal atoms. The formation of a metallomesogenic core does not suppress the nematic phase exhibited by the parent polymer. Complexation with Cu (II) increases the tensile strength of the as-spun fibres from 239 MPa to 445 MPa. Heat treatment of the fibres under tension enhances tensile strength to a value of 840 MPa. The metal ions introduce through bond interactions between the polymer chains which dramatically improve mechanical properties along with the high polarisability and paramagnetism associated with the metal atom. These polymers can undergo further processing to remove the metal atom after enhancing alignment of the fibres if required.[8]

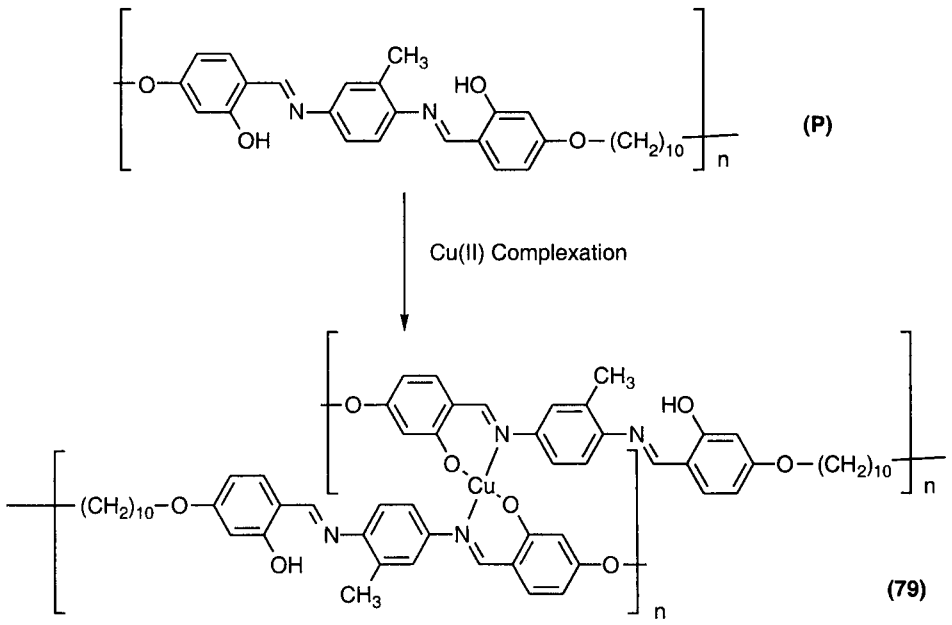

Fig. 2.78: Polyazomethine cross-linked by co-ordination to copper (II).

Section 2.4: References.

1 A-M Giroud-Godquin and P M Maitlis, *Angew. Chem., Int. Ed. Engl.*, 1991, **30**, 375.

2 J W Goodby and G W Gray *Smectic Liquid Crystals: Textures and Structures;* 1st ed.; Leonard Hill: Glasgow, 1984.

3 D W Bruce in "*Inorganic Materials*"; D W Bruce and D O'Hare Eds.; Wiley: Chichester, 1992.

4 A Fukuda, *J. Mater. Chem.*, 1994, **4**, 997.

5 D Lacey in "*An Introduction to Molecular Electronics.*"; 1st ed.; M C Petty, M R Bryce and D Bloor Eds.; Edward Arnold: London, 1995; pp 184.

6 S Chandrasekhar, *Pramana*, 1977, **9**, 471.

7 G W Gray, *Proc. R. Soc. London A*, 1985, **402**, 1.

8 L Oriol and J L Serrano, *Adv. Mat.*, 1995, **7**, 348.

9 D W Bruce, *J. Chem. Soc., Dalton Trans.*, 1993, 2983.

10 M A Esteruelas, L A Oro, E Sola, M B Ros and J L Serrano, *J. Chem. Soc., Chem. Commun.*, 1989, 55.

11 D Baxter, R H Cayton, M H Chisholm, J C Huffman, E F Putilina, S L Tagg, J L Wessemann, J W Zwanziger and F D Darrington, *J. Am. Chem. Soc.*, 1994, **116**, 4551.

12 B Xu and T M Swager, *J. Am. Chem. Soc.*, 1993, **115**, 1159.

13 E Campillos, R Deschenaux, A M Levelut and R Ziessel, *J. Chem. Soc., Dalton Trans.*, 1996, 2533.

14 K E Rowe and D W Bruce, *J. Chem. Soc., Dalton Trans.*, 1996, 3913.

15 D W Bruce and X-H Liu, *J. Chem. Soc., Chem. Commun.*, 1994, 729.

16 X H Liu, M N Abser and D W Bruce, *J. Organomet. Chem.*, 1998, **555**, 271.

17 S Morrone, G Harrison and D W Bruce, *Adv. Mat.*, 1995, **7**, 665.

18 S Morrone, D Guillion and D W Bruce, *Inorg. Chem.*, 1996, **35**, 7041.

19 X H Liu, I Manners and D W Bruce, *J. Mater. Chem.*, 1998, **8**, 1555.

20 D W Bruce and X-H Liu, *Liq. Cryst.*, 1995, **18**, 165.

21 R Deschenaux and J Santiago, *J. Mater. Chem.*, 1993, **3**, 219.

22 L Ziminski and J Malthête, *J. Chem. Soc., Chem. Commun.*, 1990, 1495.

23 J Malthête and J Billard, *Mol. Cryst., Liq. Cryst.*, 1976, **34**, 117.

24 J Bhatt, B M Fung, K M Nicholas and C-D Poon, *J. Chem. Soc., Chem. Commun.*, 1988, 1439.

25 R Deschenaux and J-L Marendaz, *J. Chem. Soc., Chem. Commun.*, 1991, 909.

26 R Deschenaux, J-L Marendaz and J Santiago, *Helv. Chim. Acta*, 1993, **76**, 865.

27 R Deschenaux, J-L Marendaz, J Santiago and J W Goodby, *Helv. Chim. Acta*, 1995, **78**, 1215.

28 R Deschenaux, I Kosztics and B Nicolet, *J. Mater. Chem.*, 1995, **5**, 2291.

29 T Kuboki, K Araki, M Yamada and S Shiraishi, *Bull. Chem. Soc. Jpn.*, 1994, **67**, 948.

30 J P Rourke, D W Bruce and T B Marder, *J. Chem. Soc., Dalton Trans.*, 1995, 317.

31 D W Bruce, D A Dunmur, M A Esteruelas, S E Hunt, R L Lagadec, P M Maitlis, J R Marsden, E Sola and J M Stacey, *J. Mater. Chem.*, 1991, **1**, 251.

32 J P Rourke, F P Fanizzi, N J S Salt, D W Bruce, D A Dunmur and P M Maitlis, *J. Chem. Soc., Chem. Commun.*, 1990, 229.

33 J P Rourke, F P Fanizzi, D W Bruce, D A Dunmur and P M Maitlis, *J. Chem. Soc., Dalton Trans.*, 1992, 3009.

34 M Lee, Y Yoo, M Choi and H Chang, *J. Mater. Chem.*, 1998, **8**, 277.

35 J Barberá, P Espinet, E Lalinde, M Marcos and J L Serrano, *Liq. Cryst.*, 1987, **2**, 833.

36 J Buey, G A Díez, P Espinet, S García-Granda and E Pérez-Carreño, *Eur. J. Inorg. Chem.*, 1998, 1235.

37 P Espinet, J Pérez, M Marcos, M B Ros, J L Serrano, J Barberá and A M Levelut, *Organomets.*, 1990, **9**, 2028.

38 A Crispini, M Ghedini, S Morrone, D Pucci and O Francescangeli, *Liq. Cryst.*, 1996, **20**, 67.

39 M J Baena, P Espinet, M B Ros and J L Serrano, *Angew. Chem., Int. Ed. Engl.*, 1991, **30**, 711.

40 M Ghedini, S Morrone, O Francescangeli and R Bartolino, *Chem. Mater.*, 1992, **4**, 1119.

41 B Neumann, T Hegmann, R Wolf and C Tschierske, *J. Chem. Soc., Chem. Commun.*, 1998, 105.

42 M Ghedini and D Pucci, *J. Organomet. Chem.*, 1990, **395**, 105.

43 A El-ghayoury, L Douce, A Skoulios and R Ziessel, *Angew. Chem., Int. Ed. Engl.*, 1998, **37**, 1255.

44 M Ghedini, D Pucci and F Neve, *J. Chem. Soc., Chem. Commun.*, 1996, 137.

45 M Ghedini, F Neve and D Pucci, *Chem. Eur. J.*, 1998, 501.

46 M J Baena, J Barberá, P Espinet, A Ezcurra, M B Ros and J L Serrano, *J. Am. Chem. Soc.*, 1994, **116**, 1899.

47 D Huang, N Xiong, J Yang, S Wang, G Li and L Zhang, *Mol. Cryst., Liq. Cryst.*, 1993, **231**, 191.

48 M J Baena, J Buey, P Espinet, H-S Kitzerow and G Heppke, *Angew. Chem., Int. Ed. Engl.*, 1993, **32**, 1201.

49 J Buey, L Díez, P Espinet, H Kitzerow and J A Miguel, *Appl. Phys. B*, 1998, **66**, 355.

50 N Hoshino, H Murakami, Y Matsunaga, T Inabe and Y Maruyama, *Inorg. Chem.*, 1990, **29**, 1177.

51 A Mori, M Takemoto, R Mori, H Takeshita, S Ujiie and V Vill, *Chem. Lett.*, 1998, 601.

52 J R Chipperfield, S Clark, J Elliott and E Sinn, *J. Chem. Soc., Chem. Commun.*, 1998, 195.

53 A El-Ghayoury, L Douce, A Skoulios and R Ziessel, *Angew. Chem., Int. Ed. Engl.*, 1998, **37**, 2205.

54 D W Bruce, E Lalinde, P Styring, D A Dumnur and P Maitlis, *J. Chem. Soc., Chem. Commun.*, 1986, 581.

55 T Kaharu, R Ishii, T Adachi, T Yoshida and S Takahashi, *J. Mater. Chem.*, 1995, **5**, 687.

56 R Ishii, T Kaharu, N Pirio, S-W Zhang and S Takahashi, *J. Chem. Soc., Chem. Commun.*, 1995, 1215.

57 P M Maitlis, D W Bruce, R Dhillon, D A Dunmur, F P Fanizzi, S E Hunt, R L Lagadec, E Lalinde, R Orr, J P Rourke, N J S Salt, J P Stacey and P Styring, *New J. Chem.*, 1990, **14**, 549.

58 M Marcos, J L Serrano, T Sierra and M J Giménez, *Angew. Chem., Int. Ed. Engl.*, 1992, **31**, 1471.

59 D Vorländer, *Z. Phys. Chem.*, 1923, **105**, 211.

60 A Omenat and M Ghedini, *J. Chem. Soc., Chem. Commun.*, 1994, 1309.

61 D W Bruce, D A Dunmur, L S Santa and M A Wali, *J. Mater. Chem.*, 1992, **2**, 363.

62 D W Bruce, M A Wali and Q M Wang, *J. Chem. Soc., Chem. Commun.*, 1994, 2089.

63 Q M Wang and D W Bruce, *Angew. Chem., Int. Ed. Engl.*, 1997, **36**, 150.

64 J Santiago, T Sugino and Y Shimizu, *Chem. Lett.*, 1998, 661.

65 H Zheng and T Swager, *J. Am. Chem. Soc.*, 1994, **116**, 761.

66 R H Clayton, M H Chisholm and F D Darrington, *Angew. Chem., Int. Ed. Engl.*, 1990, **29**, 1481.

67 B Heinrich, K Praefche and D Guillon, *J. Mater. Chem.*, 1997, **7**, 1363.

68 J Barberá, R Iglesias, J L Serrano, T Sierra, M R de-la-Fuente, B Palacios, M A Pérez-Jubindo and J T Vázquez, *J. Am. Chem. Soc.*, 1998, **120**, 2908.

69 M J Baena, P Espinet, M C Lequerica and A M Levelut, *J. Am. Chem. Soc.*, 1992, **114**, 4182.

70 C K Lai, F Chen, Y Ku, C Tsai and R Lai, *J. Chem. Soc., Dalton Trans.*, 1997, 4683.

71 J Barberá, A Elduque, R Giménez, L A Oro and J L Serrano, *Angew. Chem., Int. Ed. Engl.*, 1996, **35**, 2832.

72 J Barberá, A Elduque, R Giménez, F J Lahoz, J A López, L A Oro and J L Seranno, *Inorg. Chem.*, 1998, **37**, 2960.

73 B A Gregg, M A Fox and A J Bard, *J. Am. Chem. Soc.*, 1989, **111**, 3024.

74 B A Gregg, M A Fox and A J Bard, *J. Chem. Soc., Chem. Commun.*, 1987, 1134.

75 *Metallomesogens: Synthesis, Properties and Applications*; First ed.; J L Serrano, Ed.; VCH: Weinheim, 1996.

76 M Altman and U H F Bunz, *Angew. Chem., Int. Ed. Engl.*, 1995, **34**, 569.

77 X-H Liu, D W Bruce and I Manners, *J. Chem. Soc., Chem. Commun.*, 1997, 289.

78 M Hanack, A Beck and H Lehmann, *Synthesis*, 1987, 703.

79 C Sirlin, L Bosio and J Simon, *J. Chem. Soc., Chem. Commun.*, 1987, 379.

80 C Sirlin, L Bosio and J Simon, *J. Chem. Soc., Chem. Commun.*, 1988, 236.

81 P Cerrada, L Oriol, M Piñol and J L Serrano, *J. Am. Chem. Soc.*, 1997, **119**, 7581.

Chapter 3

Section 3.1: Preparation of 4-alkyloxy-N-(4'-alkyloxybiphenyl)benzylidenes.

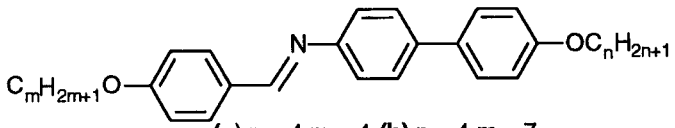

(3)

(a) n = 4 m = 4 **(b)** n = 4 m = 7
(c) n = 7 m = 4 **(d)** n = 7 m = 7

Fig. 3.1: 4-alkyloxy-N-(4'-alkyloxybiphenyl)benzylidenes.

A series of Schiff's bases **(3)** was prepared by the condensation 4-alkyloxybiphenylanilines with 4-alkyloxybenzaldehydes. These Schiff's bases were purified by recrystallisation in choroform,washing in hexane and characterised using proton and carbon NMR and microanalysis. Their thermal behaviour was examined using hot-stage polarised optical microscopy.

Section 3.2: Characterisation of 4-alkyloxy-N-(4'-alkyloxybiphenyl)benzylidenes.

n, m	Phase behaviour of 4-alkyloxy-N-(4'-alkyloxybiphenyl)benzylidenes T[°C].								
4, 4	K	191	S_F	197	S_C	201	N	276	I
4, 7	K	160	S_F	171	S_C	216	N	252	I
7, 4	K	171	S_F	178	S_C	215	N	255	I
7, 7	K	157	S_F	161	S_C	217	N	254	I

Table 3.1: Phase behaviour of 4-alkyloxy-N-(4'-alkyloxybiphenyl)benzylidene ligands.

These materials exhibited liquid crystalline behaviour, which is detailed in table 3.1. The phase diagram (figure 3.2) shows that the materials all exhibit the same three mesophases *i.e.* smectic F, smectic C and nematic phases. The melting points and clearing points decrease with increasing chain length. The phases were identifed on the basis of their optical textures. The nematic phases all displayed schlieren textures with two and four point brushes. The smectic C phase exhibited two phase textures, a broken fan texture and a schlieren texture which comprised of only four point brushes. The smectic F phase exhibited a schlieren mosaic type texture on cooling from the smectic C phase, the absence of any point disclinations ruled out the possibility of it being a smectic I phase. Where two chains of unequal length are present in the molecule, a lower transition temperature is generally seen

for when the longer chain is on the aldehydic phenyl ring. This may be due to the ability of this ring to rotate relatively more easily than the biphenyl rings (due to weaker interactions in the π-delocalised system for the aldehydic phenyl ring) augmenting the conformational disorder of the terminal chain. Examples of phase textures are given in appendix 1.

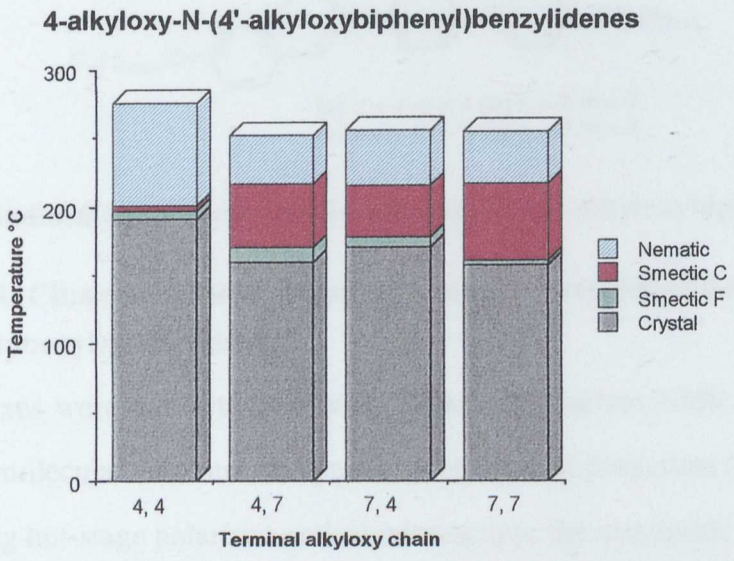

Fig. 3.2: Phase diagram of 4-alkyloxy-N-(4'-alkyloxybiphenyl)benzylidene ligands.

Section 3.3: Preparation of palladium complexes of 4-alkyloxy-N-(4'-alkyloxybiphenyl)benzylidene ligands.

The Schiff's bases **(3)** were reacted with palladium acetate in acetic acid and formed yellow cyclopalladated species. These species were isolated by removing the solvent, purified by dissolving in chloroform and filtering through celite. Analysis by proton NMR showed that these species **(4)** had a dimeric structure. No further analysis was carried out on these acetato bridged complexes.

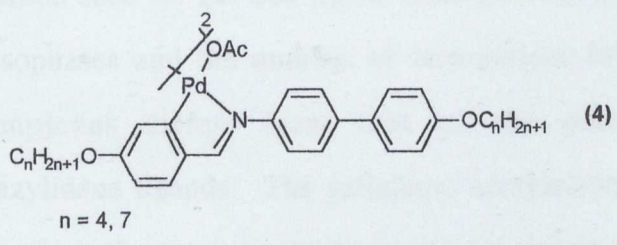

(4)

Fig. 3.3: [Palladium(μ-acetate){4-alkyloxy-N-(4'-alkyloxybiphenyl)benzylidene}].

The palladium acetato complexes (**4**) were then reacted with sodium acetylacetonate in acetone to form yellow monomeric palladium acetylacetonate derivatives (**5**). These complexes were purified by column chromatography using silica gel as the stationary phase with a 1:1 mixture of dichloromethane and hexane as the eluent.

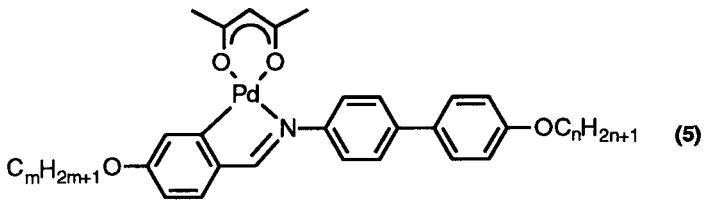

(5)

(a) n = 4 m = 4 **(b)** n = 4 m = 7
(c) n = 7 m = 4 **(d)** n = 7 m = 7

Fig. 3.4: [Palladium(acetylacetonato){4-alkyloxy-N-(4'-alkyloxybiphenyl)benzylidene}].

Section 3.4: Characterisation of [palladium(acetylacetonato){4-alkyloxy-N-(4'-alkyloxybiphenyl)benzylidene}].

These complexes were characterised using proton and carbon NMR, and microanalysis to confirm their molecular structure and purity. The thermal properties of these materials were examined using hot-stage polarised optical microscopy; the mesogenic behaviour observed is outlined in the table 3.2.

n, m	Phase behaviour of palladium acetylacetonate complexes T[°C].						
4, 4	K	184	S_A	209	N	258	I
4, 7	K	155	S_A	260[a,b]	I		
7, 4	K	162	S_A	241	N	261	I
7, 7	K	140	S_A	245	I		

a = decomposition, b = trace of nematic.

Table 3.2: Phase behaviour of palladium acetylacetonate complexes.

These materials (**5**) melt to form mesophases at temperatures comparable with the crystal to smectic F phase transition seen for the free ligand analogues (**3**) examined. However, the order within the mesophases and the number of mesophases formed by the palladium acetylacetonate complexes differs from that of the parent 4-alkyloxy-N-(4'-alkyloxybiphenyl)benzylidene ligands. The palladium acetylacetonate complexes exhibit only fluid phases in which there is very little positional order: smectic A phases were observed in all of the complexes, while nematic phases were seen in all complexes except the last member of the series which has the longest alkyloxy chains. The transitions to the

isotropic phases from the mesophase are also roughly similar (within 10°C) of the parent ligand of each complex. The absence of the more ordered smectic phases can be attributed to the reduction in shape anisotropy of the palladium complexes. The palladium metal centre and acetylacetonate co-ligand (when considered as a single component within the molecular structure) disrupts the linearity of the (biphenyl)benzylidene core making it impossible for these molecules to form the hexagonal type structures observed for smectic B, F, I phases. This reduced ability to form regular close pack arrays is reflected in the decrease in the melting of the crystal to smectic A phases where a decrease of up to 16°C was observed. Nonetheless, the expansion in planarity of the system (due to the square planar co-ordination geometry of the palladium (II) metal centre) and the *pseudo* aromatic character of the acetylacetonate group has stablised a smectic A phase which is not exhibited in the parent ligand. The smectic A phase, being the simplest lamellar phase possible for calamitic based systems, may form due to the enhancement of lateral intermolecular interactions. The increase in the "surface area" of the planar mesogenic core can only serve to increase these lateral interactions, but at the expense of more ordered smectic phases.

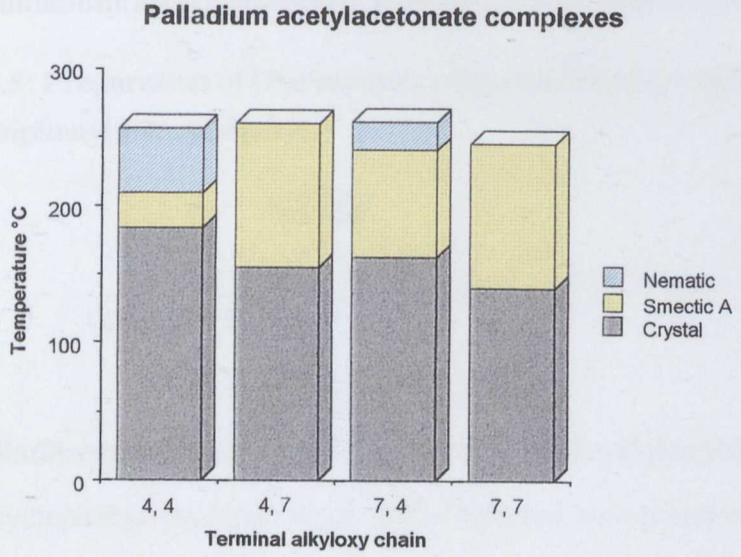

Fig. 3.5: Phase diagram of [Palladium(acetylacetonato){4-alkyloxy-N-(4'-alkyloxybiphenyl)benzylidene}].

Longer alkyloxy chains decrease the range of the nematic phase with a coincident increase in the smectic A phase range, culminating in the elimination of nematic phase behaviour for the last member of the series. These compounds show good thermal stabilty at high

temperatures, showing no sign of large scale decomposition on clearing to the isotropic liquid.

Similar materials were prepared by Espinet *et al.*[4] which are based on a 4-alkyloxy-N-(4'-alkyloxyphenyl)benzylidene system. The fliud nematic and Smectic A phases were observed in this series of compounds. However, transition temperatures were considerably lower than for series (**5**). This may be attributed to two factors: the decyloxy chain present in each of Espinets compounds, helps to reduce the melting points in each of the compounds and the presence of three phenyl rings in compound (**5**) gives added rigidity to this system, requiring more thermal energy to bring about the melting process.

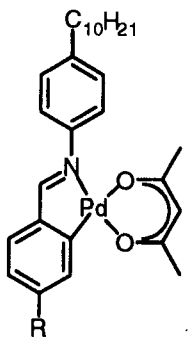

Fig. 3.6: [Palladium(acetylacetonato){4-alkyloxy-N-(4'-alkyloxyphenyl)benzylidene}].

Section 3.5: Preparation of [Palladium(cyclopentadienyl){4-alkyloxy-N-(4'-alkyloxybiphenyl)benzylidene}].

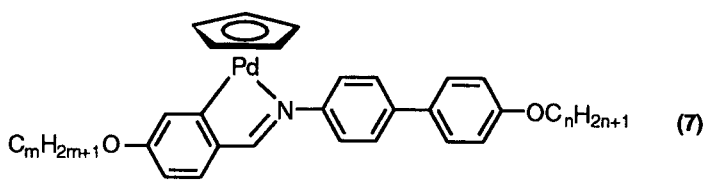

(7)

(a) n = 4 m = 4 **(b)** n = 4 m = 7
(c) n = 7 m = 4 **(d)** n = 7 m = 7

Fig. 3.7: [Palladium(cyclopentadienyl){4-alkyloxy-N-(4'-alkyloxybiphenyl)benzylidene}].

A series of cyclopentadienyl palladium (II) complexes was prepared by conversion of the acetato bridged complexes (by reaction with HCl gas in chloroform) to chloro bridged analogues (**6**) and then the reaction of this species with lithium cyclopentadienylide in tetrahydrofuran. The resulting red complexes (**7**) were purified by removing the reaction solvent, redissolving the crude product in chloroform and filtering this solution through celite. The crude product was isolated by removing the solvent and then further purified by column chromatography on silica eluting with chloroform. The complexes were characterised using

proton and carbon NMR and microanalysis to confirm their molecular structure and purity.

Section 3.6: Characterisation of [palladium(cyclopentadienyl){4-alkyloxy-N-(4'-alkyloxybiphenyl)benzylidene}].

The thermal behaviour of these complexes was also examined using hot-stage polarised optical microscopy and these observations are outlined in table 3.3.

n, m T[°C].	Phase behaviour of palladium cyclopentadienyl complexes						
4, 4	K	125	N	182[a]	I		
4, 7	K	101	N	145	I		
7, 4	K	125	N	179[a]	I		
7, 7	K	92	S_A	165	N	178	I

a = decomposition.

Table 3.3: Phase behaviour of palladium cyclopentadienyl complexes.

This series of complexes (**7**) shows marked changes in thermal behaviour in comparison to the palladium acetylacetonate complexes (**5**) and the free benzylidene ligands (**3**). The compounds in this series have a tendency to form nematic phases, with consistently low melting points. The lowest transition being a crystal to smectic A phase transition at 92°C for the last member of the series due to the presence of two heptyloxy terminal chains. The remaining members of the series all undergo crystal to nematic phase transitions at temperatures within 33°C of this value. A natural bias toward the formation of nematic phases is demonstrated by all of the members of the series. The first three compounds in this series exclusively form nematic phases, with phase ranges of the order of 40°C in each case. A discussion of the phase behaviour of these three compounds gives some insight into the effect of the terminal chains and the large cyclopentadienyl group on structure property relationships. Clearly the presence of the cyclopentadienyl group has decreased intermolecular interactions in the crystal phase by reducing the ability of these bulky molecules to pack closely. This has led to the stabilisation of nematic phases at lower temperatures. The bulk of the cyclopentadienyl ligand also hinders the formation of lamellar type smectic phases due to the structural elaboration of this molecule in three dimensions, as compared with two in the case of the palladium acetylacetonate complexes.

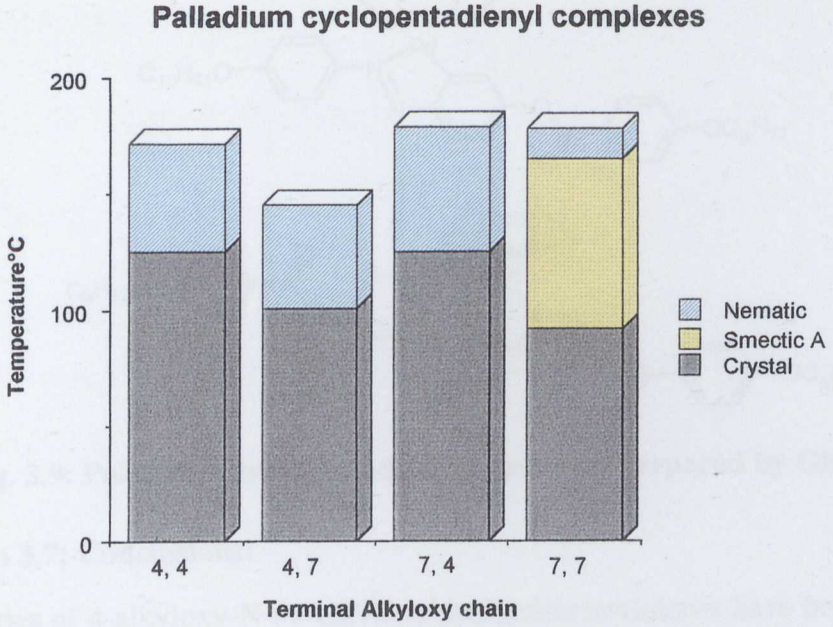

Fig. 3.8: Phase diagram of [Palladium(cyclopentadienyl){4-alkyloxy-N-(4'-alkyloxybiphenyl)benzylidene}].

The fourth member of the series forms a more ordered smectic A phase which has a broad phase range of over 70°C. The appearance of this more ordered phase may be accounted for by the presence of long terminal chains which promote lamellar ordering.

The ceiling for thermal stability of these compounds is around 180°C. This is significantly lower than the thermal stability of the acetylacetonate complexes which are stable up to about 260°C. The difference in thermal stability between the two materials arises from the molecular structure of the complexes. The square planar palladium acetylacetonate derivative of the the benzylidene ligand is formally a sixteen electron species. This is by far the most stable bonding arrangement for a palladium (II) metal centre. The cyclopentadienyl derivative of the benzylidene ligand has a distorted trigonal bipyramidal structure. Formally, it is an eighteen electron complex and is observed to have lower thermal stability.

Ghedini *et al*[2,3] have prepared similar compounds shown in figure 3.9, which also exhibit nematic phases. These azobenzene systems melt at temperatures above 117°C which is not as low as some of complexes **(7)**. Nonetheless the [palladium(cyclopentadienyl){4,4'bis(n-octyloxy)benzoyloxy)azobenzene}] complex shows the highest clearing point for this class of compound with clearing point of 226°C and increased thermal stability with respect to decomposition compared with **(7)**.

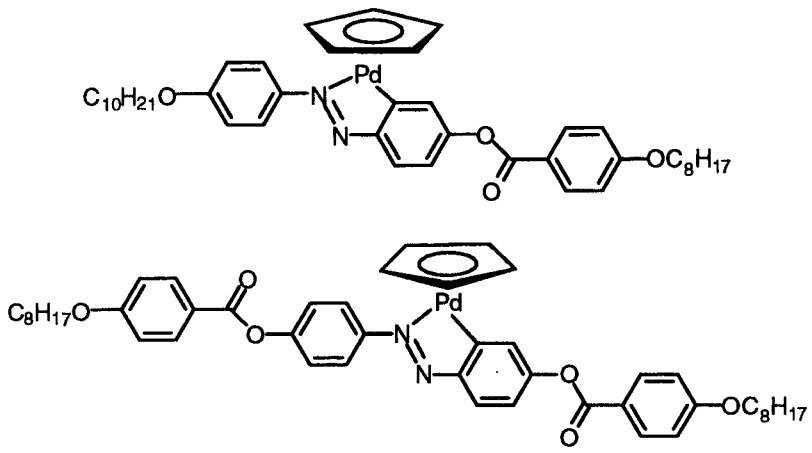

Fig. 3.9: Palladium cyclopentadienyl complexes prepared by Ghedini *et al.*

Section 3.7: Conclusions:

A short series of 4-alkyloxy-N-(4'-alkyloxybiphenyl)benzylidenes have been prepared which show mesophases ranging from the ordered smectic F to the disordered nematic phase at temperatures between 160°C and 272°C. This ligand reacts with palladium acetate to form acetato bridged dimers with an open book conformation. [1] The reaction of these materials (**4**) with sodium acetylacetonate yields monomeric complexes which have a planar geometry and these materials show smectic A and nematic phases between 140°C and 260°C. This is because the planar structure enhances intermolecular interactions and thus the ability of the molecules to order themselves.

Cyclopentadienyl complexes have also been prepared which have a three dimensional structure and generally favour the formation of nematic phases at lower temperatures (101-182°C) than those observed for the free ligand and the acetylacetonate complexes. This behaviour is attributed to the bulky nature of the cyclopentadienyl ligand. [2,3]

This work has helped to stimulate interest in a new class of metallomesogens (*i.e.* cyclopentadienyl complexes), while enabling meaningful comparison with acetylacetonate complexes with the same parent mesogenic ligand.

Section 3.8: References.

1 J Barberá, P Espinet, E Lalinde, M Marcos and J L Serrano, *Liq. Cryst.*, 1987, **2**, 833.

2 M Ghedini, D Pucci and F Neve, *J. Chem. Soc., Chem. Commun.*, 1996, 137.

3 M Ghedini, F Neve and D Pucci, *Chem. Eur. J.*, 1998, 501.

4 M J Baena, P Espinet, M B Ros and J L Serrano, *Angew. Chem., Int. Ed. Engl.*, 1991, **30**, 711.

Chapter 4

Section 4.1.1: Discussion of terephthalylidene-bis-4-N-alkyloxybenzylidenes.

The terephthalylidene-bis-4-N-alkyloxybenzylidene series of ligands **(10)** was prepared by the condensation of two equivalents of the appropriate 4-alkyloxyaminobenzene with 1,4-terephthalyldicarboxyaldehyde. These ligands were then purified by repeated recrystallisation in chloroform to give the required products, which were found to be pure by proton and carbon NMR and elemental analysis. This series of ligands are based on a conjugated aromatic core with two terminal alkyloxy chains as shown in figure 4.1. The aromatic core gives the ligand a conjugated, linear, rigid and planar core, whose length to breadth ratio is extended further by its terminal chains. This extended conjugated system enables the molecules to build up large instantaneous dipoles which favours large attractive forces between the molecules. The attractive intermolecular forces when combined with the highly linear anisotropic shape of the structure fulfil the basic requirements to produce liquid crystalline behaviour. The methoxy, ethoxy, propyloxy and butyloxy homologues have been previously reported. [1]

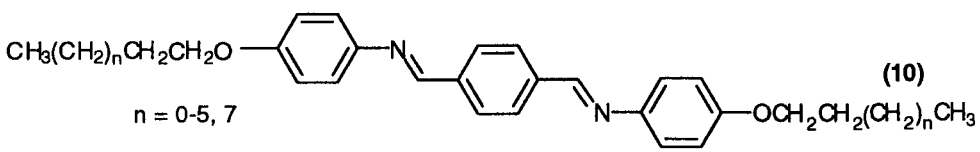

Fig. 4.1: Terephthalylidene-bis-4-N-alkyloxybenzylidene.

Section 4.1.2: Characterisation of terephthalylidene-bis-4-N-alkyloxybenzylidenes.

A homologous series of nine terephthalylidene-bis-4-N-alkyloxybenzylidenes with terminal alkyloxy chain lengths from propyloxy to octyloxy and also decyloxy has been prepared and purified. Thermal analysis data of these compounds has been obtained using DSC and their phases identified using hot-stage polarised optical microscopy.

The phase behaviour of this series is dominated by nematic phases which are observed in every member of the series at temperatures between 203°C and 308°C. The phase range monotonically decreases with increasing chain length (from 103°C to 1.5°C). This is because the increased order (due to greater intermolecular interactions as chain length increases)

coupled with a depression of the clearing point with increasing chain length reduces the range of the nematic phase moving through the series. It is quite likely that the next member of the series would not contain a nematic phase.

The smectic A phase is observed from the pentyloxy analogue to the decyloxy analogue, generally within the temperature range of 221°C to 236°C. The smectic A phase ranges observed for this series decrease with increasing terminal alkyloxy chain length from 12°C to 3°C. The smectic C phase is observed from terephthalylidene-bis-4-N-butyloxybenzylidene until the last member of the series, with phase range increasing from 30°C to 55.5°C. This phase was observed at temperatures between 169°C and 224°C. The tilted hexagonal smectic I phase was observed between the pentyloxy analogue and the decyloxy analogue of the series. The smectic I phase range increases with increasing chain length, assisted by the lowering of the crystal to mesophase transitions with increasing chain length. The phase is observed at temperatures in the phase range between 137°C to 181°C. The smectic F phase is seen in only the last two members of the series. The phase ranges are between 3-5°C in this case and these phases are observed at temperatures between 134°C and 148°C. Examples of phase textures are given in appendix 1.

All nematic to isotropic enthalpy transitions have an odd-even effect with the slope increasing locally from odd to even members of the series with a global increase in the enthalpy values passing through the series, while the temperature at which these transitions occurs monotonically decreases. The nematic phase is known to have no positional order at all and exists solely due to statistical orientational order. In such a system intermolecular interactions are quite weak. Greater conformational freedom is possible as the terminal alkyloxy chains of the molecules get longer and longer and the conformational entropy component can make a larger contribution to the total entropy change for the nematic to isotropic transition, hence leading to decreased transition temperatures. The odd-even effect arises from the greater disordering ability of odd members of the series relative to the even member directly following them in the series. Odd numbered terminal alkyloxy chains must disrupt the orientational order of neighbouring molecules more profoundly, by adopting conformations where steric interactions with neighbouring molecules disrupt the attractive

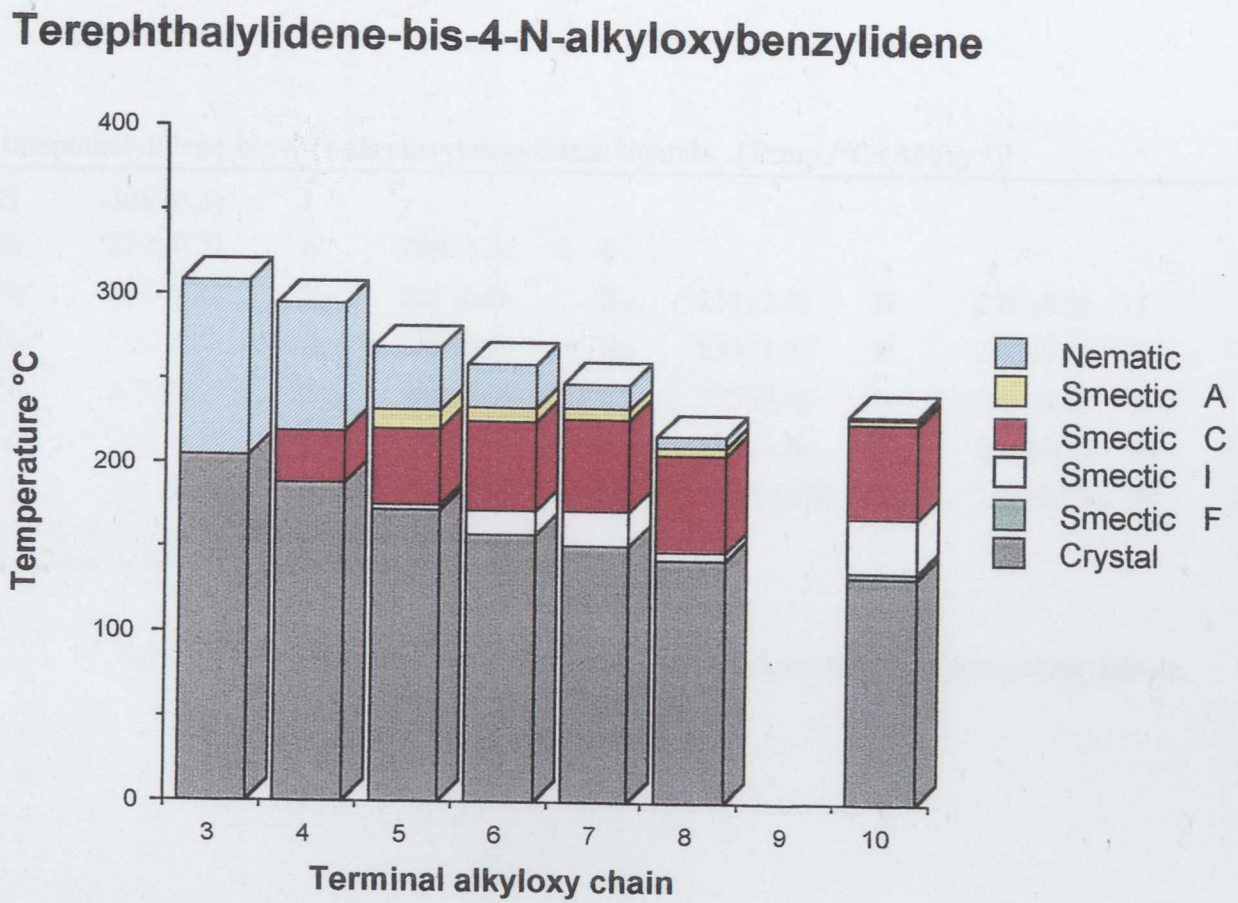
Terephthalylidene-bis-4-N-alkyloxybenzylidene
Temperature °C
400
300
200
100
0
3
4
5
6
7
8
9
10
Terminal alkyloxy chain
Nematic
Smectic A
Smectic C
Smectic I
Smectic F
Crystal

n	Phase behaviour of terephthalylidene-bis-4-N-alkyloxybenzylidene ligands. [Temp./°C ($\Delta H/Jg^{-1}$)]												
3	K	209 (114.8)	N	308 (4.3)	I								
4	K	190 (90.0)	S_C	219 (0.3)	N	296 (5.3)	I						
5	K	172 (70.8)	S_I	181 (9.3)	S_C	221 (0.3)	S_A	231 (1.9)	N	271 (3.7)	I		
6	K	158 (70.7)	S_I	173 (8.1)	S_C	228 (0.5)	S_A	233 (1.3)	N	260 (3.8)	I		
7	K	152 (76.9)	S_I	172 (8.1)	S_C	228 (0.8)	S_A	235 (0.3)	N	248 (3.8)	I		
8	K	143 (68.2)	S_F	148 (0.5)	S_I	173 (8.4)	S_C	231 (1.1)	S_A	234 (0.12	N	242 (5.6)	I
10	K	134 (93.3‡)	S_F	137 (93.3‡)	S_I	169 (8.4)	S_C	224.5 (8.0)	S_A	228 (8.2*)	N	229.5 (8.2*)	I

* incorporates enthalpy change for S_A to N and N to I transitions

‡ incorporates enthalpy change for K to S_F and S_F to S_I transitions

Table 4.1: Phase behaviour of terephthalylidene-bis-4-alkyloxybenzylidene.

intermolecular interactions. Despite the odd-even effect, the general trend suggests that the attractive Van der Waals forces of molecules with longer alkyloxy chains increase intermolecular interactions, while these additional methylene groups also contribute to increased conformational disorder as the temperature and hence thermal motion increases. As a result the loss of order of the nematic phase increases with increasing chain length as seen by an increase in enthalpy change for the transition from nematic to isotropic phase (see table 4.1).

Another notable trend in this series of compounds is the fact that for some transtions the temperatures always increase monotonically with chain length. In these transitions, the process of losing positional order through increased thermal motions is secondary to the attractive intermolecular forces which increase with increasing chain length. The phase transition of this type are: all smectic C to smectic A transitions and all smectic A to nematic phase transitions. The opposite is true of another class of phase transitions where transition temperatures decrease with increasing chain length due to the dominance of the conformational behaviour of the molecules over the attractive intermolecular interactions between them. These transitions are all the crystal to mesophase transitions; all nematic to isotropic transition temperatures and also smectic I to smectic C transitions, where transition temperatures tend to decrease with increasing chain length.

Section 4.1.3: Cyclopalladation of terephthalylidene-bis-4-N-alkyloxybenzylidenes.

The ligand **(10)** has been designed to have its sp^2 hybridised nitrogen atoms favourably positioned for co-ordination of the lone pair of electrons to the palladium (II) species and subsequent electrophilic attack of the central phenyl ring of the ligand leading to the formation of cyclopalladated ring systems. From our experimental findings, using two equivalents of palladium (II) acetate, the ligand exclusively reacts to form two cyclopalladated rings in a *trans* configuration to each other on the central aromatic ring as the final species. This acetato bridged polymeric material (which has a broad proton NMR spectrum) is then reacted with sodium acetylacetonate to form a monomeric dipalladated acetylacetonate complex **(12)**. This class of material can be studied exhaustively by proton and carbon NMR. The isomer formed, *i.e.* the five membered *endo* palladocycle has been

identified as the most favourable isomer for the cyclopalladation of benzylidenes by others. [2]

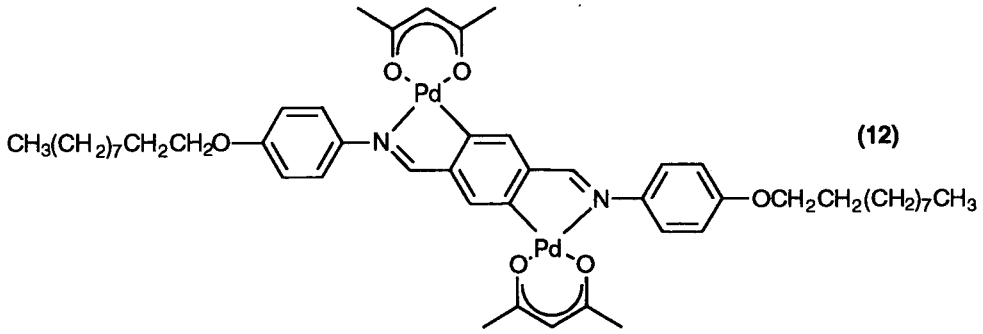

(12)

Fig. 4.3: Monomeric dipalladated terephthalylidene-bis-4-N-alkyloxybenzylidene acetylacetonate complexes .

The cyclopalladation reaction with a terephthalylidene-bis-4-N-alkyloxybenzylidene was also attempted in a 1:1 ratio of palladium (II) acetate and the ligand, again produced exclusively the *trans* dipalladated product with two five membered *endo* palladocycles. This is in agreement with recently published work by Vicente *et al.* [3] who have prepared analogous compounds. The formation of the dipalladated species in preference to the monopalladated species has also been observed for *meta* dipalladated systems by Trofimenko. [4] Doubly cyclopalladated complexes with a *meta* substitution pattern have also been prepared by Chaklader *et al.* [5,6]

This observation suggests the second cyclopalladation reaction is activated by the increase in electron density associated with the formation of the first cyclopalladated ring. Clearly, the formation of a palladocycle enlarges the delocalised system in the aromatic core. The first palladocycle bonded to the central phenyl ring is capable of delocalising the positively charged transition state of the second cyclopalladation reaction more effectively than the transition state of the first cyclopalladation reaction. This extends the delocalised system to include the palladocycle allowing it to act as an electron donating group to the phenyl ring by enhanced π-backbonding from the palladium centre to the central phenyl ring (since carbon is more electronegative than palladium) helping to cancel the effect of any positive charge arising in the transition state.

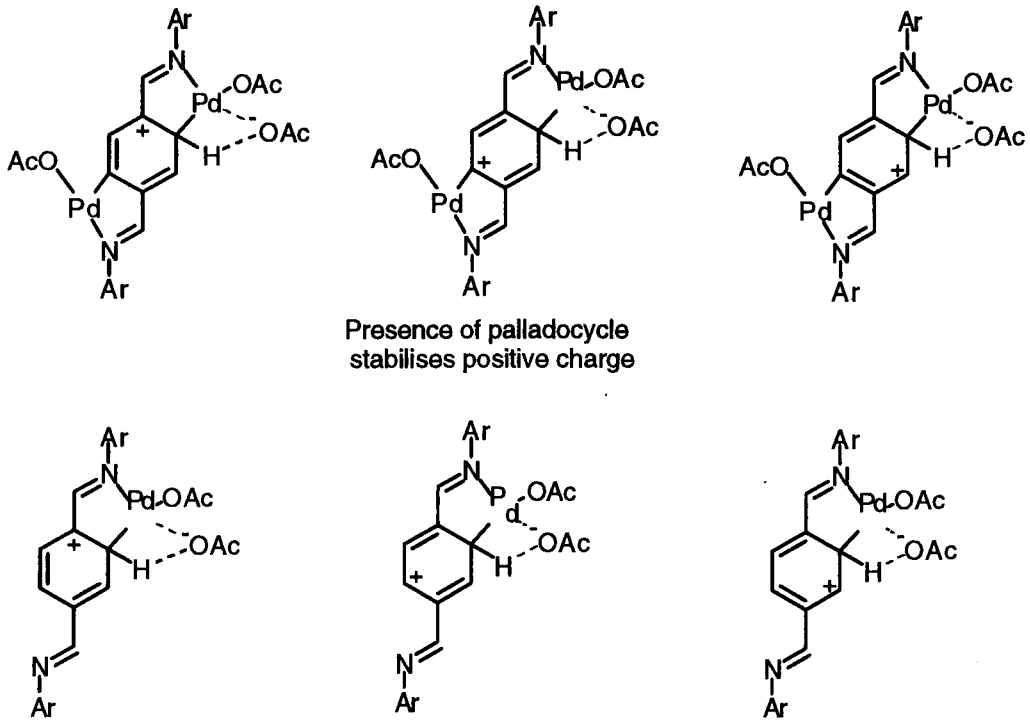

Fig. 4.4: Comparison of transition states for mono- and dipalladation.

Whilst two regioisomers are possible, *i.e.* the *cis* or *trans* isomers, dicyclopalladation of the phenyl ring using palladium (II) acetate always leads to the *trans* isomer as the final product. It is likely that the transition state for the second cyclopalladation to form the *cis* isomer would be unfavourable as it would obstructed by the palladium atom and its acetate group adjacent to it in the *ortho* position. The transition state for the *trans* isomer is in a less sterically demanding position and as a consequence favours formation of this isomer.

Section 4.1.4.0: Discussion of monomeric *trans* palladium complexes of terephthalylidene-bis-4-N-alkyloxybenzylidene (12-14).

A series of complexes based on a *trans* palladated terephthalylidene-bis-4-N-alkyl-oxybenzylidene unit have been prepared by the dicyclopalladation of the ligand **(10)** using palladium acetate as the source of palladium has been described above. These complexes were polymeric in nature, linked by bridging acetato linkages. The series consists of a group of complexes in which the alkyloxy chain is lengthened consecutively and inclusively from a n-butyloxy terminal chain to a n-octyloxy terminal chain and in addition, a complex containing a n-decyloxy terminal chain. A proton NMR spectrum was obtained for these complexes. However, due to the intractable nature of these compounds they were not purified using column chromatograpy, and hence elemental analysis of these materials was

not obtained. Since these complexes had the tendency to decompose before melting at around 270°C, no further thermal analysis was attempted. The complexes were then reacted with a series of β-diketones to form monomeric dipalladated species **(12-14)** which were characterised by proton and carbon NMR and elemental analysis. Thermal analysis was then carried out for all of the materials using hot-stage optical microscopy and for three of the complexes, (n = 8, R = n-Butyl, n-Hexyl, n-Octyl) DSC measurements were obtained. The co-ordination of palladium acetate to terephthalylidene-bis-4-N-propyloxybenzylidene was achieved forming a characteristic red product. However, the insolubility of this complex (attributed to its short terminal chains) prevented both the acquisition of NMR data and subsequent reaction of this polymeric complex to form monomeric β-diketonate complexes.

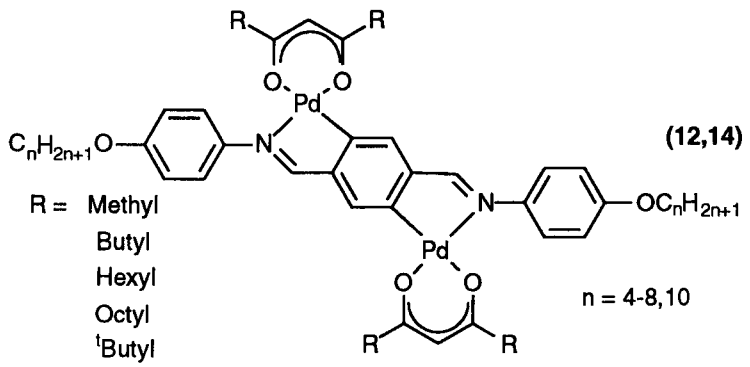

Fig. 4.5: Monomeric dipalladated β-diketonate complexes.

Section 4.1.4.1: Phase behaviour of dipalladated β-diketonate complexes (12-14).

For convenient discussion the entire series of complexes shall be divided into three sub-groups:

Section 4.1.4.1.1: The group containing the series **(12)** in which the terminal alkyloxy chain of the terephthalylidene-bis-4-N-alkyloxybenzylidene component of the complex is varied (n = 4-8, 10) while only acetylacetone (R = Me) is used as the β-diketone co-ligand in the complexes.

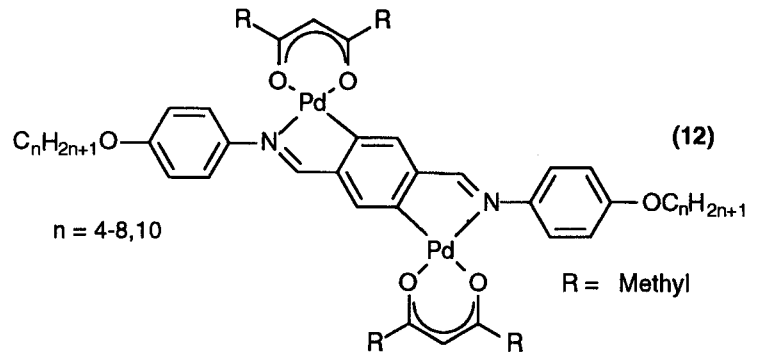

Fig. 4.6: Monomeric dipalladated β-diketonate complexes.

Section 4.1.4.1.2: The group containing the series **(13)** in which the terminal alkyloxy chain of the terephthalylidene-bis-4-N-alkyloxybenzylidene component of the complex is varied (n = 4-8, 10) while only undecane-5,7-dione (R = n-Butyl) β-diketone, is used as the co-ligand to form the complexes.

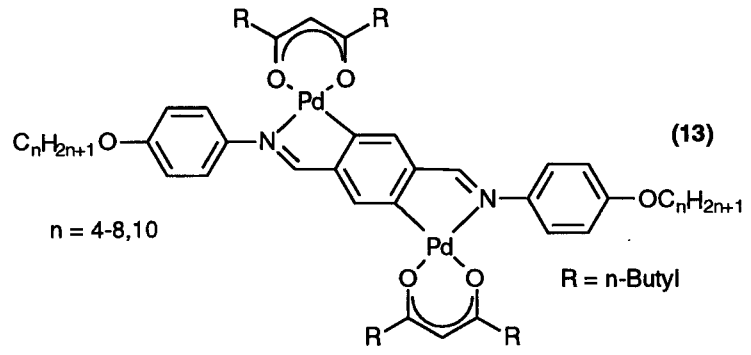

Fig. 4.7: Monomeric dipalladated β-diketonate complexes.

Section 4.1.4.1.3: The group containing compounds from the series **(12-14)** in which the Schiff's base used is terephthalylidene-bis-4-N-octyloxybenzylidene throughout the series while the β-diketone co-ligand varies (R = Me, n-Butyl, n-Hexyl, n-Octyl).

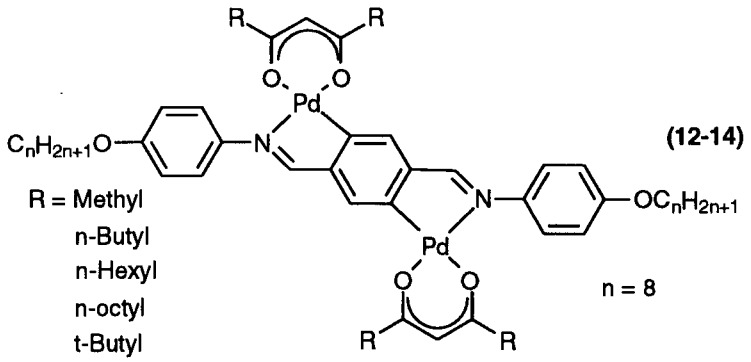

Fig. 4.8: Monomeric dipalladated β-diketonate complexes.

Section 4.1.4.1.1: Group one.

The complexes in group one **(12)** show the effect of cyclopalladation most dramatically. These complexes have melting points (or decomposition points for the early members of the series) at temperatures above the melting points observed for **(10)**. This trend is observed constantly throughout the series and arises through a number of factors. Firstly, the increase in molecular mass of these palladium complexes requires greater input of thermal energy to bring about the necessary thermal motion enabling these materials to form fluid phases. Secondly, increased attractive intermolecular interactions between molecules in the solid state

contribute to the higher transition temperatures observed. These increased intermolecular interactions are caused by the greater polarisability of the molecules arising from the presence of the palladium (II) metal in the molecules which has introduced new permanent dipole moments into the molecule arising from the difference in electronegativity between the palladium and carbon atoms in the palladium-carbon bond. Furthermore, the increase in conjugation brought about by the formation of two aromatic palladocycles augments the tendency for the formation of induced dipole moments as a result of the increased capacity of the molecule to delocalise charge more effectively over this extended aromatic core. It is true to say the net change of the dipole moment of the entire molecule is balanced by through bond interactions since the molecule retains a C_2 axis of symmetry and all forces which arise from cyclopalladation in one of the available sites are equalled and opposed by the other. Equally, through-space interactions arising from the increase in polarisability of regions within the molecule, particularly in the palladocycle and the pseudo-aromatic system arising from the co-ordination of the β-diketone group, must increase the attractive Van der Waals interactions between molecules which are nearest neighbours to help offset these induced dipole moments. Another factor which may increase interactions between planar molecules with delocalised systems is the possibility of intermolecular π-π interactions, perhaps occurring between favourably aligned metal centres.

The only mesophase observed in this group of materials is the nematic phase, identified by the two and four point brushes observed in the schlieren texture of each of the materials. This is in stark contrast to the series **(10)** where numerous ordered smectic phases (A, C, F, I) were observed over a broad range (~100°C). This is surprising because of the planar broad mesogenic core which might have been considered to promote strong lateral π-stacking effects which would lead to the formation of layered phases. The formation of the smectic phase must be dependant on achieving a length to breadth ratio of critical size. This is aptly demonstrated by the absence of smectic phases from the first member of the series **(10)**, which lacks the capability to form lamellar type phases.

The significant decrease in length to breadth ratio of the rigid aromatic core in the dipalladated acetylacetonate complexes has substantially decreased the linearity of the complex compared to the parent ligand and consequently the ability to form smectic phases.

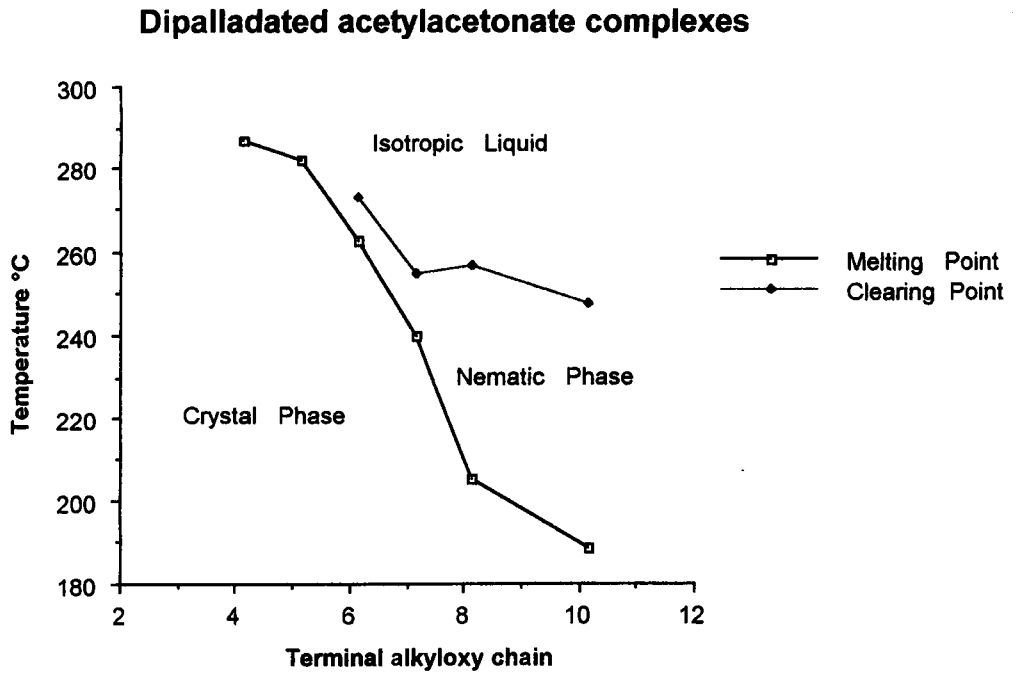

Fig. 4.9: Dipalladated acetylacetonate complexes.

The obvious strategy to pursue to bring about the formation of smectic phases with this particular molecular system would be to prepare homologues with larger terminal alkyloxy chains, to increase the linearity of the molecules.

The phase range for this series of compounds broadens substantially from the hexyloxy derivative (phase range 10°C) to the decyloxy derivative (phase range 73°C). Whilst both melting point and clearing points decrease monotonically, melting points decrease more dramatically than clearing points. This suggests that entropy factors associated with increasing chain length have a large influence in determining transition temperature of the melting point, while the stability of the nematic phase is less sensitive to the chain length for these materials. These compounds are thermally stable below 250°C for a period of time long enough to determine phase behaviour. However, above this temperature the compounds have a tendency to slowly decompose on melting, while for the butyloxy and pentyloxy members of the series, decomposition in the solid state occurs as these materials do not melt before 280°C.

Section 4.1.4.1.2: Group two.

The second group of compounds, series **(13)** is analogous to **(12)** in that it contains a series of

compounds whose terminal alkyloxy chains also increase as described from butyloxy to octyloxy, in addition to the decyloxy member of the series.

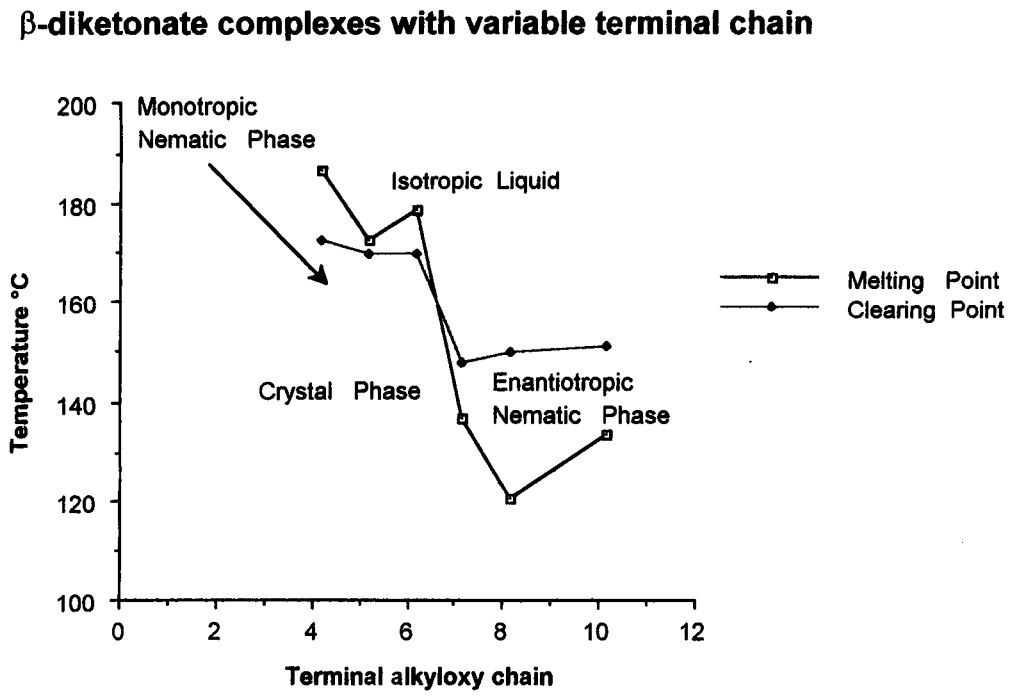

Fig. 4.10: β-diketonate complexes with variable terminal chain length.

The co-ligand in this case is undecane-5,7-dione. This has the effect of dramatically decreasing the melting point of all the compounds in the series, by at least 40°C in some cases and up to 100°C in others. The largest change in melting point is seen for the butyloxy analogue since it has a melting point of 185°C compared to a decomposition point of 285°C for the acetylacetonate derivative. A trend of a general decrease in the melting points with increasing chain length is observed, though the last member of the series actually shows an increase in melting point relative to the penultimate member of the series. The general decrease in melting points observed in series **(13)** can be explained by the four lateral alkyl chains which make significant contributions to the change in conformational entropy brought about by increased thermal motions within the chains as the temperature is increased. A significant point to note is the instability of the nematic phase for the first three members of this group: all three form only a monotropic nematic phase. The remainder of compounds in the group form enantiotropic nematic phases with the phase range generally showing a tendency to increase with longer chain lengths. The increase in the breadth of the molecules from extension of the aliphatic chains attached to the mesogenic core has reduced the

anisotropic shape of the molecules. As a consequence the tendency for self organisation between the molecules to give the degree of orientational order required for a stable nematic phase is diminished. The stabilisation of the nematic phase for longer terminal alkyloxy chains is clearly as a result of the fact that the length to breadth ratio of the molecules must be of a certain critical value in order to give a thermodynamically stable mesophase. This happens moving from the hexyloxy to heptyloxy member of the series. The reduced linearity of this group of molecules also inhibits the formation of more ordered smectic phases. The octyloxy member of this group has a nematic phase which has the largest phase range for this class of liquid crystal suggesting that it has a length to breadth ratio which can be used as a basis for further structural modification.

Section 4.1.4.1.3: Group three.

The dicyclopalladated moiety with octyloxy terminal chain was used in studying the third group of compounds. In this group the lateral side chains of the co-ligand (bonded to the mesogenic core through the palladium metal centres) were varied in size from methyl to n-butyl to n-hexyl to n-octyl and finally tertiary butyl to probe the influence of structural modification in this area of the mesogenic core. The mesogenic behaviour of this group of materials **(12, 14)** is characterised by two trends for the linear aliphatic substituents: a reduction in transition temperatures moving from methyl to larger substituents on the β-diketonate ring and the narrowing of phase ranges moving towards higher alkyl chains. This is emphatically shown by the formation of a monotropic phase for the nonadecane-9,10-dione member of the group.

The first trend can be explained by the increase in the entropy change which occurs as the chain length increases on heating these materials, as longer chains have a larger contribution to make to the conformational entropy component of the total entropy for the each transition. This reduces the melting points of the materials accordingly. The n-butyl derivative has the lowest melting point in both group two and group three. A slight rise in the melting point is observed for the n-hexyl derivative (133°C) and a further increase on this is seen for the n-octyl derivative (140°C). The rise in temperature of the latter can be explained by the fact that the melting transition occuring changes from crystal-to-nematic phase to crystal-to-isotropic phase.

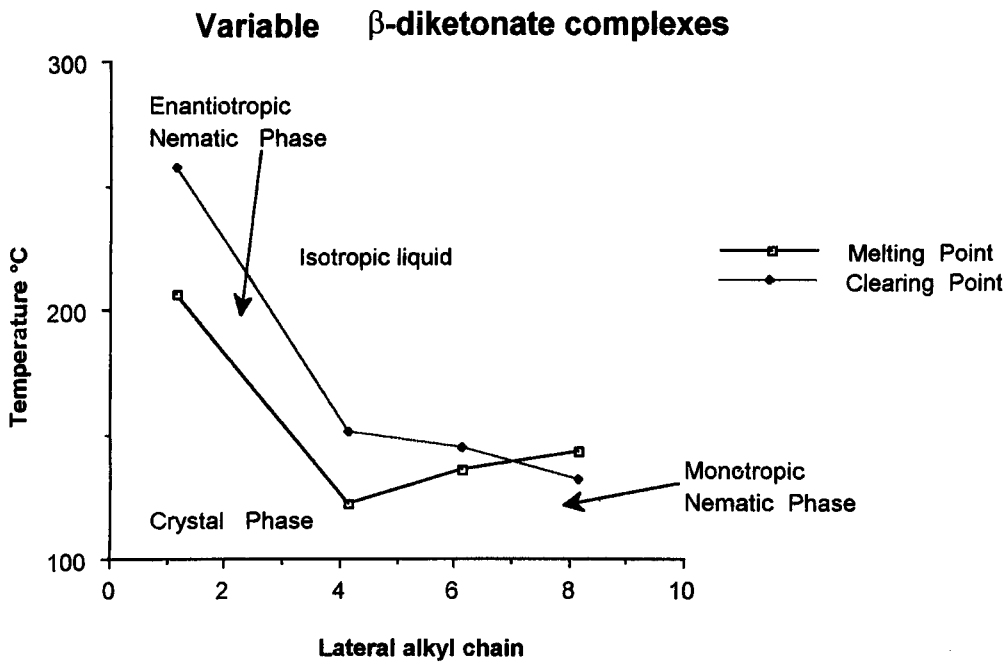

Fig. 4.11: Variable β-diketonate complexes.

The enthalpy of fusion and entropy change for the melting transition in this group decreases slightly with increasing chain length for the long chain β-diketones. This signifies more disordering of packing in the solid state as the length of the lateral chain increases. The second trend (destabilisation of the nematic phase with increasing chain length) causes a reduction in the phase range for the n-hexyl derivative followed by the formation of a monotropic phase for the n-octyl derivative. This behaviour arises due to the decrease in the length to breadth ratio of the molecules with increasing length of the alkyl substituent. These laterally substituted alkyl chains on the mesogenic core have reduced the shape anisotropy of the mesogenic core to a point where mesophase formation is inhibited.

R_1	R_2	Transition temperature °C (ΔH kJmol^{-1})[ΔS kJmol^{-1}K^{-1}]					
8	4	K	119 (32.01) [0.082]	N	148 (0.71) [0.0017]	I
8	6	K	133 (31.88) [0.079]	N	142 (0.50) [0.0012]	I
8	8	K	129 (0.61) [0.0025]	I	140 (29.33) [0.071]	N[a]

a = monotropic

Table 4.2: Temperature, enthalpy and entropy transitions for group three complexes.

An advantage of metal complexes of tertiary butyl β-diketonates is the high thermal stability of such materials. [7] However despite this enhanced thermal stability, derivative **(14)** in this

series shows no mesogenic behaviour, melting from the solid state to the isotropic liquid at 262°C. The tertiary butyl group disrupts the planar structure of the aromatic core of the molecule inhibiting the formation of mesophases. The high melting point of this analogue is comparable with some of the acetylacetonate derivatives of series **(12)**: comparison with the octyloxy derivative is particularly interesting in that this analogue melts at 203°C to give a nematic phase and clears at 255°C. This suggests the intermolecular forces are stronger for the tertiary butyl derivative than for the acetylacetonate. This could be because the large tertiary butyl groups located on the β-diketonate unit are so sterically demanding, that their initial movement must be in unison with tertiary butyl groups on neighbouring molecules and so a high barrier to rotation for any and all neighbouring tertiary butyl groups must be overcome before the solid can melt into the isotropic liquid state. Crystallisation from the melt for this material is also a stubborn process as the material can be supercooled by over 100°C before crystallisation occurs. This pattern is also seen for a series of monopalladated 2,2,6,6-tetramethylheptane-3,5-dione complexes. [8]

Section 4.1.4.1.4: Unsymmetrical β-diketonate complex.

Using octane-2,4-dione as a β-diketonate co-ligand, a mixture of at least two isomers was obtained. The proton NMR showed the presence of two imine peaks of equal intensity. This occurs because the probability of forming **(i)** is twice as much as forming the other isomers **(ii, iii)** and the proton NMR signal for the imine peaks in **(ii)** and **(iii)** are very similar leading to two equal signals. This mixture melts to the isotropic liquid at 208°C and exhibits a monotropic nematic phase at temperatures below 168°C. Separation of the isomers was not achieved.

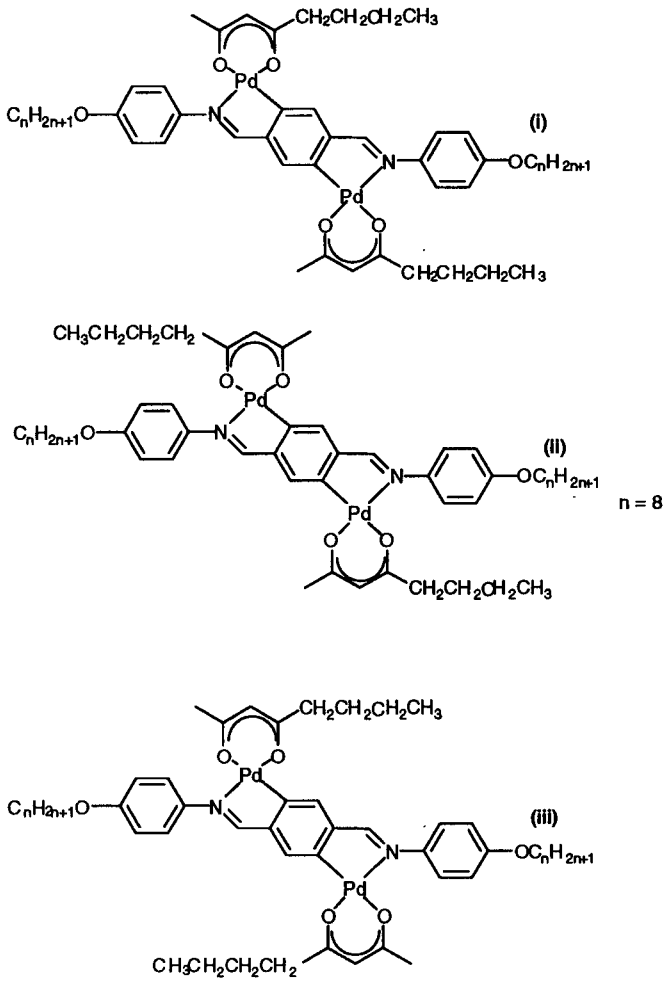

Fig. 4.12: Co-ordination of octane-2,4-dione yielding a mixture of isomers.

Section 4.1.5: Preparation of *cis* dipalladated terephthalylidene-bis-4-N-alkyloxybenzylidenes acetylacetonate complexes (16).

Section 4.1.5.1: Preparation of *cis* [dipalladium-bis(acetylacetonato) {terephthalylidene-bis-4-N-alkyloxybenzylidene} (16) via directed dicyclopalladation method.

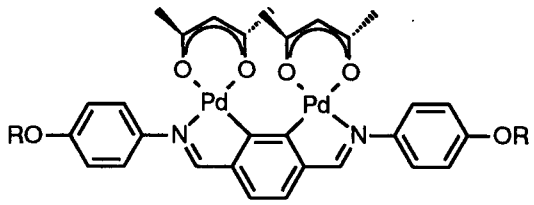

(16)

Fig. 4.13: *Cis* [dipalladium-bis(acetylacetonato){terephthalylidene-bis-4-N-alkyloxybenzylidene}.

Terephthalylidene-bis-4-N-decyloxybenzylidene was reacted with sodium tetrachloropalladate in a 1:2 ratio, in methanol (48 h) at 60°C, to form dicyclopalladated species. The products of this reacion were then reacted wth sodium acetylacetonate to yield

monomeric species. Proton NMR showed evidence of the presence of *cis* and *trans* dicyclopalladated complexes in a 1:9 ratio based on integration of the NMR spectrum. The *cis* isomer was not successfully isolated from the *trans* isomer due to decomposition during column chromatograpy.

Section 4.1.5.2: Acidolysis of *trans* [dipalladium-(μ-chloro){terephthalylidene-bis-4-N-alkyloxybenzylidene}]: a potential pathway towards *cis* [dipalladium-(μ-chloro)-{terephthalylidene-bis-4-alkyloxybenzylidene}] via a ligand exchange mechanism.

Trans [dipalladium(μ-chloro)$_2$\{terephthalylidene-bis-4-N-alkyloxybenzylidene\}] was dissolved in acetic acid and stirred overnight at 80°C. The solvent was then removed and the product was dried under vacuum. The product was then dissolved in acetone and reacted with sodium acetylacetonate to form monomeric dicyclopalladated products. Analysis of the products of this reaction showed that the palladium complex had decomposed into palladium acetylacetonate and 1,4 terephthalyldicarboxaldehyde. Therefore the strategy of forming a *cis* dipalladated species using a acidolysis mechanism was not explored further.

Section 4.2.1: Discussion of terephthalylidene-bis-n-(4'-alkyloxybenzoate)aniline.

The analogous terephthalylidene-bis-N-(4'-alkyloxybenzoate)aniline system **(19)** has also been prepared to probe the effect of an extended mesogenic core on the phase behaviour of the free ligand and on cyclopalladated derivatives.

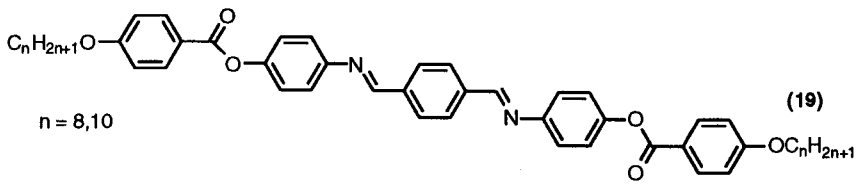

Fig. 4.14: Terephthalylidene-bis-N-(4'-alkyloxybenzoate)anilines.

Section 4.2.2: Discussion of phase behaviour of terephthalylidene-bis-N-(4'-alkyloxybenzoate)anilines.

The octyloxy and decyloxy dervatives of this system have been prepared and they both show smectic F, I, C and nematic phases. These phases are seen in the range from 120°C to above 400°C where extensive decomposition was observed under the microscope. In comparison with the octyloxy and decylocy analogues of **(10)**, the extension of the mesogenic core by the addition of two benzoate groups has extended the range of the smectic C phase to above a temperature of 300°C in each case (n = 8, 10) and also increased the range of the nematic

phase to above 400°C. However the lifetime of these materials is poor at 400°C.

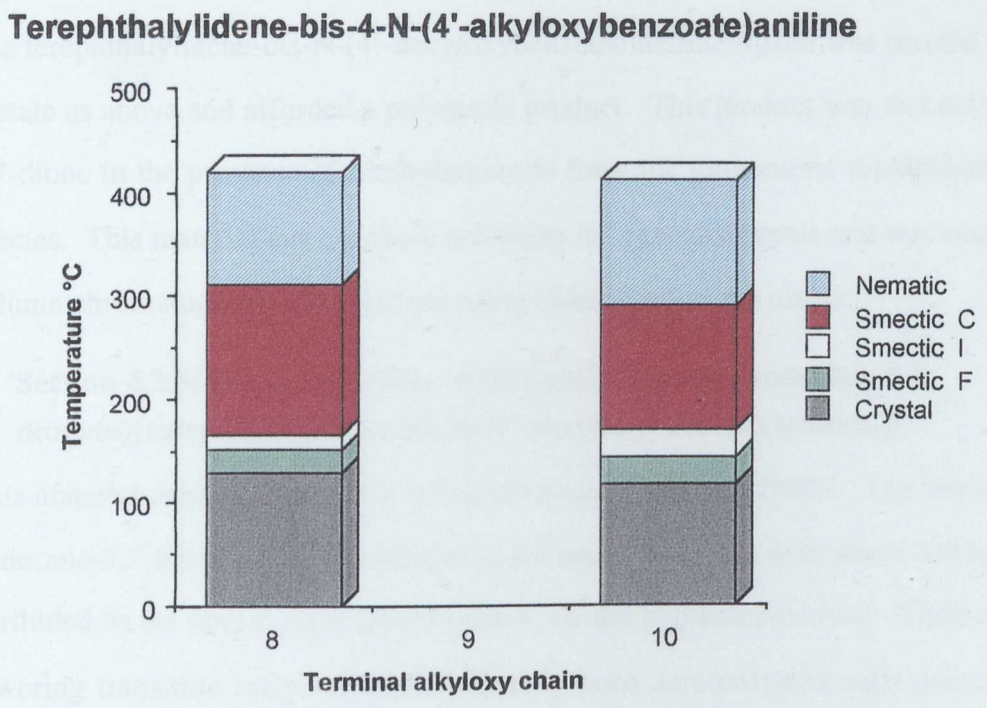

Fig. 4.15: Phase diagram of terephthalylidene-bis-N-(4'-octyloxybenzoate)anilines.

Section 4.2.3: Cyclopalladation of terephthalylidene-bis-N-(4'-octyloxybenzoate)anilines.

The ligand **(19)** was reacted with palladium acetate in acetic acid at 60°C which afforded a dicyclopalladated polymeric product. This product was reacted with sodium acetylacetonate to form the monomeric dipalladated species **(21)**.

This material was poorly soluble in the usual solvents which presented difficulties in purifying the material by column chromatography and also in gaining analysis. A proton NMR spectrum was obtained but no ^{13}C NMR was obtained due to solubility problems. This material melts with rapid decompostion above 290°C with no mesophases observed.

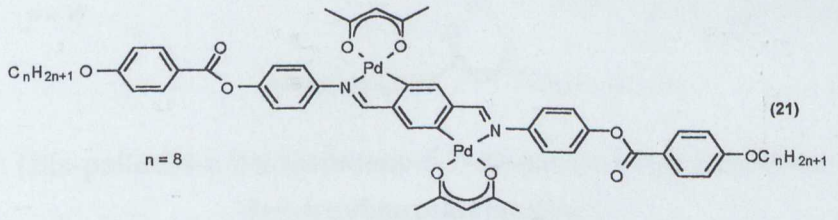

Fig. 4.16: [Bis-palladium-bis(acetylacetonato){terephthalylidene-bis-N-(4'-decyloxybenzoate)aniline}].

Section 4.2.4: Preparation of [Bis-palladium-bis(undecane-5,7-dionato){terephthalylidene-bis-N-(4'-decyloxybenzoate)aniline}].

The terephthalylidene-bis-N-(4'-decyloxybenzoate)aniline ligand was reacted with palladium acetate as above and afforded a polymeric product. This product was reacted with undecane-5,7-dione in the presence of triethylamine to form the monomeric dipalladated β-diketonate species. This material had excellent solubility in organic solvents and was readily purified by column chromatography on silica gel using chloroform as the eluent.

Section 4.2.5: Phase behaviour of [Bis-palladium-bis(undecane-5,7-dionato){terephthalylidene-bis-N-(4'-decyloxybenzoate)aniline}].

This material exhibited a nematic phase between 166°C and 280°C. The lower melting of the undecane-5,7-dione derivative relative to the acetylacetonate derivatives above can be largely attributed to the lateral alkyl chains present on the β-diketonate ring. Their effectiveness in lowering transition temperatures has already been demonstrated with series **(13)** and **(14)**. The increase in the length of the mesogenic core has broadened the nematic phase range, giving a system with a nematic phase of over 110°C. The attenuation of the mesogenic core has however failed to produce more ordered smectic phases such as the smectic C or smectic A phase with this increase in length to breadth ratio. This would suggest that the *trans* dipalladocycles dictate the primary intermolecular interaction for these systems, forming exclusively nematic phases and variation of this basic structure modifies the temperatures at which the nematic phase is observed, but does not alter the degree of order within the phases. This is true for all derivatives that have been prepared.

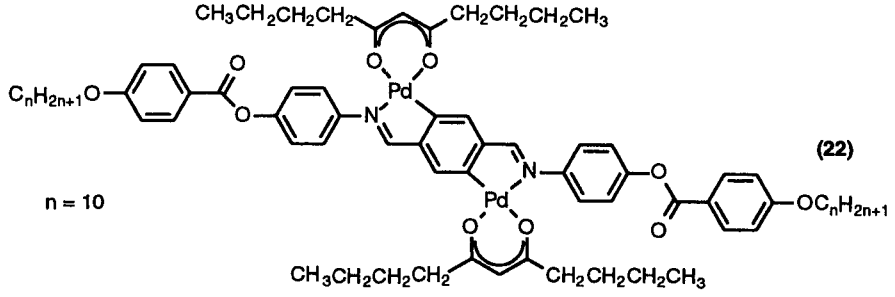

Fig. 4.17: [Bis-palladium-bis(undecane-5,7-dionato{terephthalylidene-bis-N-(4'-decyloxybenzoate)aniline}].

Section 4.3.1: Preparation of bis(4-N-alkyloxybenzylidene)-1,4-phenylenediamines.

For comparison the octyloxy and decyloxy derivatives of **(23)** were prepared. These are

isomers of the ligand **(10)**. They also undergo double cyclopalladation reaction forming *endo* palladocycles but cyclopalladation occurs singly on each of the outer rings of the ligand.

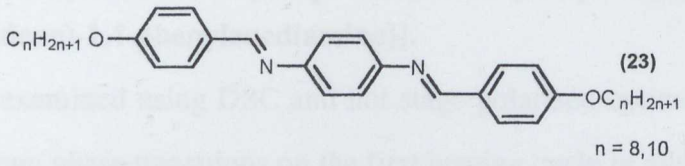

Fig. 4.18: Bis(4-N-alkyloxybenzylidene)-1,4-phenylenediamines.

Section 4.3.2: Phase behaviour of bis(4-N-alkyloxybenzylidene)-1,4-phenylenediamines.

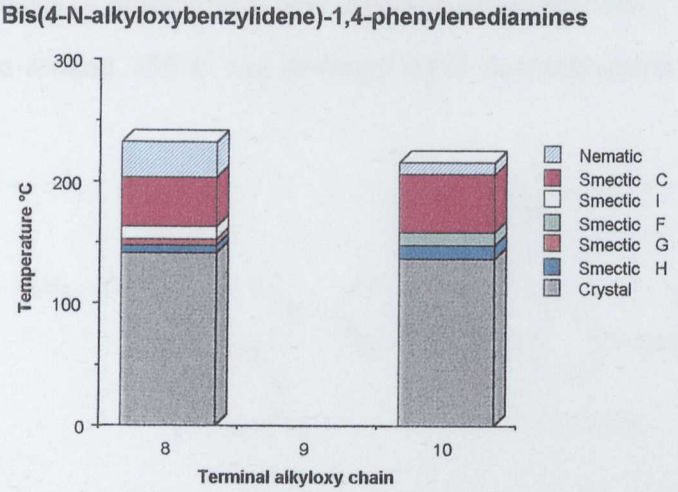

Fig. 4.19: Phase diagram of bis(4-N-alkyloxybenzylidene)-1,4-phenylenediamines.

The phase behaviour of the ligands is shown in figure 4.19, and exhibits the more ordered smectic G' and H' phases in addition to the smectic C, smectic I and nematic phases observed in the analogous isomers from the series **(10)**.

Section 4.3.3: Preparation of [bis-palladium-(acetylacetonato){bis(4-N-alkyloxybenzylidene)-1,4-phenylenediamine}].

While this series of ligands has been prepared previously, [9,10] it has not been used as substrate for the preparation of metallomesogens. Ligand **(23)** undergoes cyclopalladation with palladium (II) acetate in toluene at 60°C forming polymeric systems. These acetato complexes readily react with sodium acetylacetonate to form monomeric systems **(25)**. Due to poor solubility of these acetylacetonate complexes, ^{13}C spectra were not obtained. Proton NMR was sucessfully obtained. Microanalysis was obtained for both materials, though in each instance the percenatge of carbon was about 1% below that expected. Nitrogen and

hydrogen analyses were satisfactory.

Section 4.3.4: Characterisation of [bis-palladium-bis-(acetylacetonato){bis(4-N-alkyloxybenzylidene)-1,4-phenylenediamine}].

The materials were examined using DSC and hot stage polarised optical microscopy. Both materials exhibited two phase transitions on the first heating cycle in addition to the clearing transition, however on a second heating of each material, only a single transition was observed in addition to the clearing transition. The polarised optical microscopy identified the reversible phase transition as a crystal to smectic A transition. The smectic A phase was identified on the basis of homeotropic and myelinic phase textures. These materials clear to the isotropic state around 255°C and undergo rapid decomposition at temperatures above 250°C.

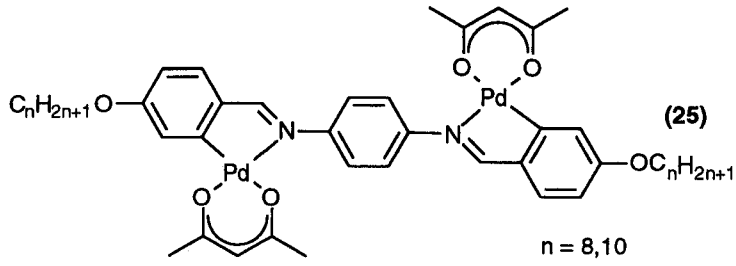

Fig. 4.20: [Bis-palladium-bis-(acetylacetonato){(bis(4-N-alkyloxybenzylidene)-1,4-phenylenediamine)}].

The melting transition for each of the analogues **(25)** is at least 20°C higher than for the corresponding dicyclopalladated isomer **(12)**. The increase in positional order (the formation of lamellar smectic A phases in these isomers when compared with disordered nematic phases in the isomers **(12)** must depend primarily on intermolecular interactions which originate from the palladocycles.

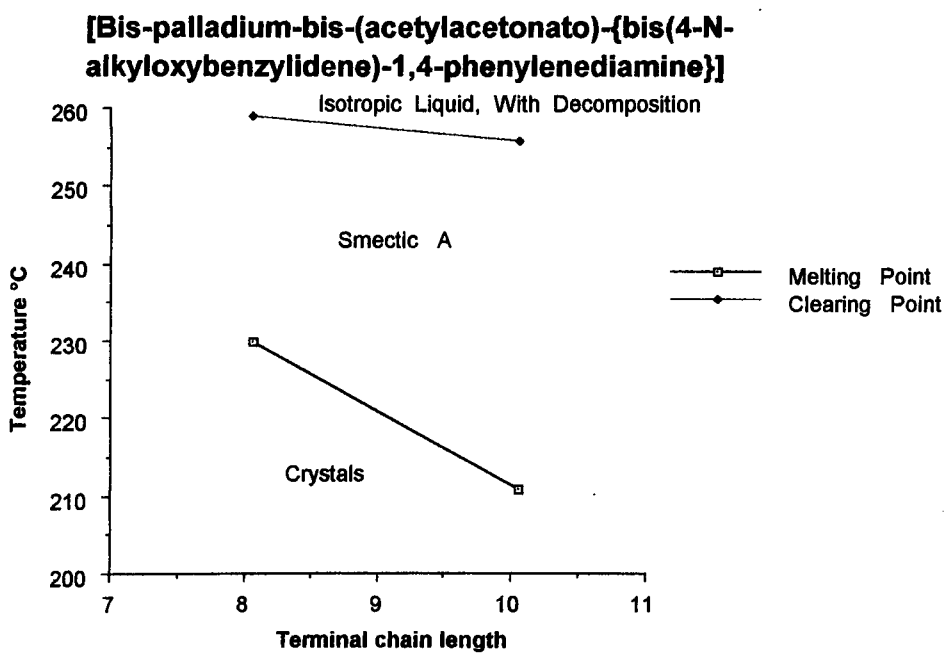

Fig. 4.21: Phase diagram of [bis-palladium-bis(acetylacetonato){bis(4-N-alkyloxybenzylidene)-1,4-phenylenediamine}].

The difference in structure between the two systems can be can be usefully described in the following manner. The system **(12)** has a five membered ring system across the centre of the molecule producing a point of high intermolecular interaction at the centre of the molecule, which is distributed over the area of those five ring systems. These interactions arise from an entirely rigid system and this reduces the range of interactions which are possible. In the case of the complex **(25)**, there are two flexible palladacycles from which strong intermolecular interaction can arise, allowing a larger range of possible intermolecular interactions from each system incorporating three rings. The positioning of the palladocycle leads to more rigid interactions for the two isolated palladated rings compared to the single interaction in the extended dipalladocycle. This is suggested as an explanation of the formation of the more ordered smectic A phases for the system **(25)**. Interdigitation type inertactions may also play a role in the formation of this lamellar phase since molecules in a smectic A phase are known to pass freely between layers.

Section 4.4: Conclusions.

The highly anisotropic, linear terephthalylidene-bis-4-N-alkyloxybenzylidenes system **(10)** is a rich source of mesogenic behaviour, with many analogues in the series showing four or more mesophases. This can be attributed to the planarity of the mesogenic core coupled with

the increased linearity achieved with varying the terminal chain length. Dicyclometallation has been achieved with palladium acetate yielding *trans* substituted products. Monocyclopalladated products were not observed in any of the analysis carried out suggesting that the primary cyclopalladation step activates the ligands towards secondary cyclopalladation. Monomeric dicyclopallated acetylacetonate complexes with hexyloxy terminal chain lengths or greater exhibited nematic phases at temperatures between 187-271°C. No other phases were observed for this class of compound. Dicyclopalladated *trans* complexes containing β-diketonate co-ligands with alkyl substituents groups were also prepared. These exclusively exhibit the nematic phases which occur at temperatures in the range 129-171°C. The phases exhibit enantiotropic or monotropic phases, depending on the length to breadth ratio of the molecules. A tertiary butyl derivative was also prepared which showed enhanced thermal stability, however no mesogenic behaviour was observed.

Attempts to prepare substantial quantities of *cis* dipalladated terephthalylidene-bis-4-N-alkyloxybenzylidenes **(16)** using sodium tetrachloropalladate were unsuccessful either due to formation of *trans* substituted dicyclopalladated complexes or decompostion of the starting materials.

A related terephthalylidene-bis-N-(4'-alkyloxybenzoate)aniline system **(19)** was prepared to probe the effect of an extended aromatic core. The octyloxy and decyloxy derivatives were prepared and these exhibit mesophases similar to **(10)**, however the range of the nematic phase in each case extends to above 400°C, where extensive decomposition occurs. The dicyclopalladated *trans* acetylacetonate complex of terephthalylidene-bis-n-(4'-octyloxybenzoate)aniline **(21)** was prepared, but failed to show mesogenic behaviour, instead decomposing rapidly at temperatures above 290°C. The dicyclopalladated *trans* undecane-5,7-dione complex of terephthalylidene-bis-N-(4'-decyloxybenzoate)aniline **(22)** was also prepared and this material showed a nematic phase from 160°C to 280°C.

The bis(4-N-alkyloxybenzylidene)-1,4-phenylenediamine system **(23)** was also examined for comparison of mesogenic behaviour of the free ligands and the cyclopalladated acetyacetonate complexes **(25)** with that of **(12)**. The free ligands shows slightly more ordered mesophases than are present in the isomeric **(10)** analogues. The complexes **(25)** are

remarkable in that lamellar smectic A phases are observed. This contrasts strongly with the exclusive formation of the nematic phase observed for the isomeric system **(12)**, regardless of terminal chain length. Therefore the presence of two cyclopalladated rings on the outer phenyl groups enhances lamellar ordering while dicyclopalladation on the central ring of promotes the formation of the more disordered nematic phase.

As consequence of this work, trends in the reactivity with palladium (II) and the thermal behaviour of terephthalylidene-bis-4-N-alkyloxybenzylidenes, bis(4-N-alkyloxybenzylidene)-1,4-phenylenediamine and their palladium compounds have been examined. This work has initiated the study of dicyclopalladated metallomesogens as a method for preparing novel liquid crystalline materials.

Section 4.5: References.

1 C Wiegand, *Z. Naturforschg.*, 1957, **12 b**, 512.

2 M Goméz, J Granell and M Martinéz, *J. Chem. Soc., Dalton Trans.*, 1998, 37.

3 J Vincente, J A Abad, B Rink, F S Hernández and M C R de Arellano, *Organomets.*, 1997, **16**, 5269.

4 S Trofimenko, *Inorg. Chem.*, 1973, **12**, 1215.

5 S Chakladar, P Paul, A K Mukherjee, S K Dutta, K K Nanda, D Podder and K Nag, *J. Chem. Soc., Dalton Trans.*, 1992, 3119.

6 S Chakladar, P Paul, K Venkatsubramanian and K Nag, *J. Chem. Soc., Dalton Trans.*, 1991, 2669.

7 E I Tsyganova and L M Dyagileva, *Russ. Chem. Rev.*, 1996, **65**, 315.

8 G W V Cave, D P Lydon and J P Rourke, *J. Organomet. Chem.*, 1998, **555**, 81.

9 S L Arora, T R Taylor, J L Fergason and A Saupe, *J. Am. Chem. Soc.*, 1969, **91**, 3671.

10 J Barberá, M Marcos and J L Serrano, *Mol. Cryst., Liq. Cryst.*, 1987, **149**, 225.

Chapter 5

Section 5.1: Preparation of 3,6-bis(4'-alkyloxyphenyl)pyridazines.

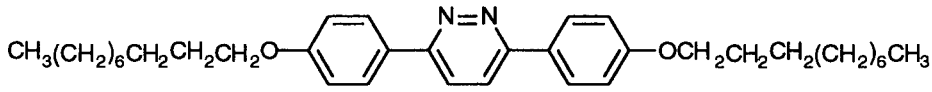

(30)

Fig. 5.1: 3,6-bis(4'-alkyloxyphenyl)pyridazines .

A series of 3,6-bis(4'-alkyloxyphenyl)pyridazines **(30)** was prepared by the elimination of hydrogen sulfide from 3,6-bis(4'-alkyloxyphenyl)-2,7-dihydro-1,4,5-thiadiazepine **(29)** leading to a heterotriene species which which undergoes an electrocyclic ring closure yielding the desired product. Four such pyridazines were prepared with variation in the terminal alkyloxy chains yielding hexyloxy to octyloxy and also decyloxy derivatives.

Section 5.2: Characterisation of 3,6-bis(4'-alkyloxyphenyl)pyridazines.

Analysis was carried out using proton and carbon NMR and microanalysis to confirm the molecular structure and purity of the materials. The thermal behaviour was examined using hot-stage polarised optical microscopy and DSC. These materials exhibited liquid crystalline behaviour, which is detailed in table 5.1.

n	Phase behaviour of 3,6-bis(4'-alkyloxyphenyl)pyridazine ligands. [Temp./°C ($\Delta H/Jg^{-1}$)]												
6	K	87 (20.4)	K'	94 (35.6)	K''	139 (0.40)	K'''	158 (24.4)	S_F	165 (2.09)	S_I	258 (25.9)	I
7	K	112 (87.4)	K'	143 (22.4)	S_G	145 (0.09)	S_F	165 (3.2)	S_I	252 (28.4)	I		
8	K	109 (67.3)	K'	131 (20.7)	S_G	142 (0.18)	S_F	166 (2.7)	S_I	249 (27.2)	I		
10	K	113 (18.9)	K'	121 (18.4)	K''	129 (18.4)	S_G	163 (3.6)	$S_{F/I}$	238 (28.9)	I		

Table 5.1: Thermal analysis of 3,6-bis(4'-alkyloxyphenyl)pyridazine.

These materials show rich mesomorphic behaviour, with examples of smectic G, F and I phases formed within the series. The molecular structure of the 3,6-bis(4'-alkyloxyphenyl)pyridazines favours the formation of ordered smectic phases. A further similarity of the mesophases observed in this series is that they are all based on a hexagonal net. The compact linearity of the mesogenic core (three directly connected *para* substituted aromatic rings) is a near perfect example of a "rigid rod" on a molecular scale. Hence it is

not surprising that these molecules adopt hexagonal close packed structures and modifications of this structure. The ability of these materials to sustain hexagonal type arrays until the isotropic point is reached, (with the total exclusion of phases such as smectic C, smectic A and nematic phases) demonstrates the innate stability of these mesophase structures, when assembled from the rigid planar bis(phenyl)pyridazine core. Examples of phase textures are given in appendix 1.

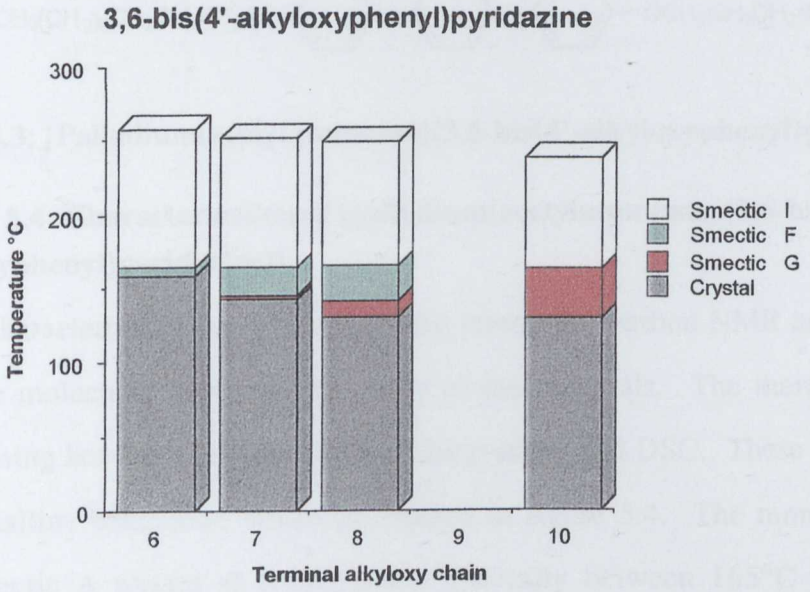

Fig. 5.2: Phase diagram of 3,6-bis(4'-alkyloxyphenyl)pyridazine.

As might be expected, these materials melt to smectic G phases from the crystal phase at lower temperatures with increasing chain length. Clearing points also decrease on increasing chain length, but with smaller magnitude than for melting transitions and therefore mesophase ranges generally increase with increasing chain length.

Section 5.3: Preparation of [palladium(acetylacetonato){3,6-bis(4'-alkyloxyphenyl)pyridazine}].

The pyridazine ligands were then used to carry out various cyclometallation reactions to determine their potential as ligands for metallomesogens. The series of reactions undertaken were monocyclopalladation and dicyclopalladation

Monocyclopalladation of the 3,6-bis(4'-alkyloxyphenyl)pyridazine ligands has been achieved selectively by reaction of one equivalent of palladium acetate with one equivalent of 3,6-bis-

(4'-alkoxyphenyl)pyridazine in acetic acid (16 h) by stirring at 60°C, yielding a bright yellow product. These materials have been characterised by proton NMR and found to be dimeric acetate bridged systems **(31)**. These dimers can split into monomers using sodium acetylacetonate **(32)**.

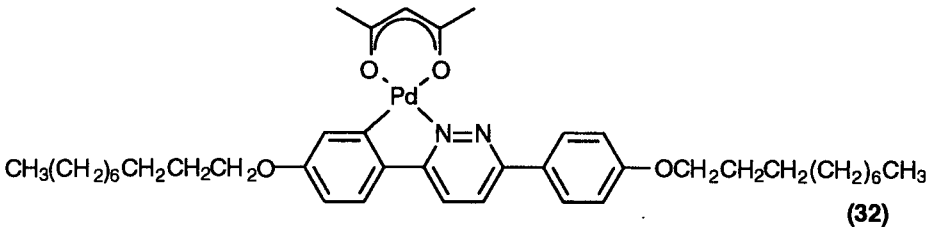

(32)

Fig. 5.3: [Palladium(acetylacetonato){3,6-bis(4'-alkyloxyphenyl)pyridazine}].

Section 5.4: Characterisation of [palladium(acetylacetonato){3,6-bis(4'-alkyloxyphenyl)pyridazine}].

Structural characterisation was obtained using proton and carbon NMR and microanalysis to confirm the molecular structure and purity of the materials. The thermal behaviour was examined using hot-stage polarised optical microscopy and DSC. These materials exhibited liquid crystalline behaviour, which is detailed in figure 5.4. The monomeric complexes exhibit smectic A phases at temperatures generally between 165°C and 290°C, where isotropic phases are observed with the onset of extensive decomposition. The presence of a palladocycle has a disruptive effect on molecular packing relative to the free pyridazine ligand which has shows ordered hexagonal smectic phases for all chain lengths in this series. The formation of the relatively disordered smectic A phase can be attributed to the reduction in linearity coupled with the extension of the planarity in the structure and increased intermolecular interaction arising from increased polarity due to the presence of the palladium (II) metal centre. These features enhance lateral intermolecular interactions, giving rise to the disordered lamellar phase formation.

The compact nature of this system is demonstrated by comparison with the monopalladated complexes in the chapter 3. The most meaningful comparison can be made between [palladium(acetylacetonato){3,6-bis(4'-heptyloxyphenyl)pyridazine}]**(32)** (which forms a smectic A phase at 196°C and clears to the isotropic phase at 290°C) and [palladium-(acetylacetonato){4-heptyloxy-N-(4'-heptyloxybiphenyl)benzylidene}] **(5)** (which forms a smectic A phase at 140°C and clears to the isotropic phase at 245°C). These molecules are

systems based on three aromatic rings, a palladocycle and two heptyloxy terminal chains. The pyridazine complex is a more compact system; the direct linearity of three para substituted contiguous aromatic rings is contrasted with a biphenyl unit coupled discontinuously to a phenyl unit through imine group. This compact structure is the basis for the formation of a more compact palladium acetylacetonate complex. As a consequence, it shows the same liquid crystal phase as the benzylidene structure, but with higher crystal to smectic A and smectic A to isotropic transition temperatures (over 40°C higher in each case) due to greater interaction of the molecules in the crystal phase and in the mesophase.

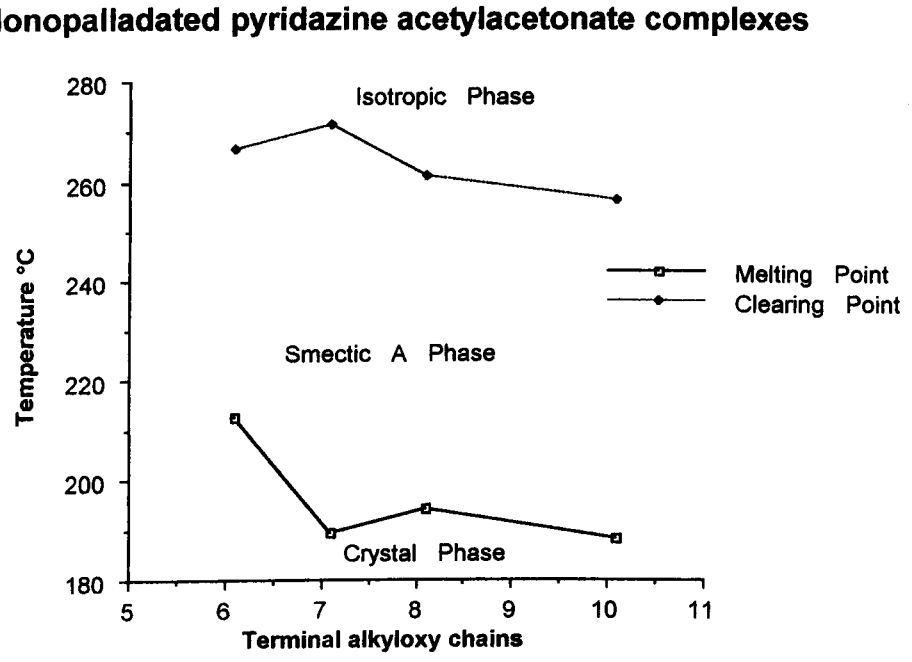

Fig. 5.4: Phase diagram of [palladium(acetylacetonato){3,6-bis (4'-alkoxyphenyl)pyridazine}].

Section 5.5: Preparation of [bis-palladium-bis(acetylacetonato){3,6-bis (4'-alkoxyphenyl)pyridazine}].

3,6-bis(4'-heptyloxyphenyl)pyridazine reacts with two equivalents of palladium (II) acetate in acetic acid (48 h) to form a red dipalladated polymeric complex **(33)**.

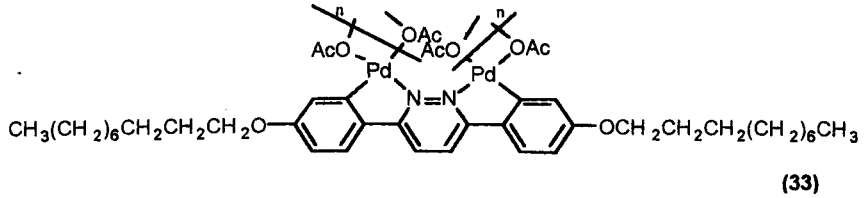

(33)

Fig. 5.5: [Bis-palladium-bis(μ-acetato){3,6-bis (4'-decyloxyphenyl)pyridazine}].

This material (**33**) reacts with sodium acetylacetonate to form a monomeric dipalladated yellow complex. This material is difficult to purify as column chromatography with silica and alumina leads to decomposition of the material with formation of the monopalladated acetylacetonate complex. This material was purified by filtering a solution of the material in chloroform and washing the material as a powder in diethyl ether and hexane.

Section 5.6: Charaterisation of [bis-palladium-bis(acetylacetonato){3,6-bis (4'-alkoxyphenyl)pyridazine}].

Structural characterisation was obtained using proton and carbon NMR and microanalysis to confirm the molecular structure and gauge the purity of the material. The material was found to be 3% lower than required for carbon content and within acceptable limits for nitrogen and hydrogen. A complex with a similar geometry, prepared by Trofimenko[1] is shown in figure 5.6. The nonequivalence of the benzylic hydrogens (^{1}H δ6.80, 4.62) and the N-ethyl substituents (^{1}H δ3.7-2.4) in Trofimenko's complex demonstrates that the acetylacetonate rings and the central phenyl ring are not co-planar, but twisted to give a chiral complex. The proton signals on the central ring of the pyridazine complex have the same chemical shift (^{1}H δ7.76), and the acetylacetonate methyl groups are chemical shift equivalent (^{1}H δ2.06). This suggests that the twisting of the acetylacetonate groups may be restricted to some extent by the phenyl groups in the para position of the pyridazine ring.

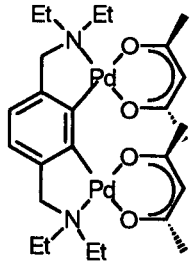

Cis

Fig. 5.6: *Cis* [Bis-palladium(acac)$_2$ {N,N,N',N'-tetraethyl-p-xylene- α,α'-diamine}].

The thermal behaviour was examined using hot stage polarised optical microscopy and DSC. This material showed a smectic A phase observed at 169°C using DSC while the clearing point was observed as 210°C with extensive decomposition. The poor stability of this

material can be accounted for by the ring strain present due to the steric clash of neighbouring acetylacetonate rings.

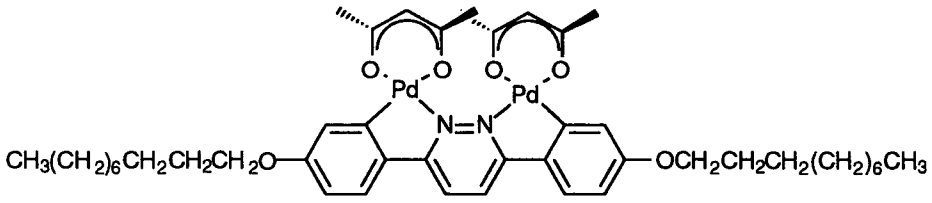

(34)

Fig. 5.7: [Bis-palladium-bis(acetylacetonato){3,6-bis(4'-alkoxyphenyl)pyridazine}]

Section 5.7: Conclusions.

The series of 3,6-bis(4'-alkoxyphenyl)pyridazines prepared exclusively exhibit ordered hexagonal mesophases (smectic I, smectic F and smectic G) between 130°C and 258°C. This highly ordered mesogenic behaviour can be attributed to the compact, planar, linear structure arising from the contiguous bonding of three aromatic rings in a *para* substitution pattern. This enables highly efficient intermolecular hexagonal packing interactions between the molecules in the mesophases that is sustained until the point of isotropization. The ligand reacts with one equivalent of palladium acetate to exclusively form yellow monopalladated dimeric acetate bridged complexes. These form yellow monomeric planar systems when reacted with sodium acetylacetonate which show exclusively smectic A phases between 162°C and 290°C. This lamellar ordering is attributed to enhanced intermolecular interactions arising due to the presence of the palladium metal and a decrease in linearity arising from the presence of the cyclopalladated ring and the acetylacetonate group. Controlled dicyclopalladation of this system is also possible using two equivalents of palladium acetate over longer periods of time. The acetylacetonate dervattive **(34)** of the dicyclopalladated 3,6-bis(4'-decyloxyphenyl)pyridazine acetate complex exhibits a smectic A phase at 169°C which clears to the isotropic state at 210°C. The low thermal stability of this material is attributed to the ring strain arising from the steric clash of the two acetylacetonate groups.

This work has identified 3,6-bis(4'-alkyloxyphenyl)pyridazines as a novel meosgenic system and a versatile ligand for cyclopalladation. This ligand has large potential for cyclometallation with other metals to give a diverse range of complexes.

Section 5.8: References.

1 S Trofimenko, *Inorg. Chem.*, 1973, **12**, 1215.

Chapter 6

Section 6.0: General.

All chemicals were used as supplied, unless noted otherwise. Unless noted otherwise, all NMR spectra were obtained on a Bruker AC250 in $CDCl_3$ and are referenced to external TMS. Thermal analyses were performed on an Olympus BH2 microscope equipped with a Linkam HFS 91 heating stage and a TMS90 controller, at a heating rate of 10 K min^{-1}. DSC measurements were carried out on a Perkin Elmer Pyris 1 Differential Scanning Calorimeter at a heating rate of 10 K min^{-1}. All elemental analyses were performed by Warwick Analytical Service.

Section 6.1: Preparation and characterisation of 4-heptyloxy-N-(4'-heptyloxybiphenyl)benzylidene (3).

Preparation of 4'-heptyloxy-4-nitro-biphenyl (1).

Potassium carbonate (5 equiv., 21.19g, 1.53 x 10^{-1} mol) was added to a solution of 4'-hydroxy-4-nitro-biphenyl (6.00g, 2.8 x 10^{-2} mol) and 1-bromoheptane (1.1 equiv., 5.50 g, 3.07 x 10^{-2} mol) in butanone (150 cm^3). The reaction mixture was refluxed (24 h). The mixture was filtered, the solvent removed and the crude product collected. The product was washed with hexane to remove excess alkyl halide and yield the pure product.

Yield: 7.90g (2.52 x 10^{-2} mol), 90%.

NMR Data ($CDCl_3$):

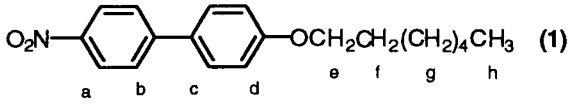

δ_H:	8.23	2H, AA'XX', H_a
	7.66	2H, AA'XX', H_b
	7.55	2H, AA'XX', H_c
	6.99	2H, AA'XX', H_d
	4.00	3H, t, ^3J(HH) 6.5Hz, H_e
	1.80	2H, m, ^3J(HH) 7Hz, H_f
	1.40	8H, m, H_g
	0.90	3H, t, ^3J(HH) 7Hz, H_h

Preparation of 4'-heptyloxy-4-amino-biphenyl (2).

4-Heptyloxy-4-nitro-biphenyl (7.90g, 2.52 x 10^{-2} mol) was dissolved in ethanol (100cm^3) and tin (II) chloride dihydrate (31.05g, 1.39 x 10^{-1} mol) was added. The mixture was refluxed (2 h) under nitrogen and then cooled slowly to room temperature. A mixture of ice/water (200 cm^3) was added turning the mixture cloudy. Potassium carbonate was added until the solution was alkaline (pH = 7-8). The mixture was extracted with dichloromethane and the organic fraction was washed (2 x water [500 cm^3], sat NaCl [500cm^3]) and dried ($MgSO_4$). The solvent was removed yielding the product.

Yield: 6.48g (2.29 x 10^{-2} mol), 90%.

NMR Data ($CDCl_3$):

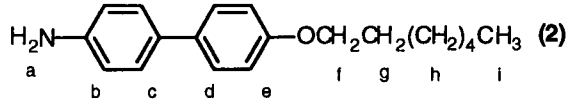

δ_H:

7.45	2H, AA'XX', H_c
7.36	2H, AA'XX', H_d
6.93	2H, AA'XX', H_b
6.74	2H, AA'XX', H_e
3.98	2H, t, ^3J(HH) 6.5Hz, H_f
3.68	2H, br. s, H_a
1.80	2H, m, H_g
1.30	8H, m, H_h
0.90	3H, t, ^3J(HH) 7Hz, H_i

Preparation of 4-heptyloxy-N-(4'-heptyloxybiphenyl)benzylidene (3).

4-heptyloxy-benzaldehyde (1.61g, 7.10 x 10^{-3} mol) was added to 4'-heptyloxy-4-amino-biphenyl (2.00g, 7.10 x 10^{-3} mol) dissolved in toluene (200cm^3), and refluxed (2 h) using a Dean Stark water trap and in the presence of molecular sieves. The product was repeatedly recrystallised from chloroform to give the pure ligand.

Yield: 2.47g (5.1 x 10^{-3} mol), 72%.

NMR Data ($CDCl_3$):

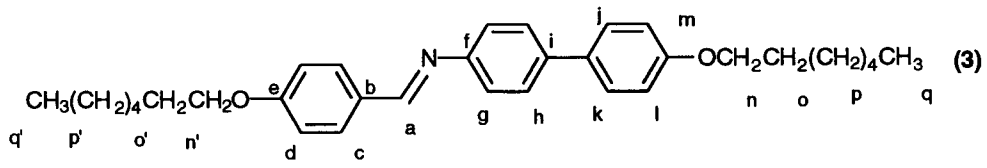

δ_H:

8.44	1H, s, H_a
7.87	2H, AA'XX', H_c
7.57	2H, AA'XX', H_h
7.55	2H, AA'XX', H_k
7.28	2H, AA'XX', H_g
6.96	2H, AA'XX', H_d
6.95	2H, AA'XX', H_l
4.03	2H, t, ^{3}J(HH) 7Hz, $H_{n'}$
4.01	2H, t, ^{3}J(HH) 7Hz, H_n
1.81	4H, m, $H_{o,o'}$
1.40	16H, m, $H_{p,p'}$
0.89	6H, t, ^{3}J(HH) 7Hz, $H_{q,q'}$

δ_C:

159.2 (C_a)	158.5 ($C_{e,m}$)	138.1 (C_i)	132.9 ($C_{b/j}$)
13.05(C_c)	127.7 (C_h)	127.2 (C_k)	121.2 (C_g)
114.7 ($C_{d/l}$)	114.6 ($C_{d/l}$)	68.0 (C_n)	67.8 ($C_{n'}$)
31.7 ($C_{p,p'}$)	29.1 ($C_{o,o'}$)	28.9 ($C_{p,p'}$)	25.9 ($C_{p,p'}$)
14.0 ($C_{q,q'}$)			

A number of homologues were prepared in a similar fashion: elemental and thermal analysis data is detailed in table 6.1 and table 6.2 respectively.

n, m	C % found	(expected)	H % found	(expected)	N % found	(expected)
4, 4	80.9	(80.8)	7.8	(7.8)	3.4	(3.5)
4, 7	81.2	(81.2)	8.4	(8.4)	3.1	(3.2)
7, 4	81.6	(81.2)	8.4	(8.4)	3.2	(3.2)
7, 7	81.3	(81.6)	8.7	(8.9)	3.0	(2.9)

Table 6.1: Microanalysis of 4-alkyloxy-N-(4'-alkyloxybiphenyl)benzylidene ligands (3).

n, m	Phase behaviour of 4-alkyloxy-N-(4'-alkyloxybiphenyl)benzylidene T[°C].								
4, 4	K	191	S_F	197	S_C	201	N	276	I
4, 7	K	160	S_F	171	S_C	216	N	252	I
7, 4	K	171	S_F	178	S_C	215	N	255	I
7, 7	K	157	S_F	161	S_C	217	N	254	I

Table 6.2: Phase behaviour of 4-alkyloxy-N-(4'-alkoxybiphenyl)benzylidene ligands (3).

Section 6.1.2: Preparation and characterisation of [palladium (acetylacetonato){4-heptyloxy-N-(4'-heptyloxybiphenyl)benzylidene}] (5).

Preparation of [bis-palladium-(μ-acetato){4-heptyloxy-N-(4'-heptyloxybiphenyl) benzylidene}] (4).

Palladium acetate (0.191g, 8.5 x 10^{-4} mol) was dissolved in a solution of 4-heptyloxy-N-(4'-heptyloxybiphenyl)benzylidene (0.41g, 8.5 x 10^{-4} mol) in acetic acid (250cm^3) and stirred (60°C, 20 h). The solvent was then removed, the crude product redissolved in chloroform, filtered to remove traces of palladium black and the yellow solution obtained was evaporated to dryness yielding the acetato complex.

Yield: 0.55g (4.2 x 10^{-4} mol), 98%.

NMR Data ($CDCl_3$):

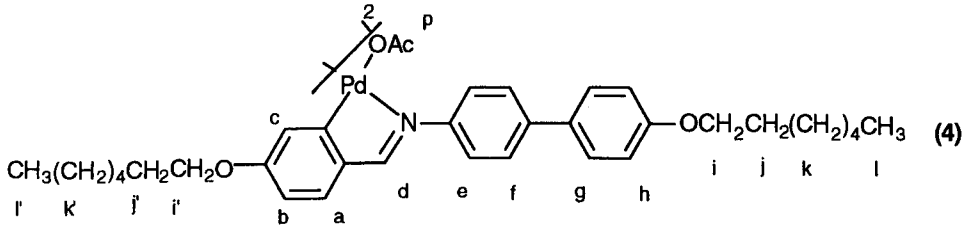

δ_H:

7.59	1H, s,	H_d
7.51	2H, AA'XX',	H_f
7.35	2H, AA'XX',	H_g
7.18	1H, d, ^{3}J(HH) 8.5Hz,	H_a
6.95	2H, AA'XX',	H_e
6.78	2H, AA'XX',	H_h
6.59	1H, dd, ^{3}J(HH) 8.5Hz, ^{4}J(HH) 2.5Hz,	H_b
6.03	1H, d, ^{4}J(HH) 2.5Hz,	H_c
4.05	4H, t, ^{3}J(HH) 6.5Hz,	$H_{i/i'}$
4.00	4H, t, ^{3}J(HH) 6.5Hz,	$H_{i/i'}$
1.90	3H, s,	H_p
1.81	4H, m, ^{3}J(HH) 6.5Hz,	$H_{j,j'}$

1.40 16H, m, $H_{k,k'}$

0.88 6H, m, $H_{l,l'}$

Preparation of [palladium(acetylacetonato){4-heptyloxy-N-(4'-heptyloxybiphenyl)benzylidene}] (5).

Sodium acetylacetonate (0.018g, 1.54 x 10^{-1} mol) was added to a solution of the acetate bridged palladium complex **(4)**, (0.200g, 1.54 x 10^{-4} mol) in acetone (150cm^3) at room temperature and stirred (2 h). The solvent was removed and the product was purified by column chromatography on silica, eluting with a 50/50 mixture of dichloromethane and hexane.

Yield: 0.135g (1.96 x 10^{-4} mol), 62%.

NMR Data ($CDCl_3$):

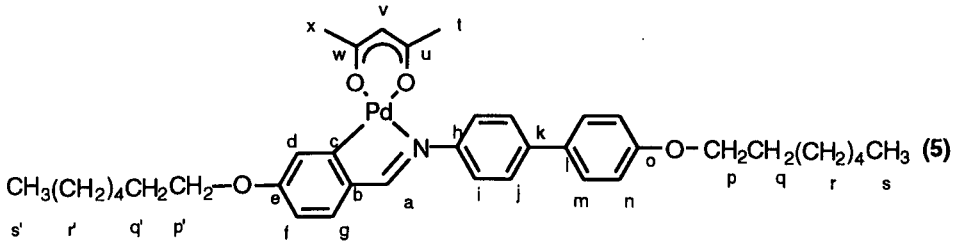

δ_H: 8.03 1H, s, H_a

7.58 2H, AA'XX', H_j

7.51 2H, AA'XX', H_m

7.46 2H, AA'XX', H_i

7.31 1H, d, ^{3}J(HH) 8.5Hz, H_g

7.14 1H, d, ^{4}J(HH) 2.5Hz, H_d

6.97 2H, AA'XX', H_n

6.60 1H, dd, ^{3}J(HH) 8.5Hz, ^{4}J(HH) 2.5Hz, H_f

5.36 1H, s, H_v

4.08 2H, t, ^{3}J(HH) 6.5Hz, $H_{p'}$

4.02 4H, t, ^{3}J(HH) 6.5Hz, H_p

2.10 3H, s, H_x

1.91 3H, s, H_t

1.84 4H, m, $H_{q,q'}$

1.40 16H, m, $H_{r,r'}$

0.90 6H, m, $H_{s,s'}$

δ_C:	188.3 ($C_{u/w}$)	185.7 ($C_{u/w}$)	172.4 (C_a)	160.4 (C_e)
	158.7 (C_o)	146.3 (C_h)	139.7 ($C_{b/c}$)	138.8 ($C_{b/c}$)
	132.6 (C_k)	129.5 (C_g)	127.9 (C_m)	127.6 (C_l)
	126.5 (C_j)	123.6 (C_i)	115.7 (C_d)	114.7 (C_n)
	111.4 (C_f)	100.1 (C_v)	67.7 (C_p)	67.5 ($C_{p'}$)
	31.2 ($C_{q/q'}$)	31.1 ($C_{q/q'}$)	29.2 ($C_{r,r'}$)	27.8 ($C_{t'}$)
	27.4 (C_x)	25.9 ($C_{r,r'}$)	19.1 ($C_{r,r'}$)	13.8 ($C_{s,s'}$)

A number of analogues were prepared in a similar fashion: elemental and thermal analysis data is detailed in table 6.3 and table 6.4 respectively.

n, m	C % found	(expected)	H % found	(expected)	N % found	(expected)
4, 4	63.4	(63.4)	6.2	(6.2)	2.3	(2.3)
4, 7	64.5	(64.4)	6.6	(6.7)	2.0	(2.2)
7, 4	64.7	(64.4)	6.7	(6.7)	2.3	(2.2)
7, 7	66.3	(66.0)	7.2	(7.3)	1.9	(2.0)

Table 6.3: Microanalysis of series of palladium acetylacetonate complexes (5).

n, m	Phase behaviour of palladium acetylacetonate complexes T[°C].						
4, 4	K	184	S_A	209	N	258	I
4, 7	K	155	S_A	260[a]	I		
7, 4	K	162	S_A	241	N	261	I
7, 7	K	140	S_A	245	I		

a = decomposition.

Table 6.4: Phase behaviour of palladium acetylacetonate complexes (5).

Section 6.1.3: Preparation and characterisation of [palladium (cyclopentadienyl){4-heptyloxy-N-(4'-heptyloxybiphenyl)benzylidene}] (7).

Preparation of chloro bridged palladium complex (6).

One equivalent of 0.4N methanolic hydrogen chloride was added to [palladium-(μ-acetato){4-heptyloxy-N-(4'-heptyloxybiphenyl)benzylidene}] **(4)** (0.356g, 3.1 x 10^{-4} mol) dissolved in chloroform (250cm^3) at room temperature. This caused the clear yellow solution to become cloudy. The solvent was removed and the crude product was washed with acetone (15 cm^3) and filtered to collect the product.

Yield: 0.21g (1.72 x 10^{-4} mol), 54%.

NMR Data ($CDCl_3$):

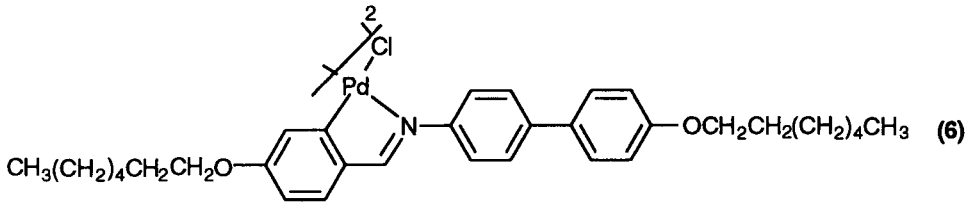

(6)

NMR data: Compound (**6**) has not been fully characterised by NMR. However, comparison with the NMR spectrum for the acetato complex (**4**) shows the absence of the proton resonances asssociated with the bridging acetato group.

Preparation of palladium cyclopentadienyl complex (7).

Lithium cyclopentadiene (4 equiv. 0.055g, 7.64 x 10^{-4} mol) was added to a solution of the chloro bridged palladium complex, (**7**), (0.239g,1.91 x 10^{-4} mol), in THF (250cm^3) and gently refluxed (1 h). The solvent was removed and the mixture was filtered. The crude product was purified by column chromatography on silica, eluting with chloroform yielding a red solid.

Yield: 0.020g (2.58 x 10^{-5} mol), 14%.

NMR Data ($CDCl_3$):

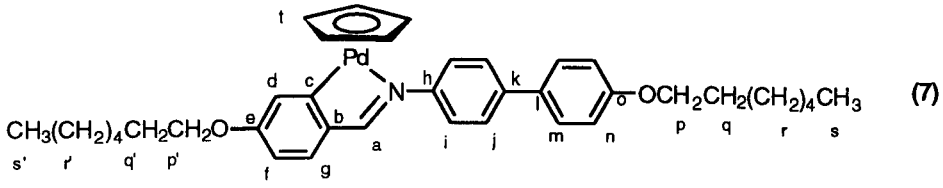

(7)

δ_H:

7.86	1H, s,	H_a
7.54	4H, m,	$H_{i,m}$
7.52	1H, d, ^{3}J(HH) 8.5Hz,	H_g
7.35	2H, AA'XX',	H_j
7.24	1H, d, ^{4}J(HH) 2.5Hz,	H_d
6.97	2H, AA'XX',	H_n
6.59	1H, dd, ^{3}J(HH) 8.5Hz, ^{4}J(HH) 2.5 Hz,	H_f
5.80	5H, s,	H_t
4.02	2H, t, ^{3}J(HH) 7Hz,	$H_{p'}$
4.02	2H, t, ^{3}J(HH) 7Hz,	H_p
1.84	4H, m,	$H_{q/q'}$
1.40	16H, m,	$H_{r,r'}$
0.90	6H, m,	$H_{s,s'}$

δ_C:	164.3 (C_a)	158.9 (C_e)	157.7 (C_o)	139.6 ($C_{b/c/h}$)
	138.9 ($C_{b/c/h}$)	138.4 ($C_{b/c/h}$)	132.4 (C_k)	131.8 (C_g)
	130.58 (C_l)	128.0 ($C_{j/m}$)	127.9 ($C_{j/m}$)	125.6(C_d)
	123.0 (C_i)	114.8 (C_n)	110.5 (C_f)	95.8 (C_t)
	68.0 (C_p)	67.8 ($C_{p'}$)	31.8 (C_q)	31.3 ($C_{q'}$)
	29.2 ($C_{r,r'}$)	26.0 ($C_{r,r'}$)	19.2 ($C_{r,r'}$)	14.1 ($C_{s/s'}$)
	13.8 ($C_{s/s'}$)			

A number of analogues were prepared in a similar fashion: microanalysis and thermal analysis data is detailed in table 6.5 and table 6.6 respectively.

n, m	C % found	(expected)	H % found	(expected)	N % found	(expected)
4, 4	67.4	(67.2)	6.2	(6.3)	2.4	(2.5)
4, 7	68.5	(69.5)	6.7	(7.1)	2.2	(2.3)
7, 4	67.1	(68.5)	7.0	(6.7)	1.5	(2.3)
7, 7	69.3	(69.6)	7.4	(7.2)	2.1	(2.1)

Table 6.5: Microanalysis of the series of palladium cyclopentadienyl complexes (7).

n, m	Phase behaviour of palladium cyclopentadienyl complexes T[°C].							
4, 4	K	125	N	182[a]	I			
4, 7	K	101	N	145	I			
7, 4	K	125	N	179[a]	I			
7, 7	K	92	S_A	165	N	178	I	

a = decomposition.

Table 6.6: Phase behaviour of palladium cyclopentadienyl complexes (7).

Section 6.2.1: Preparation and characterisation of terephthalylidene-bis-4-N-(4'-alkyloxybenzylidene) (10).

Preparation of 4-decyloxynitrobenzene (8).

Potassium carbonate (5 equiv., 21.19g, 1.53 mol) was added to a solution of 4-nitro-phenol (4.25g, 3.06 x 10^{-2} mol) and 1-bromodecane (1.1 equiv., 7.46g, x 3.37 x 10^{-2} mol) in butanone (150 cm^3). The reaction mixture was refluxed (24 h). The mixture was filtered and the solvent removed.

Yield: 7.26g (2.60 x 10^{-2} mol), 85%.

NMR Data ($CDCl_3$):

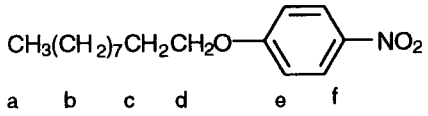

(8)

δ_H: 8.13 2H, AA'XX', H_f
6.89 2H, AA'XX', H_e
4.00 2H, t, ^3J(HH) 6.5Hz, H_d
1.78 2H, m, H_c
1.40 14H, m, H_b
0.88 3H, t, ^3J(HH) 6.5Hz, H_a

Preparation of 4-decyloxyaminobenzene (9).

Tin(II) chloride dihydrate (31.05g, 15.6 x 10^{-1} mol) was added to a solution of 4-decyloxynitrobenzene (7.26g, 2.60 x 10^{-2} mol) in ethanol (100cm^3). The mixture was refluxed (2 h) under nitrogen and cooled slowly to room temperature. A mixture of ice/water (200 cm^3) was added turning the mixture cloudy. Potassium carbonate was added until the solution was alkaline (pH = 7-8). The mixture was extracted with dichloromethane, the organic fraction washed (H_2O, sat NaCl soln.) and dried ($MgSO_4$). The solvent was removed yielding the product.

Yield: 5.84g (2.34 x 10^{-2} mol), 90%.

NMR Data ($CDCl_3$):

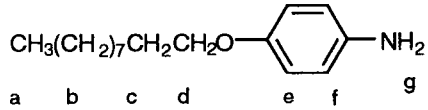

(9)

δ_H: 6.52 2H, AA'XX', H_e
6.35 2H, AA'XX', H_f
3.98 2H, t, ^3J(HH) 6.5Hz, H_d
3.68 2H, br. s, H_a
1.78 2H, m, ^3J(HH) 7Hz, H_c
1.40 14H, m, H_b
0.88 3H, t, ^3J(HH) 6.5Hz, H_a

Preparation of terephthalylidene-bis-4-N-(4'-decyloxybenzylidene) (10).

Terephthaldicarboxaldehyde (1.57g, 1.17 x 10^{-2} mol) was added to 4-decyloxyaminobenzene (5.84g, 2.34 x 10^{-3} mol) dissolved in toluene (200cm^3), and refluxed for (2 h) using a Dean Stark water trap and in the presence of molecular sieves. The product was repeatedly recrystallised from chloroform, to give the pure ligand.

Yield: 5.45g (9.13 x 10^{-3} mol), 78%.

NMR Data ($CDCl_3$):

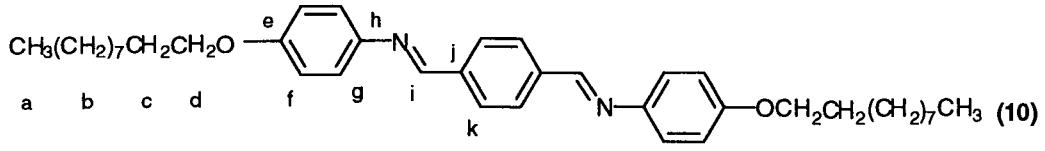

(10)

δ_H: 8.54 2H, s, H_i
8.00 4H, s, H_k
7.28 4H, AA'XX', H_g
6.94 4H, AA'XX', H_f
3.98 4H, t, ^3J(HH) 6.5Hz, H_d
1.78 4H, m, ^3J(HH) 7Hz, H_c
1.40 28H, m, H_b
0.88 6H, t, ^3J(HH) 6.5Hz, H_a

δ_C:	128.82 (C_k)	122.2 (C_g)	114.9 (C_f)	68.2 (C_d)
	31.8 (C_c)	29.5 (C_b)	29.29 (C_b)	29.2 (C_b)
	25.9 (C_b)	22.6 (C_b)	14.0 (C_a)	

Due to poor solubility of **(10)**, and despite running an overnight carbon accumulation, signals were not obtained for the following carbon nuclei: (e, h, j, i)

A homlogous series of compounds were prepared: microanalysis and thermal analysis are

detailed in tables 6.7 and 6.8 respectively.

n	C % found	(expected)	H % found	(expected)	N % found	(expected)
3	78.3	(78.0)	7.1	(7.1)	7.1	(7.0)
4	78.5	(78.3)	7.5	(7.5)	6.5	(6.6)
5	78.9	(79.0)	8.0	(7.9)	6.1	(6.3)
6	79.0	(79.3)	8.2	(8.3)	5.6	(5.7)
7	79.2	(79.7)	8.4	(8.7)	5.2	(5.5)
8	80.1	(79.9)	8.9	(8.9)	5.3	(5.2)
10	80.6	(80.2)	9.4	(9.2)	4.8	(4.9)

Table 6.7: Microanalysis of terephthalylidene-bis-4-N-(4'-alkyloxybenzylidene) (10).

n	Phase behaviour of terephthalylidene-bis-4-N-alkyloxybenzylidene ligands. [Temp./°C ($\Delta H/Jg^{-1}$)]												
3	K	209 (114.8)	N	308 (4.3)	I								
4	K	190 (90.0)	S_C	219 (0.3)	N	296 (5.3)	I						
5	K	172 (70.8)	S_I	181 (9.3)	S_C	221 (0.3)	S_A	231 (1.9)	N	271 (3.7)	I		
6	K	158 (70.7)	S_I	173 (8.1)	S_C	228 (0.5)	S_A	233 (1.3)	N	260 (3.8)	I		
7	K	152 (76.9)	S_I	172 (8.1)	S_C	228 (0.8)	S_A	235 (0.3)	N	248 (3.8)	I		
8	K	143 (68.2)	S_F	148 (0.5)	S_I	173 (8.4)	S_C	231 (1.1)	S_A	234 (0.12	N	242 (5.6)	I
10	K	134 (93.3‡)	S_F	137 (93.3‡)	S_I	169 (8.4)	S_C	224.5 (8.0)	S_A	228 (8.2*)	N	229.5 (8.2*)	I

* incorporates enthalpy change for S_A to N and N to I transitions

‡ incorporates enthalpy change for K to S_F and S_F to S_I transitions

Table 6.8: Phase behaviour of terephthalylidene-bis-4-alkyloxybenzylidene.

Section 6.2.2: Preparation and characterisation of [bis-palladium(β-diketonato){terephthalylidene-bis-4-N-(4'-decyloxybenzylidene)}] (12), (13), (14).

Preparation of [bis-palladium-bis(μ-acetato){terephthalylidene-bis-4-N(4'-decyloxybenzylidene)}] (11).

Palladium acetate (0.150g, 6.7 x10^{-4} mol) was added to terephthalylidene-bis-4-n-decyloxybenzylidene (0.200g, 3.35 x 10^{-4} mol) dissolved in acetic acid (200cm^3) and stirred (60°C, 48 h). The product was then dissolved in chloroform and filtered through celite.

Yield: 0.278g (3.00 x 10^{-4} mol), 90%.

NMR Data ($CDCl_3$):

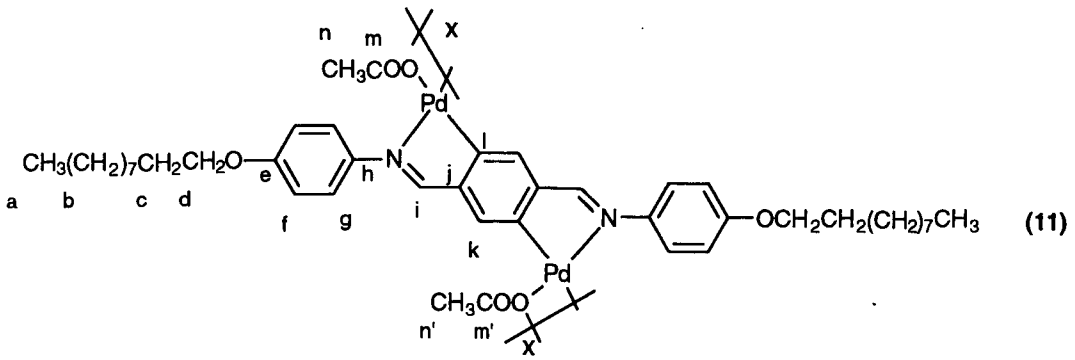

(11)

δ_H: 7.90 2H, s, H_i
7.05 4H, AA'XX', H_g
6.55 4H, AA'XX', H_f
6.20 2H, s, H_k
3.99 4H, ^3J(HH) 7Hz, H_d
2.07 3H, s, $H_{n/n'}$
2.00 3H, s, $H_{n/n'}$
1.78 4H, m, H_c
1.23 28H, m, H_b
0.88 6H, t, ^3J(HH) 6.5Hz, H_a

Preparation of [bis-palladium-bis(acetylacetonato){terephthalylidene-bis-4-N(4'-decyloxybenzylidene)}] (12).

Sodium acetylacetonate (0.073g, 6.00 x 10^{-4} mol) was added to [bis-palladium-bis(μ-acetato){terephthalylidene-bis-4-N(4'-decyloxybenzylidene)}] (0.180g, 1.00 x 10^{-4} mol) suspended in acetone (200cm^3) and heated under reflux (24 h). The solvent was then removed and the crude product extracted with chloroform, washed twice with water and once with sodium chloride solution and dried ($MgSO_4$).

Yield: 0.154g (1.53×10^{-4} mol), 77%.

The product was then purified by column chromatography on a silica column eluting with chloroform and washed with hexane.

Yield: 0.054g (5.40×10^{-5}mol), 27%.

NMR Data ($CDCl_3$):

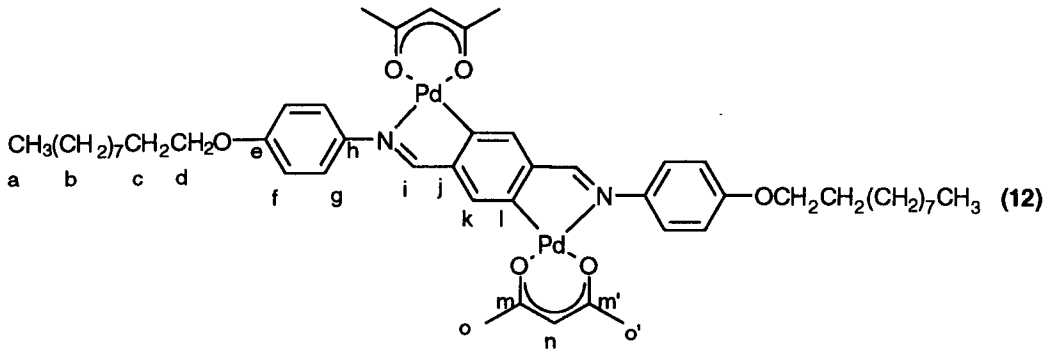

(12)

δ_H:	8.13	2H, s, H_i
	7.56	2H, s, H_k
	7.39	4H, AA'XX', H_g
	6.88	4H, AA'XX', H_f
	5.34	2H, s, H_n
	3.99	4H, t, ^3J(HH) 6.5Hz, H_d
	2.07	6H, s, $H_{o/o'}$
	1.89	6H, s, $H_{o/o'}$
	1.40	28H, m, H_b
	0.89	6H, t, ^3J(HH) 6.5Hz, H_a

δ_C:	188.3 ($C_{m/m'}$)	185.60 ($C_{m/m'}$)	172.9 (C_i)	158.9 (C_e)
	151.7 ($C_{h/j}$)	147.1 ($C_{h/j}$)	140.8 (C_l)	129.3 (C_k)
	124.5 (C_g)	114.0 (C_f)	100.1 (C_n)	68.0 (C_d)
	31.5 (C_c)	29.1 (C_b)	27.4 ($C_{o/o'}$)	27.8 ($C_{o/o'}$)
	25.6 (C_b)	22.5 (C_b)	13.9 (C_a)	

A homologous series of compounds was prepared: microanalysis and thermal analysis are detailed in tables 6.9 and 6.10 respectively.

n	C % found	(expected)	H % found	(expected)	N % found	(expected)
4	54.0	(54.5)	5.3	(5.3)	3.1	(3.3)
5	55.3	(55.5)	5.5	(5.6)	3.2	(3.3)
6	56.9	(56.5)	5.7	(5.9)	2.9	(3.1)
7	57.7	(57.3)	6.2	(6.1)	2.8	(3.0)
8	58.0	(58.2)	6.3	(6.4)	3.1	(3.0)
10	59.5	(59.7)	6.8	(6.8)	2.9	(2.8)

Table 6.9: Microanalysis of [bis-palladium-bis(acetylacetonato){terephthalylidene-bis-4-N(4'-decyloxybenzylidene)}] (12).

n	Bis-palladium[di-acac-(terephthalylidene-bis-4-N-(4'-alkyloxybenzylidene))]. T. /°C				
4	K	285	I^a		
5	K	280	I^a		
6	K	261	N	271	I^a
7	K	238	N	253	I^a
8	K	203	N	255	I^a
10	K	187	N	246	I

a = decomposition

Table 6.10: Phase behaviour of [bis-palladium-bis(acetylacetonato){terephthalylidene-bis-4-N(4'-decyloxybenzylidene)}] (12).

Preparation of [bis-palladium-bis(undecane-5,7-dione){terephthalylidene-bis-4-N(4'-octyloxybenzylidene)}] (13).

Undecane-5,7-dione (0.128g, 6.90 x 10^{-4} mol) and triethylamine (0.35g, 0.5cm^3, 4.8 x10^{-3} mol) were added to [bis-palladium-bis(μ-acetato){terephthalylidene-bis-4-N(4'-octyloxybenzylidene)}] (0.150g, 8.62 x 10^{-5} mol) suspended in acetone (300cm^3) and heated under reflux (24 h). The solvent was then removed and the product extracted with chloroform, washing with water (x2), with sodium chloride solution (x1) and dried ($MgSO_4$). The solvent was then removed and the orange powder was then washed with acetone.

Yield: 0.072g (3.28 x 10^{-5} mol), 38%.

NMR Data ($CDCl_3$):

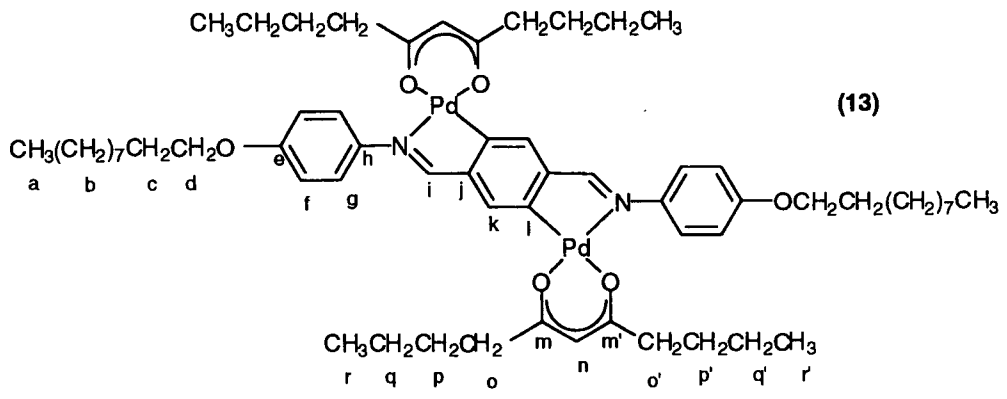

(13)

δ_H:	8.15	2H, s, H_i
	7.60	2H, s, H_k
	7.39	4H, AA'XX', H_g
	6.90	4H, AA'XX', H_f
	5.33	2H, s, H_n
	3.98	4H, t, ^3J(HH) 6.5Hz, H_d
	2.30	4H, t, ^3J(HH) 7.5Hz, $H_{o/o'}$
	2.15	4H, t, ^3J(HH) 7.5Hz, $H_{o/o'}$
	1.80	4H, m, H_c
	1.65	4H, m, $H_{p/p'}$
	1.40	40H, m, $H_{p/p'}$, $H_{q,q'}$, H_b
	0.93	6H, t, ^3J(HH) 7.5Hz, $H_{a/r/r'}$
	0.89	6H, m, $H_{a/r/r'}$
	0.86	6H, t, ^3J(HH) 7.5Hz, $H_{a/r/r'}$

δ_C:	191.3 ($C_{m/m'}$)	188.7 ($C_{m/m'}$)	172.9 (C_i)	158.8 (C_e)
	151.9 ($C_{h/j}$)	147.1 ($C_{h/j}$)	140.9 (C_l)	129.3 (C_k)
	124.5 (C_g)	114.1 (C_f)	99.4 (C_n)	68.2 (C_d)
	40.5 ($C_{o/o'}$)	40.3 ($C_{o/o'}$)	31.5 (C_c)	29.2 ($C_{p/p'}$)
	29.1 (C_b)	28.1 ($C_{p/p'}$)	25.9 (C_b)	22.5 (C_b)
	22.4 ($C_{q/q'}$)	22.3 ($C_{q/q'}$)	14.0 ($C_{r, r'/a}$)	13.98 ($C_{r, r'/a}$)

Preparation of [bis-palladium-bis(2,2,6,6 tetra-methyl-heptane-3,5-dionato){terephthalylidene-bis-4-N(4'-octyloxybenzylidene)}] (14).

To [bis-palladium-bis(μ-acetato){terephthalylidene-bis-4-N(4'-octyloxybenzylidene)}] (0.160g, 0.184 x 10^{-3} mol) suspended in acetone (500cm^3) 2,2,6,6 tetra-methyl-heptanedione (0.135g, 0.736 x 10^{-3} mol) and triethylamine (0.35g, 0.5cm^3, 4.8 x10^{-3} mol) was added and stirred (72 h). The solvent was then removed, the product extracted with chloroform, washing with water (x2)

and with sodium chloride solution. The solvent was then removed. The orange powder was then washed with hexane and chromatographed using chloroform on silica gel.

Yield: 0.100g (8.90×10^{-5} mol), 56%.

Tert-butyl NMR Data ($CDCl_3$):

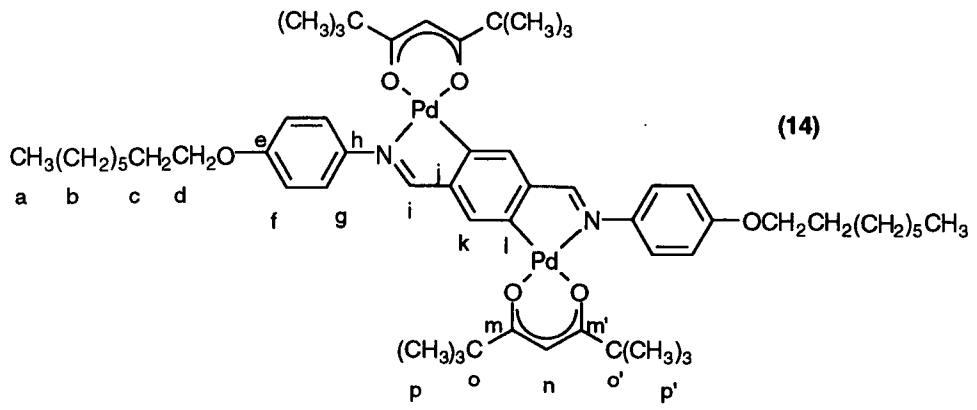

δ_H:

8.14	2H, s,	H_i
7.64	2H, s,	H_k
7.40	4H, AA'XX',	H_g
6.89	4H, AA'XX',	H_f
5.68	2H, s,	H_n
4.00	4H, t, ^3J(HH) 6.5Hz,	H_d
1.80	4H, m,	H_c
1.40	20H, m,	H_b
1.24	18H, s,	$H_{p/p'}$
1.02	18H, s,	$H_{p/p'}$
0.89	6H, t, ^3J(HH) 6.5Hz,	H_a

δ_C:

197.7 ($C_{m/m'}$)	195.4 ($C_{m/m'}$)	173.2 (C_i)	158.7 (C_e)
152.5 ($C_{h/j}$)	147.1 ($C_{h/j}$)	141.1 (C_l)	129.6 (C_k)
124.6 (C_g)	114.3 (C_f)	90.9 (C_n)	68.4 (C_d)
41.6 ($C_{o/o'}$)	41.0 ($C_{o/o'}$)	31.8 (C_c)	29.3 (C_b)
29.2 (C_b)	29.1 (C_b)	29.0 ($C_{p/p'}$)	28.5 ($C_{p/p'}$)
25.9 (C_b)	22.6 (C_b)	14.10 (C_a)	

A series of analogues were prepared: microanalysis and phase behaviour are detailed in tables 6.11. and 6.12 respectively. The octane-5,7-dione derivative was obtained as a mixture of isomers (concluded from the presence of two peaks for H_i at δ 8.12 and δ 8.16) due to the unsymmetrical nature of the ligand.

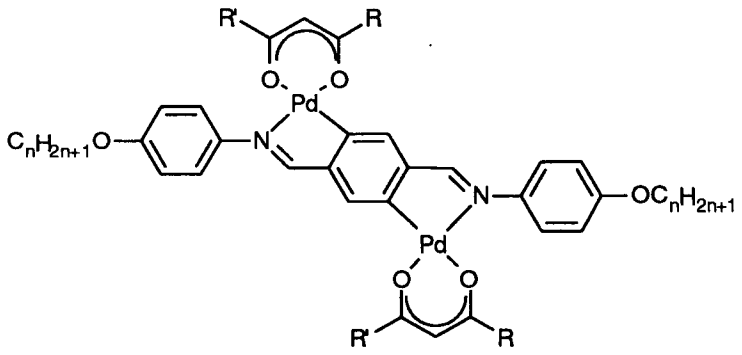

n	R	R'	C% found	(expected)	H% found	(expected)	N% found	(expected)
4	4	4	59.4	(59.7)	6.7	(6.8)	2.9	(2.8)
5	4	4	59.9	(60.4)	7.0	(6.7)	2.2	(2.7)
6	4	4	61.0	(61.0)	7.3	(7.2)	2.8	(2.6)
7	4	4	61.8	(61.7)	7.4	(7.4)	2.6	(2.6)
8	4	1	60.4	(60.3)	7.0	(7.0)	2.7	(2.7)
8	4 ^{n}Bu	4 ^{n}Bu	62.5	(62.3)	7.6	(7.6)	2.4	(2.5)
8	6	6	64.5	(64.4)	8.1	(8.2)	2.2	(2.3)
8	8	8	66.2	(66.1)	8.7	(8.9)	2.1	(2.1)
8	4 ^{t}Bu	4 ^{t}Bu	62.0	(62.3)	7.5	(7.6)	2.9	(2.5)
10	4	4	63.5	(63.4)	7.9	(7.9)	2.4	(2.4)

Table 6.11: Microanalysis of β-diketone complexes (13), (14).

n	R	R'	Phase behaviour of β-diketone complexes. T. /°C.				
4	4	4	K	185	I	171	N^{a}
5	4	4	K	171	I	168	N^{a}
6	4	4	K	177	I	168	N^{a}
7	4	4	K	135	N	146	I
8	4	1	K	208	I	170	N^{a}
8	4 ^{n}Bu	4 ^{n}Bu	K	119	N	148	I
8	6	6	K	133	N	142	I
8	8	8	K	140	I	129	N^{a}
8	4 ^{t}Bu	4 ^{t}Bu	K	260	I		
10	4	4	K	132	N	149	I

a = monotropic

Table 6.12: Phase behaviour of β-diketone complexes (13), (14).

Section 6.2.3: Preparation of *cis* dipalladated terephthalylidene-bis-4-N-(4'-alkyloxybenzylidene) acetylacetonate complexes (15).

Preparation of *cis* dipalladated terephthalylidene-bis-4-N-(4'-alkyloxybenzylidenes (15), (16).

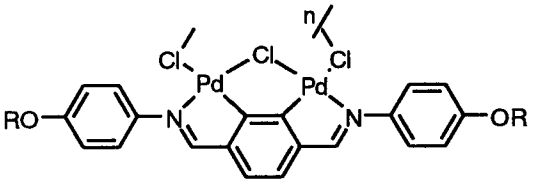

(15)

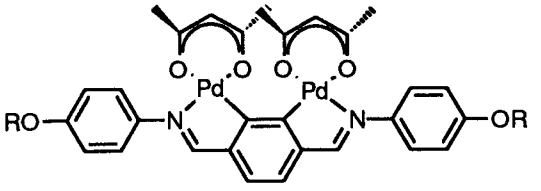

(16)

Terephthalylidene-bis-4-N-(4'-decyloxybenzylidene) (0.050g, 8.4 x 10^{-5} mol) and Na_2PdCl_4 (0.049g, 1.68 x 10^{-4} mol) were stirred in methanol (48 h) at 60°C. The solvent was then removed and the orange product was redissolved in acetone. Sodium acetylacetonate was added and the mixture was stirred overnight at room temperature. The solvent was then removed and the crude product was dried under vacuum.

This afforded the *cis* isomer **(16)** in 10% yield and the *trans* isomer in 90% yield observed using proton NMR. Attempts to isolate the *cis* isomer in large quantities failed, due to its decomposition when undergoing column chromatography on silica gel using chloroform.

NMR Data ($CDCl_3$):

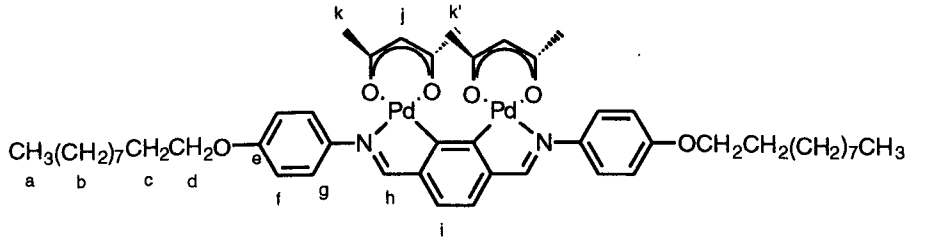

(16)

δ_H:

8.14	2H, s,	H_i
7.65	2H, s,	H_h
7.40	4H, AA'XX',	H_g
6.92	4H, AA'XX',	H_f
5.38	2H, s,	H_j
4.00	4H, m,	H_d
2.12	6H, s,	$H_{k/k'}$

1.90 6H, s, $H_{k/k'}$

1.40 28H, m, H_b

0.90 6H, m, H_a

Acidolysis of *trans* [dipalladium-(μ-chloro){terephthalylidene-bis-4-N-(4'-alkyloxybenzylidene}]: a potential pathway towards *cis* [dipalladium-(μ-chloro){terephthalylidene-bis-4-N-(4'-alkyloxybenzylidene}] (15) via a ligand exchange mechanism.

Trans [dipalladium-(μ-chloro){terephthalylidene-bis-4-N-(4'-alkyloxybenzylidene}] (0.100g,1.30 x 10^{-4} mol) was dissolved in acetic acid and stirred overnight at 80°C. The solvent was then removed and the product was dried under vacuum. The product was then dissolved in acetone and reacted with sodium acetylacetonate (0.031g, 2.60 x 10^{-4} mol) (24 h). The solvent was then removed and the product dried under vacuum.

Section 6.3.1: Preparation and characterisation of terephthalylidene-bis-4-N-(4'-alkyloxybenzoate)anilines (19).

Preparation of terephthalylidene-4-N-hydroxyaniline (17).

To hydroxyaniline (2.00g, 1.83 x 10^{-2} mol) dissolved in toluene (200ml), 1,4-terephthaldicarboxyaldhyde (1.23g, 9.16 x 10^{-3} mol) was added and the mixture was refluxed using a Dean Stark apparatus. The solvent was then removed.

Yield 2.60g (8.21 x 10^{-3} mol), 87%.

NMR Data (Acetone d^6):

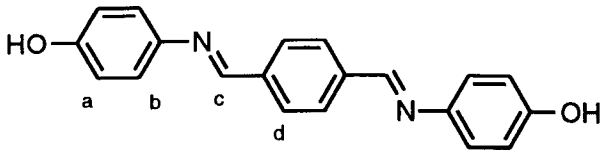

(17)

δ_H: 8.68 2H, s, H_c

8.05 4H, s, H_d

7.28 4H, AA'XX', H_b

6.91 4H, AA'XX', H_a

Preparation of 4-decyloxybenzoic acid (18).

To 4-hydroxybenzoic acid (10.00g, 7.24 x 10^{-2} mol) dissolved in an ethanol/water solution (85%/15%), (300ml), potassium hydroxide (10.00g, 1.78 x 10^{-2} mol), bromodecane (17.61g, 7.96 x 10^{-2} mol) and potassium iodide (0.050g, 3.00 x 10^{-4} mol) were added and refluxed (72 h). The solvent was then removed and a dilute solution of HCl (300ml) was added to the reaction mixture. The resulting suspension was then boiled until a clear aqueous layer was obtained with a white organic layer floating on the surface. The mixture was then extracted with chloroform (2 x 150 ml). The organic phase was then washed with a sodium chloride solution and dried ($MgSO_4$). The solvent was then removed and the crude product was recrystallised in chloroform.

Yield 7.45g (2.68 x 10^{-2} mol), 37%.

NMR Data ($CDCl_3$):

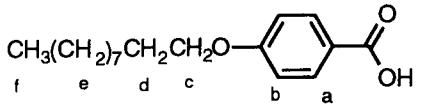

(18)

δ_H:	8.06	2H, AA'XX', H_a
	6.90	2H, AA'XX', H_b
	4.01	2H, t, ^3J(HH) 6.7Hz, H_c
	1.90	2H, m, H_d
	1.40	14H, m, H_e
	0.88	3H, t, ^3J(HH) 6.7Hz, H_f

Preparation of terephthalylidene-bis-4-N-(4'-decyloxybenzoate)aniline (19).

To 4-decyloxybenzoic acid (2.20g, 7.91 x 10^{-3} mol), dissolved in dichloromethane (50ml), oxalyl chloride (1.10g, 8.69 x 10^{-3} mol, 0.76ml) was added. To this solution a catalytic quantity of DMF was added and the reaction mixture was refluxed (2 h) resulting in a clear yellow solution. The solvent was then removed and the yellow solid was dried under vacuum, removing any residual oxalyl chloride. The 4-decyloxybenzoyl chloride was then redissolved in dichloromethane. A solution of terephthalylidene-bis-4-n-hydroxyaniline (1.25g, 3.96 x 10^{-3} mol) in dichloromethane (40ml) was then added. To the resulting orange solution, triethylamine (1.20g, 1.19 x 10^{-2} mol, 1.7ml) was added and the reaction was allowed to reflux overnight. The

solvent was then removed and the crude product was recrystallised in ethyl acetate yielding a yellow powder.

Yield: 0.68g (8.3×10^{-4} mol), 21%.

NMR Data ($CDCl_3$):

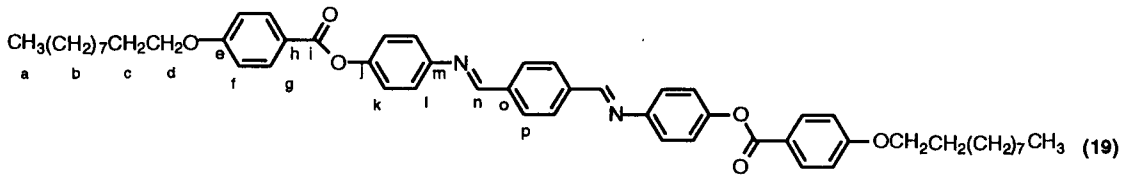

(19)

δ_H: 8.54 2H, s, H_n
8.15 4H, AA'XX', H_g
8.00 4H, s, H_p
7.33 4H, AA'XX', H_k
7.26 4H, AA'XX', H_l
6.98 4H, AA'XX', H_f
4.04 4H, t, ^3J(HH) 6.4Hz, H_d
1.84 4H, m, H_c
1.40 28H, m, H_b
0.88 6H, t, ^3J(HH) 6.4Hz, H_a

δ_C: 165.0 (C_h) 163.6 (C_l) 159.4 (C_c) 149.5 (C_d)
149.2 (C_g) 138.6 (C_b) 132.3 (C_j) 129.2 (C_a)
122.5 (C_k) 121.9 (C_e) 121.4 (C_h) 114.3 (C_f)
68.3 (C_m) 31.8 (C_n) 29.3 (C_o) 29.2 (C_o)
29.1 (C_o) 26.0 (C_o) 22.6 (C_o) 14.1 (C_p)

The octyloxy analogue was prepared in addition to the decyloxy analogue and microanalysis and phase behaviour are presented in tables 6.13 and 6.14 respectively.

	C %	H %	N %
n	found (expected)	found (expected)	found (expected)
8	75.0 (76.9)	7.1 (7.2)	3.2 (3.6)
10	75.3 (77.5)	7.6 (7.7)	3.0 (3.4)

Table 6.13: Microanalysis of terephthalylidene-bis-4-N-(4'-alkoxybenzoate)aniline (19).

n	Phase behaviour of terephthalylidene-bis-4-N-(4'-alkoxybenzoate)aniline. T. /°C ($\Delta H/Jg^{-1}$)										
8	K	130 (22.13)	S_F	152 (0.040)	S_I	165 (2.36)	S_C	311 (3.41)	N	420	I
10	K	117 (9.78)	S_F	143 (0.30)	S_I	169 (2.76)	S_C	291 (0.188)	N	411	I

Table 6.14: Phase behaviour of terephthalylidene-bis-4-N-(4'-alkoxybenzoate)aniline.

Section 6.3.2: Preparation of [bis-palladium-bis(acetylacetonato){terephthalylidene-bis-4-N-(4'-octyloxybenzoate)aniline}] (21).

Preparation of [bis-palladium-bis(μ-acetato){terephthalylidene-bis-4-N-(4'-octyloxybenzoate)aniline}] (20).

To terephthalylidene-bis-4-N-(4'-octyloxybenzoate)aniline) (0.250g, 3.65 x 10^{-4} mol) in acetic acid (300ml) at 60°C palladium acetate (0.163g, 7.30 x 10^{-4} mol) was added and stirred (48 h). The solvent was then removed and the product dried under vacuum.

Yield: 0.29g (2.9 x 10^{-4} mol), 80%.

NMR Data ($CDCl_3$):

No NMR data was recorded due to the insolubility of **(20)**.

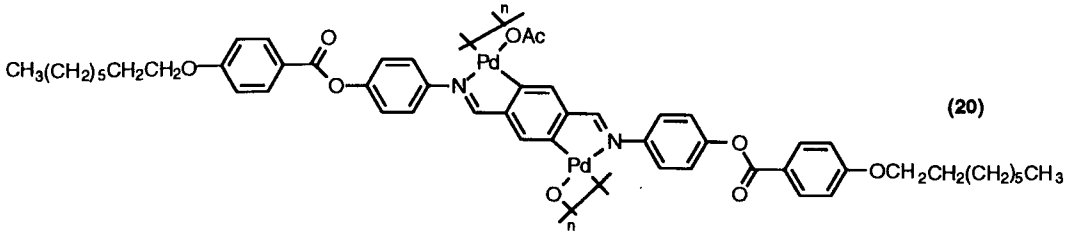

(20)

Preparation of [bis-palladium-bis(acetylacetonato){terephthalylidene-bis-4-N-(4'-octyloxybenzoate)aniline}] (21).

To [bis-palladium-bis(μ-acetato){terephthalylidene-bis-4-N-(4'-octyloxybenzoate)aniline}] (0.200g, 2.08 x 10^{-4} mol) **(20)** suspended in acetone (300ml), sodium acetylacetonate (0.101g, 8.32 x 10^{-4} mol) was added and refluxed (48 h). The solvent was then removed, the product extracted with chloroform, washing with water, (2) and with sodium chloride solution and dried ($MgSO_4$).

Yield: 0.092g (8.9 x 10^{-5} mol), 43%.

NMR Data ($CDCl_3$):

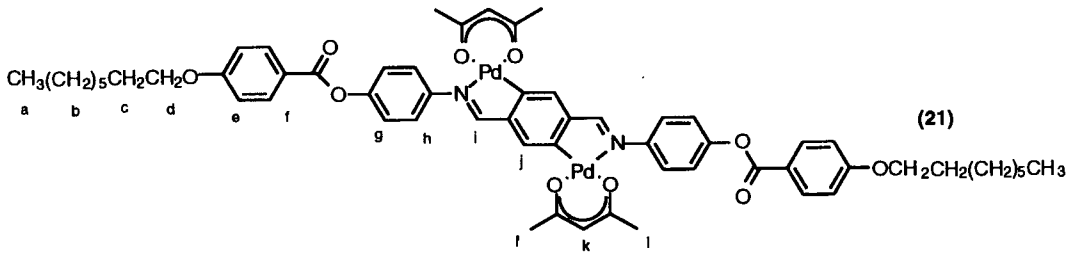

(21)

δ_H:

8.26	2H, s,	H_i
8.14	4H, AA'XX',	H_f
7.64	2H, s,	H_j
7.51	4H, AA'XX',	H_g
7.26	4H, AA'XX',	H_h
7.00	4H, AA'XX',	H_e
5.36	2H, s,	H_k
4.04	4H, t, ^3J(HH) 6.4Hz,	H_d
2.09	6H, s,	$H_{l/l'}$
1.88	6H, s,	$H_{l/l}$
1.80	4H, m,	H_c
1.60	20H, m	H_b
0.89	6H, t, ^3J(HH) 6.4Hz,	H_a

δ_C: **(21)** is not sufficently soluble in common solvents to allow acquisition of a carbon NMR.

Thermal behaviour: rapid decomposition on melting at 290°C.

Preparation of [bis-palladium-bis(undecane-5,7-dionato){terephthalylidene-bis-4-N-(4'-decyloxybenzoate)aniline}] (22).

To [bis-palladium-bis(μ-acetato){terephthalylidene-bis-4-N-(4'-decyloxybenzoate)aniline}] (0.115g, 1.03 x 10^{-2} mol) suspended in acetone (300ml), undecane-5,7-dione (0.075g, 4.12 x 10^{-2} mol) was added with triethylamine (0.041g, 4.12 x 10^{-2} mol) and refluxed (48 h). The solvent was then removed, the product extracted with chloroform, washing with water, (x 2) and with sodium chloride solution and dried ($MgSO_4$). The solvent was then removed and the orange powder was then columned on silica using a chloroform as the eluent and finally washed with acetone.

Yield: 0.050g (3.7 x 10^{-5} mol), 35%.

NMR Data ($CDCl_3$):

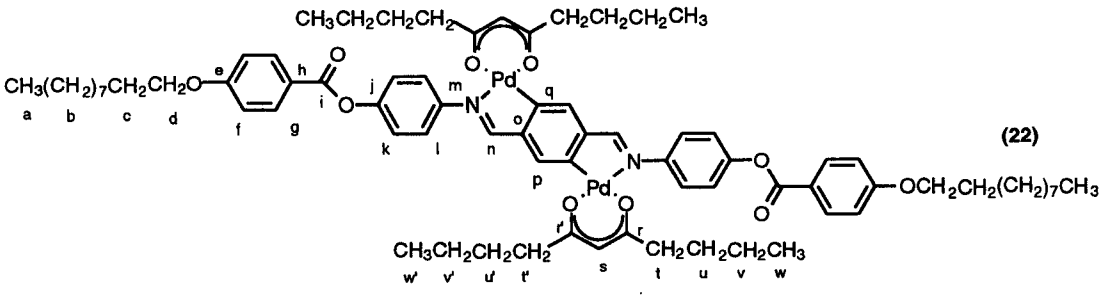

(22)

δ_H:

8.24	2H, s,	H_n
8.14	4H, AA'XX',	H_g
7.66	2H, s,	H_p
7.51	4H, AA'XX',	H_k
7.26	4H, AA'XX',	H_l
7.00	4H, AA'XX',	H_f
5.34	2H, s,	H_s
4.04	4H, t, ^3J(HH) 6.4Hz,	H_d
2.32	4H, m,	$H_{t/t'}$
2.15	4H, m,	$H_{t/t'}$
1.80	4H, m,	H_c
1.67	4H, m,	$H_{u/u'}$
1.30	40H, m,	$H_{u/u'}$, $H_{v,v'}$, H_b
0.93	6H, m,	$H_{a/w/w'}$
0.87	6H, m,	$H_{a/w/w'}$
0.85	6H, m,	$H_{a/w/w'}$

δ_C:

191.4 ($C_{r/r'}$)	188.7 ($C_{r/r'}$)	174.5 (C_n)	164.6 (C_i)
163.5 (C_e)	152.4 ($C_{m/o}$)	150.5 ($C_{m/o}$)	147.3 (C_j)
145.1 (C_q)	132.2 (C_g)	129.9 (C_p)	124.5 (C_l)
121.8 (C_k)	121.2 (C_h)	114.2 (C_f)	99.6 (C_s)
68.3 (C_d)	40.5 ($C_{t/t'}$)	40.3 ($C_{t/t'}$)	31.8 (C_c)
29.5 (C_b)	29.3 ($C_{b/u/u'}$)	29.0 ($C_{b/u/u'}$)	28.0 ($C_{u/u'}$)
25.9 (C_b)	22.6 (C_b)	22.4 ($C_{v/v'}$)	22.2 ($C_{v/v'}$)
14.1 ($C_{a/w/w'}$)	14.0 ($C_{a/w/w'}$)	13.9 ($C_{a/w/w'}$)	

	Phase behaviour of [bis-Pd-(undecane-5,7-dione){C10/C10 ester}] . T. /°C ($\Delta H/Jg^{-1}$)				
4,4	K	166 (29.46)	N	280[a]	I

a = decomposition

Table 6.15: Phase behaviour of [bis-palladium-bis(undecane-5,7-dionato){terephthalylidene-bis-4-N-(4'-decyloxybenzoate)aniline}] (22).

Section 6.4.1: Preparation and characterisation of bis(4-N-alkyloxybenzylidene)-1,4-phenylenediamines (23).

Preparation of bis(4-N-alkyloxybenzylidene)-1,4-phenylenediamines (23).

1,4-Phenylenediamine (1.57g, 1.45 x 10^{-2} mol) was added to 4-decyloxybenzaldehyde (7.61g, 2.90 x 10^{-2} mol) dissolved in toluene (200cm^3) and refluxed (2 h) using a Dean Stark water trap and in the presence of molecular sieves. The product was repeatedly recrystallised from chloroform and washed with hexane, to give the pure ligand.

Yield: 5.45g (9.19 x 10^{-3} mol), 78%.

NMR Data ($CDCl_3$):

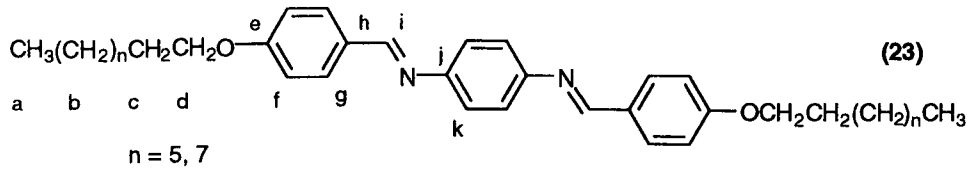

(23)

δ_H:

8.43	2H, s,	H_i
7.86	4H, AA'XX',	H_g
7.26	4H, s,	H_k
6.98	4H, AA'XX',	H_f
4.05	4H, t, ^3J(HH) 6.5Hz,	H_d
1.78	4H, m, ^3J(HH),	H_c
1.40	28H, m,	H_b
0.88	6H, t, ^3J(HH) 6.5Hz,	H_a

δ_C:

161.7 (C_i)	158.9 (C_e)	149.8 (C_f)	130.3 (C_h)
129.0 (C_k)	121.6 (C_g)	114.6 (C_f)	68.1 (C_d)
31.7 (C_c)	29.1 (C_b)	28.9 (C_b)	25.9 (C_b)
22.5 (C_b)	14.0 (C_a)		

The octyloxy analogue was also prepared: microanalysis and thermal analysis are detailed in

tables 6.16 and 6.17 respectively.

n	C % found (expected)	H % found (expected)	N % found (expected)
8	80.1 (80.0)	9.0 (9.0)	5.5 (5.2)
10	80.9 (80.5)	9.6 (9.5)	5.0 (4.7)

Table 6.16: Microanalysis of bis(4-N-alkoxybenzylidene)-1,4-phenylenediamines (23).

n	Phase behaviour of bis(4-N-alkoxybenzylidene)-1,4 phenylenediamine. T. /°C ($\Delta H/Jg^{-1}$)
8	K 142 (11.53) $S_{H'}$ 148 (3.35) $S_{G'}$ 153 (0.66) S_I 163 (5.67) S_C 203 (6.59) N 232 (3.78) I
10	K 137 (15.33) $S_{H'/G'}$ 147 (5.74) S_F 158 (5.83) S_C 206 (9.63) N 215 (4.35) I

Table 6.17: Phase behaviour of bis(4-N-alkoxybenzylidene)-1,4-phenylenediamines (23).

Section 6.4.2: Preparation of [bis-palladium-bis(acetylacetonato){bis(4-N-decyloxybenzylidene)-1,4 phenylenediamine}] (25).

Preparation of [bis-palladium-bis(μ-acetato){bis(4-N-decyloxybenzylidene)-1,4 phenylenediamine}] (24).

Palladium acetate (0.235g, 1.15 x 10^{-3} mol) was added to bis(4-N-decyloxybenzylidene)-1,4 phenylenediamine (0.300g, 5.23 x 10^{-4} mol) dissolved in toluene (200cm^3) and stirred (60°C, 26 h) to form a brown solution. The solvent was then removed and the product was then dissolved in chloroform and filtered through celite and the solvent was removed and the product was dried under vacuum.

Yield: 0.386g (4.49 x 10^{-4} mol), 86%.

NMR Data ($CDCl_3$):

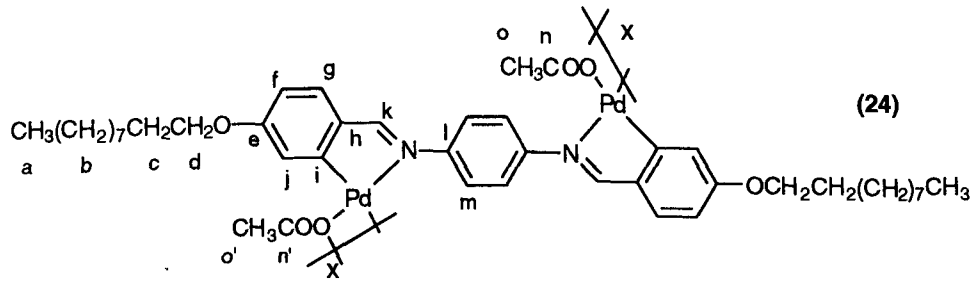

(24)

δ_H: 7.80 2H, s. H_k
7.02 4H, s, H_m
6.96 2H, d, $^3J(HH)$ 8.5Hz
6.55 2H, AA'XX', H_f

6.35 2H, dd, $^3J(HH)$ 8.5Hz, $^5J(HH)$ 2.5Hz, H_f

6.30 2H, d, $^5J(HH)$ 2.5Hz, H_j

3.99 4H, t, $^3J(HH)$ 7Hz, H_d

2.07 3H, s, $H_{n/n'}$

2.00 3H, s, $H_{n/n'}$

1.78 4H, m, H_c

1.23 28H, m, H_b

0.88 6H, t, $^3J(HH)$ 6.5Hz, H_a

Preparation of [bis-palladium-bis(acetylacetonato){bis(4-N-decyloxybenzylidene)-1,4 phenylenediamine}] (25).

Sodium acetylacetonate (0.109g, 8.98 x 10^{-4} mol) was added to [bis-palladium-bis(μ-acetato){bis(4-N-decyloxybenzylidene)-1,4 phenylenediamine}] (0.386g, 4.49 x 10^{-4} mol) suspended in acetone (200cm^3) and stirred (12 h). The solvent was then removed and the crude product extracted with chloroform, washed with water (x2) and with sodium chloride solution (x1) and dried ($MgSO_4$). The solvent was then removed and the product was then purified by chromatography on silica gel using chloroform as the eluent.

Yield: 0.080g (8.03 x 10^{-5} mol), 18%.

NMR Data ($CDCl_3$):

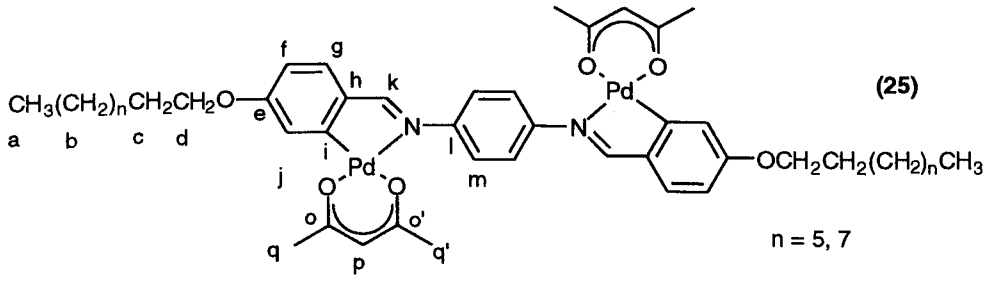

(25)

δ_H: 8.02 2H, s, H_k

7.43 4H, s, H_m

7.32 2H, d, $^3J(HH)$ 8.5Hz, H_g

7.11 2H, d, $^5J(HH)$ 2.5Hz, H_j

6.60 2H, dd, $^3J(HH)$ 8.5Hz, $^5J(HH)$ 2.5Hz, H_f

5.35 2H, s, H_p

4.07 4H, t, $^3J(HH)$ 6.5Hz, H_d

2.09 6H, s, $H_{q/q'}$

1.89 6H, s, $H_{q/q'}$

1.78 4H, m, H_c

1.30 28H, m, H_b

0.86 6H, t, $^3J(HH)$ 6.5Hz, H_a

δ_C: No Carbon-13 spectrum acquired due to the poor solubilty of product (25).

Two compounds of this type were prepared: microanalysis and thermal analysis are detailed in tables 6.18 and 6.19 respectively.

n	C % found (expected)	H % found (expected)	N % found (expected)
8	57.1 (58.2)	6.2 (6.4)	2.4 (3.0)
10	58.4 (59.7)	6.7 (6.8)	2.3 (2.8)

Table 6.18: Microanalysis of [bis-palladium-bis(acetylacetonato){bis(4-N-alkyloxybenzylidene)-1,4 phenylenediamine}] (25).

n	Bis-Pd[di-acac-(bis(4-N-alkyloxybenzylidene)-1,4 phenylenediamine)]. T. /°C ($\Delta H/Jg^{-1}$)			
8	K229 (26.86)	S_A	258[a]	I
10	K210 (7.36) S_A	255[a]	I	

a = decomposition

Table 6.19: Phase behaviour of [bis-palladium-bis(acetylacetonato){bis(4-N-alkyloxybenzylidene)-1,4 phenylenediamine}] (25).

Section 6.6.1: Preparation and characterisation of 3,6-bis(4'-alkoxyphenyl)pyridazine (30).

Preparation of 4-decyloxyacetophenone (26).

Potassium carbonate (20.00g, 1.47 x 10^{-2} mol) was added to a solution of 4-hydroxyacetophenone (10.00g, 7.34 x 10^{-2} mol) and bromodecane (17.87g, 8.08 x 10^{-2} mol) in butanone (200cm^3). The reaction mixture was heated under reflux (24 h) resulting in a colour change in the suspension from yellow to white. The reaction mixture was cooled to room temperature and the potassium carbonate was filtered off. The solvent was then removed from the filtrate. The product was purified by distillation (160°C, 1mmHg) to give a colourless liquid which formed white crystals at room temperature.

Yield: 17.88g (6.47 x 10^{-2} mol), 88%.

NMR Data ($CDCl_3$):

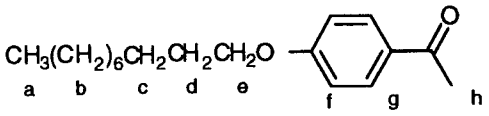

(26)

δ_H: 7.86 2H, AA'XX', H_g
6.86 2H, AA'XX', H_f
3.97 2H, t, $^3J(HH)$ 6.5Hz, H_e
2.49 3H, s, H_h
1.75 2H, m, H_d
1.41 2H, m, H_c
1.26 12H, m, H_b
0.84 3H, t, $^3J(HH)$ 6.5Hz, H_a

Preparation of α-bromo-4-decyloxyacetophenone (27).

Bromine (10.34g, 3.30 cm^3, 6.47 x 10^{-2} mol) was added drop-wise to a stirred solution of 4-decyloxyacetophenone (17.88g, 6.47 x 10^{-2} mol) dissolved in a 2:1 diethyl ether-dioxane solvent system[1] (200cm^3). A colour change in the solution from red to yellow was observed. The solvent was then removed and a purple crystalline solid was obtained.

Yield: 15.86g (4.46 10^{-2} mol), 60%.

NMR Data ($CDCl_3$):

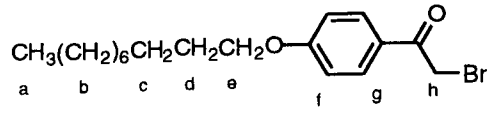

(27)

δ_H: 7.94 2H, AA'XX', H_g
6.93 2H, AA'XX', H_f
4.36 2H, s, H_h
4.01 2H, t, $^3J(HH)$ 6.5Hz, H_e
1.79 2H, m, H_d
1.44 2H, m, H_c
1.28 12H, m, H_b
0.88 3H, t, $^3J(HH)$ 6.5Hz, H_a

Preparation of 1,5-bis(4'-decyloxyphenyl)-3-thiapentane-1,5-dione (28).

A solution of sodium sulphide (1.74g, 2.23 x 10^{-2} mol) in water (15cm^3) was added to a stirred solution (0°C) of α-bromo-4-decyloxyacetophenone (15.86g, 4.46 x 10^{-2} mol) in acetone (100cm^3). The reaction mixture was then allowed to warm to room temperature and stirred (2

h). The white precipitate was removed by filtration and washed with cold water ($10cm^3$) and cold methanol ($10cm^3$).

Yield: 5.46g (0.94×10^{-2} mol), 29%.

NMR Data ($CDCl_3$):

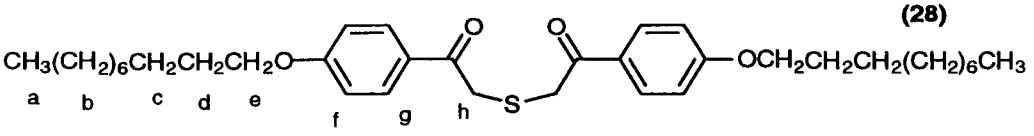

δ_H: 7.92 4H, AA'XX', H_g
6.89 4H, AA'XX', H_f
3.99 4H, t, $^3J(HH)$ 6.5Hz, H_e
3.92 4H, s, H_h
1.78 4H, m, H_d
1.44 4H, m, H_c
1.29 24H, m, H_b
0.87 6H, t, $^3J(HH)$ 6.5Hz, H_a

Preparation of 3,6-bis(4'-decyloxyphenyl)-2,7-dihydro-1,4,5-thiadiazepine (29).

A mixture of 1,5-bis(4-decyloxyphenyl)-3-thiapentane-1,5-dione (5.46g, 0.94×10^{-2} mol) and hydrazine monohydrate (0.47g, 0.94×10^{-2} mol) was heated in acetic acid ($100cm^3$) (95°C, 1.5h). The solvent was removed and the yellow powder was washed with cold ethanol ($10cm^3$).

Yield: 3.70g (6.77×10^{-2} mol), 72%.

NMR Data ($CDCl_3$):

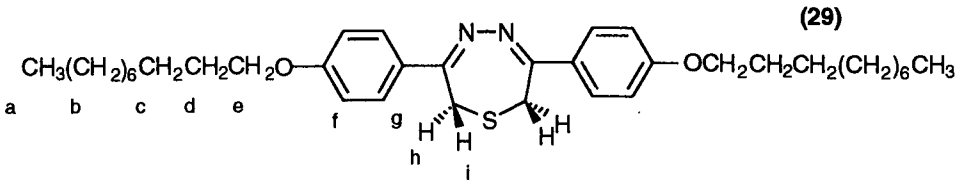

δ_H: 7.81 4H, AA'XX', H_g
6.95 4H, AA'XX', H_f
3.99 4H, t, $^3J(HH)$ 6.5Hz, H_e
3.63 2H, d, $^2J(HH)$ 13Hz, $H_{h/i}$
3.30 2H, d, $^2J(HH)$ 13Hz, $H_{h/i}$
1.79 4H, m, H_d
1.44 4H, m, H_c
1.29 24H, m, H_b
0.88 6H, t, 6.5Hz, H_a

Preparation of 3,6-bis(4-decyloxyphenyl)pyridazine (30).

Diethylene glycol ($30cm^3$) was added to 3,6-bis(4-decyloxyphenyl)-2,7-dihydro-1,4,5-thiadiazepine (2.00g, 0.37×10^{-2} mol) and heated to 230°C (0.5 h), causing the evolution of hydrogen sulphide gas. The dark brown solution was cooled to room temperature and cold water was added to the resulting mixture. The brown precipitate was then removed by filtration and washed with cold acetone ($10cm^3$). The crude product contained 4-decyloxyacetophenone (in a 1:1 ratio with the product) as a by-product of the reaction. This was removed by sublimation at 180°C under vacuum (1mmHg) The product was then recrystallised in butanone to give a white crystalline solid.

Yield: 0.60g (0.11×10^{-2} mol), 30%.

NMR Data ($CDCl_3$):

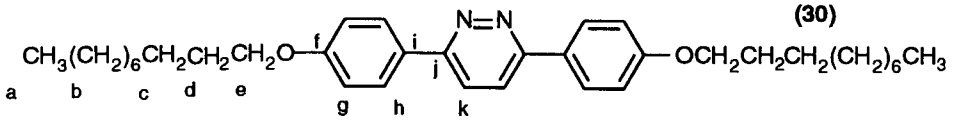

δ_H:	8.08	4H, AA'XX', H_h
	7.81	2H, s, H_k
	7.03	4H, AA'XX', H_g
	3.99	4H, t, ^3J(HH) 6.5Hz, H_e
	1.71	4H, m, H_d
	1.47	4H, m, H_c
	1.27	24H, m, H_b
	0.87	6H, t, ^3J(HH) 6.5Hz, H_a

δ_C:	160.7 (C_f)	156.5 (C_i)	128.3 (C_j)	128.0 (C_h)
	123.3 (C_k)	114.8 (C_g)	68.1 (C_e)	31.8 (C_d)
	29.5-22.5 ($C_{b,c}$)	14.0 (C_a)		

A number of homologues were prepared in a similar fashion: microanalysis and thermal analysis data is detailed in table 6.20 and table 6.21 respectively.

n	C % found (expected)	H % found (expected)	N % found (expected)
6	77.6 (77.7)	8.3 (8.4)	6.5 (6.5)
7	78.0 (78.2)	8.7 (8.8)	6.2 (6.1)
8	78.3 (78.7)	8.9 (9.1)	5.7 (5.7)
10	79.3 (79.4)	9.6 (9.6)	5.3 (5.1)

Table 6.20: Microanalysis of series of 3,6-bis (alkoxyphenyl)pyridazines (30).

n	Phase behaviour of 3,6-bis(4-alkoxyphenyl)pyridazines. Temp. /°C ($\Delta H/Jg^{-1}$)
6	K 87 (20.4) K' 94 (35.6) K'' 139 (0.40) K''' 158 (24.4) S_F 165 (2.09) S_I 258 (25.9) I
7	K 112 (87.4) K' 143 (22.4) S_G 145 (0.09) S_F 165 (3.2) S_I 252 (28.4) I
8	K 109 (67.3) K' 131 (20.7) S_G 142 (0.18) S_F 166 (2.7) S_I 249 (27.2) I
10	K 113 (18.9) K' 121 (18.4) K'' 129 (18.4) S_G 163 (3.6) $S_{F/I}$ 238 (28.9) I

Table 6.21: Phase behaviour of 3,6-bis (alkoxyphenyl)pyridazines (30).

Section 6.6.2: Preparation and characterisation of [palladium-(acetylacetonato){3,6-bis(4'-alkoxyphenyl)pyridazine}] (32).

Preparation of [palladium-bis(μ-acetato){3,6-bis(4-decyloxyphenyl)pyridazine}] (31).

Palladium acetate (0.122g, 5.45 x 10^{-4} mol) was added to a solution of 3,6-bis(4'-decyloxyphenyl)pyridazine (0.300g, 5.45 x 10^{-4} mol) in acetic acid (200cm^3) and stirred overnight (60°C, 16 h). The solvent was then removed and the crude product was dried under vacuum (1mmHg). The yellow powder was then dissolved in chloroform and filtered through celite and the solvent was removed.

Yield: 0.355g (5.01 x 10^{-4} mol), 92%.

NMR Data ($CDCl_3$):

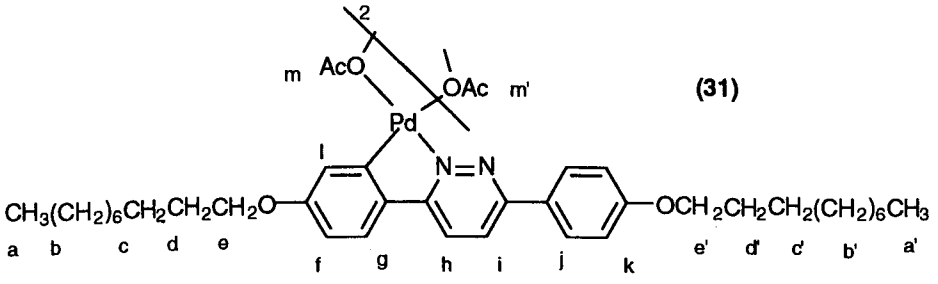

(31)

δ_H: 7.90 2H, AA'XX', H_j

7.46 1H, d, ^3J(HH) 9Hz, $H_{h/i}$

7.02 1H, d, ^3J 9Hz, $H_{h/i}$

6.98 2H, AA'XX', H_k

6.75 1H, d, $^3J(HH)$ 8.5Hz, H_g

6.27 1H, d, $^4J(HH)$ 2.5Hz, H_l

6.68 1H, dd, $^3J(HH)$ 8.5Hz, $^4J(HH)$ 2.5Hz, H_f

4.00 4H, m, $H_{e,e'}$

2.34 3H, s, $H_{m/m'}$

1.80 4H, m, $H_{d,d'}$

1.46 4H, m, $H_{c,c'}$

1.30 24H, m, $H_{b,b'}$

0.89 6H, m, $H_{a,a'}$

Preparation of [palladium-(acetylacetonato){3,6-bis(4-decyloxyphenyl)pyridazine}] (32).

Sodium acetylacetonate (0.073g, 6.00 x 10^{-4} mol) was added to [palladium-bis(μ-acetato){3,6-bis(4-decyloxyphenyl)pyridazine}] (0.200g, 2.82 x 10^{-4} mol) dissolved in tetrahydrofuran ($100cm^3$). The solution was heated under reflux (16 h) yielding a yellow solution. The solvent was removed and the yellow powder was chromatographed on silica using chloroform as an eluent.

Yield: 0.119g (1.60 x 10^{-4} mol), 57%.

NMR Data ($CDCl_3$):

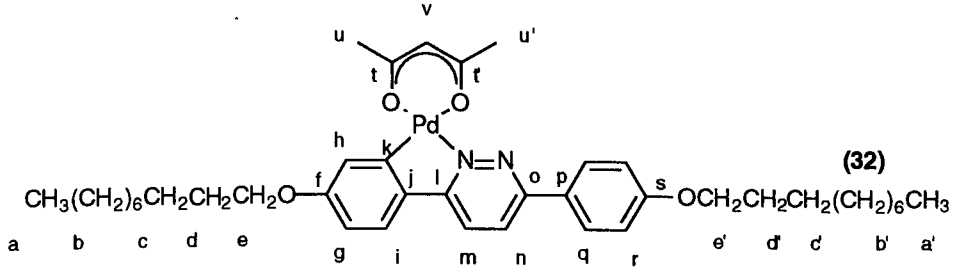

(32)

δ_H: 8.03 2H, AA'XX', H_q

7.88 1H, d, $^3J(HH)$ 9Hz, $H_{m/n}$

7.67 1H, d, $^3J(HH)$ 9Hz, $H_{m/n}$

7.31 1H, d, $^3J(HH)$ 8.5Hz, H_i

7.23 1H, d, $^4J(HH)$ 2.5Hz, H_h

6.98 2H, AA'XX', H_r

6.68 1H, dd, $^3J(HH)$ 5.5Hz, $^4J(HH)$ 2.5Hz, H_g

5.44 1H, s, H_v

4.07 2H, t, $^3J(HH)$ 6.5Hz, $H_{e/e'}$

4.00 2H, t, $^3J(HH)$ 6.5Hz, $H_{e/e'}$

2.16 3H, s, $H_{u/u'}$

2.12 3H, s, $H_{u/u'}$

1.80 4H, m, $H_{d,d'}$
1.45 4H, m, $H_{c,c'}$
1.30 24H, m, H_b
0.88 6H, m, $H_{a,a'}$

δ_C: 189.2 ($C_{t/t'}$) 186.1 ($C_{t/t'}$) 165.7 (C_l) 161.1 (C_f)
159.7 (C_s) 157.9 (C_j) 155.2 (C_p) 132.7 (C_k)
127.9 (C_q) 127.0 (C_o) 124.9 (C_i) 124.5 (C_m)
123.5 (C_q) 115.9 (C_h) 114.8 (C_r) 112.1 (C_g)
100.4 (C_v) 68.1 (C_e) 67.8 ($C_{e'}$) 31.7 (C_d)
29.2 (C_c) 29.1 (C_b) 29.1 (C_b) 28.3 ($C_{u/u'}$)
27.5 ($C_{u/u'}$) 26.0 (C_b) 25.9 (C_b) 22.5 (C_b)
14.0 ($C_{a/a'}$).

A number of homologues were prepared in a similar fashion: microanalysis and thermal analysis data is detailed in table 6.22 and table 6.23 respectively.

n	C % found (expected)	H % found (expected)	N % found (expected)
6	61.9 (62.2)	6.7 (6.6)	4.1 (4.4)
7	63.5 (63.2)	7.1 (7.0)	4.2 (4.2)
8	64.5 (64.1)	7.4 (7.3)	3.8 (4.0)
10	65.6 (65.7)	7.8 (7.8)	3.7 (3.7)

Table 6.22: Microanalysis of series of [palladium-(acetylacetonato){3,6-bis(4-alkyloxyphenyl)pyridazine}] (32).

n	Phase behaviour of palladium (acetylacetonate)-3,6-bis(4-alkoyphenyl)pyridazines. T. /°C ($\Delta H/Jg^{-1}$)				
6	K	196 (34.38)	S_A	280[a] (0.90)	I
7	K	196 (34.38)	S_A	290[a] (1.43)	I
8	K	162 (33.57)	S_A	264[a] (2.18)	I
10	K	184 (30.28)	S_A	281[a] (2.36)	I

a = decomposition

Table 6.23: Thermal analysis of series of [palladium(acetylacetonato){3,6-bis(4-alkyloxyphenyl)pyridazine}] (32).

Section 6.6.3: Preparation of and characterisation of [bis-palladium-bis-(acetylacetonato){3,6-bis(4-decyloxyphenyl)pyridazine}] (34).

Preparation of [bis-palladium-bis(μ-acetato){3,6-bis(4-decyloxyphenyl)pyridazine}] (33).

Palladium acetate (0.169g, 7.54 x 10^{-4} mol) was added to 3,6-bis(4-decyloxyphenyl)pyridazine (0.196g, 3.77 x 10^{-4} mol) dissolved in acetic acid (60cm^3) and stirred (60°C, 48 h). The solvent was then removed and the red product was dried under vacuum (1mmHg). The product was then dissolved in chloroform and filtered through celite.

Yield: 271g (335 x 10^{-4} mol), 90%.

NMR Data:

Proton NMR specturm of **(33)** broad. No other characterisation attempted.

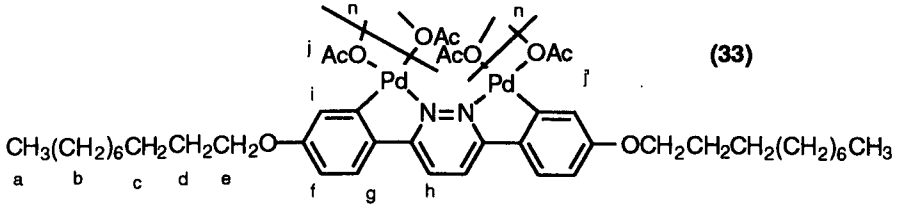

(33)

Preparation of [bis-palladium-bis(acetylacetonato){3,6-bis(4-decyloxyphenyl)pyridazine}] (34).

Sodium acetylacetonate (0.028g, 2.32 x 10^{-4} mol) was added to [bis-palladium-bis(μ-acetato){3,6-bis(4-decyloxyphenyl)pyridazine}] (0.100g, 1.16 x 10^{-4} mol) was dissolved in tetrahydrofuran (100cm^3) and was stirred overnight. The solvent was removed and the product dried under vacuum (1mmHg). The product was then washed in diethyl ether and hexane.

Yield: 0.052g (7.11 x 10^{-5} mol), 62%.

NMR Data ($CDCl_3$):

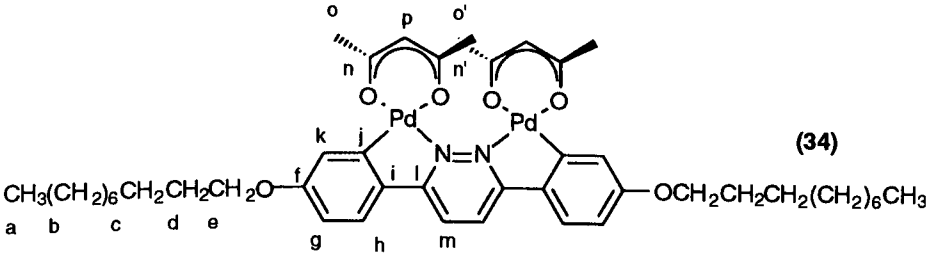

(34)

δ_H: 7.76 2H, s, H_m

7.27 2H, d, ^3J(HH) 8.5 Hz, H_h

7.10 2H, d, ^4J(HH) 2.5 Hz, H_k

6.64 2H, dd, ^3J(HH) 8.5Hz, ^4J(HH) 2.5Hz, H_g

5.27 2H, s, H_p

4.04 4H, t, $^3J(HH)$ 6.5Hz, H_e

2.06 12H, s, $H_{o,o'}$

1.78 4H, m, H_d

1.48 4H, m, H_c

1.28 24H, m, H_b

0.88 6H, t, $^3J(HH)$ 6.5Hz, H_a

δ_C:

186.5 ($C_{n,n'}$)	164.2(C_i)	159.4 (C_f)	156.8 (C_l)
132.8 (C_j)	125.1 (C_h)	124.6 (C_m)	116.0 (C_k)
111.8 (C_g)	99.8 (C_p)	67.8 (C_e)	31.7 (C_d)
29.3 (C_c)	29.2 (C_b)	27.4 ($C_{o,o'}$)	26.0 (C_b)
22.6 (C_b)	14.0 (C_a)		

n	C % found (expected)	H % found (expected)	N % found (expected)
10	56.9 (59.9)	6.7 (7.0)	2.8 (3.0)

Table 6.24: Microanalysis of [bis-palladium-bis(acetylacetonato){3,6-bis(4-decyloxyphenyl)pyridazine}] (34).

n	Phase behaviour of bis Pd [di-acac-3,6-bis(4-decyloxyphenyl)pyridazine]. T. /°C ($\Delta H/Jg^{-1}$)			
10	K	169 (30.51)	S_A	$210^{a,b}$ I

a = clears with decomposition.

Table 6.25: Phase behaviour of [bis-palladium-bis(acetylacetonato){3,6-bis(4-decyloxyphenyl)pyridazine}] (34).

Section 6.7: References.

1 S E Whitney, M Winters and B Ricborn, *J. Org. Chem.*, 1990, 55, 929.

Appendix 1: Examples of Liquid Crystal Phase Textures.

Appendix 1:

Smectic I

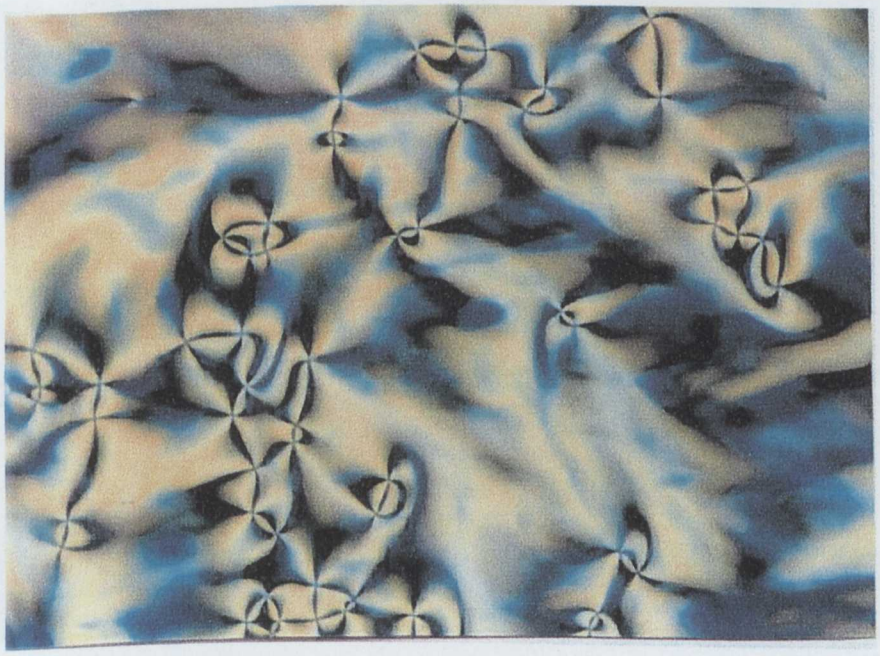

Smectic F

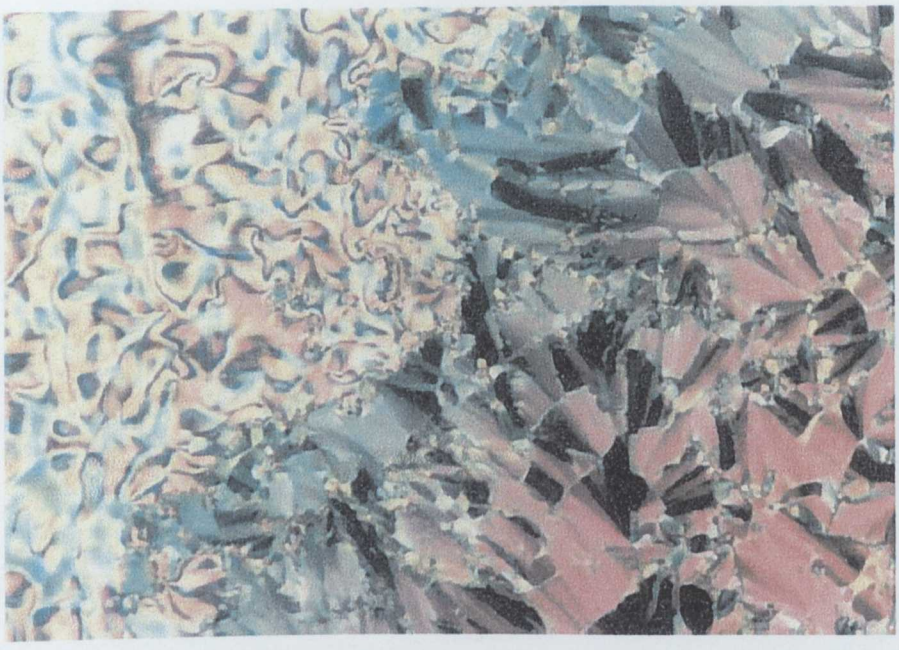

Smectic C

Smectic A

Nematic

APPENDIX NOT COPIED

ON INSTRUCTION FROM

UNIVERSITY